

# Quantification of structural loading, during race scenarios, and initial frame stiffness optimization using Finite Element Analysis of a handbike

MATHIAS SONSBY MOURIDSEN & RASMUS KOKHOLM PEDERSEN  
Aalborg University, Faculty of Medicine and Health, Sports Technology.

## Abstract

**Purpose:** This study determined the forces acting on a handbike, using strain gauges, in three field test scenarios - accelerating, braking and road irregularities. In addition an initial optimization study was conducted using the determined acceleration forces.

**Methods:** Free Body Diagrams and Finite Element Analysis (FEA) was used to determine strain gauge positions. Laboratory calibrations were carried out to transform the measured strains into forces. One healthy male subject performed five trials of each field test scenario – all out acceleration for three pedal cycles, braking the handbike from a velocity of  $41.7 \pm 0.3$  km/h and riding across wooden list, simulating a cobblestone road (velocity of  $37.3 \pm 1.1$  km/h). A FE-model of the handbike, used for optimization, was validated by carrying out a calibration study for each field test scenario. Lastly, an initial optimization study, in regard to frame stiffness, was conducted by applying the acceleration force, calculated with the laboratory calibration, to the FE-model of the handbike.

**Results:** For the acceleration scenario the tangential and radial force peaks were 407.6 N and 380.0 N, respectively, the peak brake force was 1571.1 N and the peak forces caused by road irregularities, were 12952.4 N and 21586.7 N, at the front and rear wheel, respectively, calculated with the laboratory calibrations. The tangential and radial force peaks were 25.2 percent higher and 8.4 percent lower, respectively, while the peak brake and road irregularity forces, at the front wheel, were 96.4 and 1328.3 percent higher, respectively, calculated with the laboratory calibrations compared to the SW calibrations. The lowest displacement of the crankbox, 0.494mm, was found by thickening the front V-tube of the FE-model.

**Conclusion:** The acceleration forces found was considered slightly overestimated and the brake force was considered valid, while the road irregularity forces was not. As disagreement between the results of the FE-model and laboratory calibration were present, the FE-model cannot fully be trusted for FEA, especially in regard to brake and road irregularity force. The initial optimization study revealed that the highest stiffness by least weight increase was obtained by thickening the frontal V-tube.

**Keywords:** Handcycling | Structural loading | Frame | Stiffness | Compliance | Finite Element Analysis

## 1. Introduction

The use of hand-cycling has become popular, both in daily as well as recreational use, over the last decades, due to the high efficiency in propulsion and low loads on the body, compared to traditional wheelchairs (Hettinga, Valent et al. 2010). This high efficiency in propulsion enables higher peak performance, as well as higher endurance compared to wheelchairs (Dallmeijer, Zentgraaff et al. 2004). This have made it possible for hand-bikers to participate in cycling training sessions with able-bodies participants (Hettinga, Valent et al. 2010). An example of such a handbike, used for racing, is the Race bandit (Wolturnus A/S) with synchronous propulsion, Figure 1, which is also the handbike used in this study.

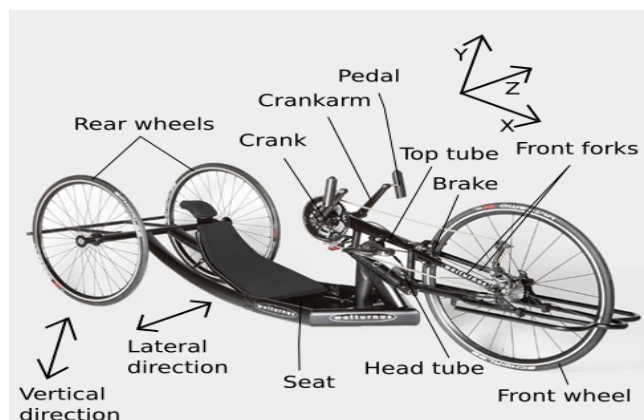


**Figure 1:** Race bandit (Wolturnus A/S), which is the handbike used in this study.

Research has been made to determine the mechanics and design of standard bicycles. Bicycles with a human on top can, in a simple interpretation, be considered a system with a mass on top of a spring and a damper (Vanwalleghem 2009), where the bicycle is the spring and damper, and the human is the mass. The spring constant, which is a measure of the stiffness of the bicycle, is defined by Hooke's law,  $F = -k \cdot X$ , where  $F$  is force,  $k$  is a constant factor of the spring stiffness and  $X$  is distance. This influences the force transfer to the human, caused by bumps in imperfect surfaces. For a more vertical compliant bicycle the same amount of force is transferred slower, thereby lowering the peak forces experienced by the rider. Damping is a measure of how fast the amplitude of vibrations dissipates, which gives a smoother ride, if the damping increases, to some extent (Vanwalleghem 2009). This is important, as the vibrations has shown to negatively affect physical performance and comfort (Vanwalleghem 2009, Sperlich, Kleinoeder et al. 2009, Le'pine, Champoux et al. 2015). Vertical compliance is therefore desired in order to reduce vibrations. Furthermore, lateral stiffness, which is the stiffness causing the bicycle not to bend around the X-axis, illustrated on Figure 2, is desired, as less lateral deflection of the bicycle frame leaves more energy to create propulsion (Vanwalleghem 2009). This means that high lateral stiffness, helps to maximize the load transfer from feet and hands to the chain (Covill, Begg et al. 2014).

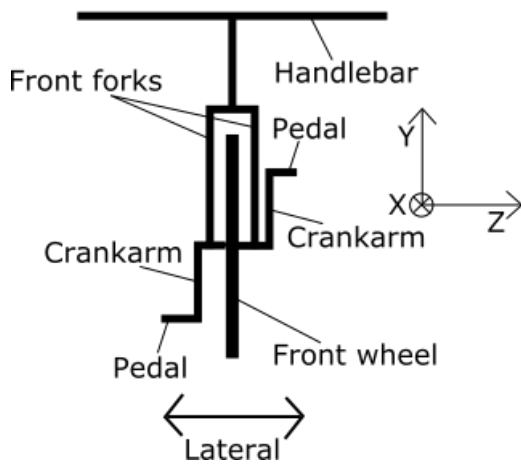


Figure 2: Front view of a bicycle, defining the lateral direction.

To sum up, a good bicycle will have a different stiffness in the vertical and lateral direction. Composite materials, like carbon fiber has the advantage of being able to apply stiffness in the desired directions by customizing the directions of the fibers (Calfeedesign.com). Because of this, and the high strength to weight ratio, composite materials are becoming more and more commonly used, when designing new bicycles. In metallic materials it is only possi-

ble to customize the directional stiffness by doing geometry changes. This can i.e. be done by making tubes oval, thereby altering the area moment of inertia. Less research has been focusing on three-wheel handbikes, as the one used in this study, Figure 1. It is therefore necessary to consider if the vertical compliance and lateral stiffness, relevant for a standard bicycle, is relevant for the handbike used in this study. It must be assumed that a compliant vertical system is also advantageous in the handbike, as that lowers vibrations, which have proven disadvantageous in standard bicycles (Vanwalleghem 2009, Sperlich, Kleinoeder et al. 2009, Le'pine, Champoux et al. 2015). However, the propulsion created in the push phase of the pedal cycle pushes the rider down in the seat, Figure 3, which causes vertical deflection, leading to a loss of energy. A handbike design, with a very high vertical stiffness, at the frame and crank, and vertical compliance at the wheels, would be preferred.

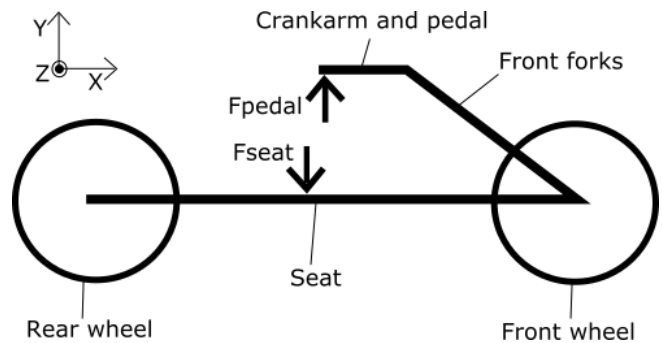


Figure 3: The push force and corresponding force from the rider getting pushed down in the seat, which causes vertical deflection.

Lateral stiffness is not a relevant design criterion for the handbike, as it was for a standard bicycle, because the synchronous propulsion, at the pedals, does not cause any forces that would make the handbike deflect laterally.

In terms of optimizing the handbike in terms of stiffness, it is necessary to know, which forces are present when riding a handbike. Those forces can be split into two categories, namely rider induced forces and forces occurring from imperfections in the road. The rider induced forces comes from the riders weight and when applying forces to the pedals i.e. during acceleration and normal riding, but also when braking. The forces that occur from imperfections in the road are when riding across bumps etc. (Wilson 2004). A previous study, conducted on standard bicycles, found that the stresses occurring from accelerating during starting and brake cases are quite high, but that the stresses occurring from constant high speed cycling is significantly lower (Soden, Millar et al. 1986). Because of this, it is expected that accelerating and brake forces are the upper

limit scenarios, for the rider induced loads on a handbike as well. In terms of road irregularities, the forces will vary depending on how big the bumps are. Realistic race scenarios for the type of handbike, should be used to determine how big the bumps tested should be. In this study the focus is on acceleration, brake force, and road irregularities, as those are considered the upper limit structural loading scenarios of the handbike. A commonly used method to determine forces applied to bicycles are by using strain gauges (SG) (Wilson 2004). As the method is applicable for bicycles, it is also applicable for handbikes. In order to go from strains measured when the handbike is rode, to forces applied, it is necessary to place the SGs strategically on the handbike.

Once the forces acting on the handbike is found, it is possible by Finite Element Analysis (FEA) to investigate deflection in different locations on the structure. In that way, it is possible to investigate where the structure should be made stiffer, thereby optimizing the structure in terms of deflection. This can i.e. be done by adding material or changing the geometry. The use of FEA is, however, only as good as the inputs you give the program, it is therefore important to use a representative FE-model of the handbike, as well as applying correct constraints and forces in the FE-model of the handbike, to get useful outputs from the FEA.

The purpose of this study is twofold. Firstly, to determine the forces acting on the handbike, riding the handbike with SGs attached in three field test scenarios - accelerating, braking and road irregularities. Secondly, to optimize the front part of the handbike design in terms of stiffness by FEA, using the determined acceleration forces as inputs.

## 2. Methods

In order to determine the forces acting on the handbike, which in the end was used for optimization, several steps were made. The steps are illustrated, as a flow chart, Figure 4, where each block is described through the method. Firstly however, a custom made three-wheel handbike, which was manufactured in heat-treated 7020 aluminum, with a recumbent frame and riding style was acquired from Wolturnus A/S (RaceBike model), Figure 1. Furthermore, Wolturnus A/S supplied a SolidWorks (SW) made CAD-model of the handbike. However, the CAD-model was only used for technical drawings and not simulations, why modifications and repairs was required in order to run simulations.

### 2.1 Modifications of the CAD-model

Several geometry changes and simplifications were made, on the acquired CAD-model, as it was initially not suitable for FEA. Firstly, the dimensions of the CAD-model were altered, as they did not correspond to the real handbike. This was due to the CAD-model being an overall design, and not the exact handbike acquired. To correct this, length measurement were made on the real handbike and adjusted in the CAD-model. Secondly, several geometry changes and simplifications were made. Common to all geometry changes and simplifications, were that the strains, at and close to the geometries that were altered from the acquired CAD-model, could not be trusted, as the CAD-model and the real handbike did not correspond. However, geometries that were made like the geometries on the real handbike could still be trusted.

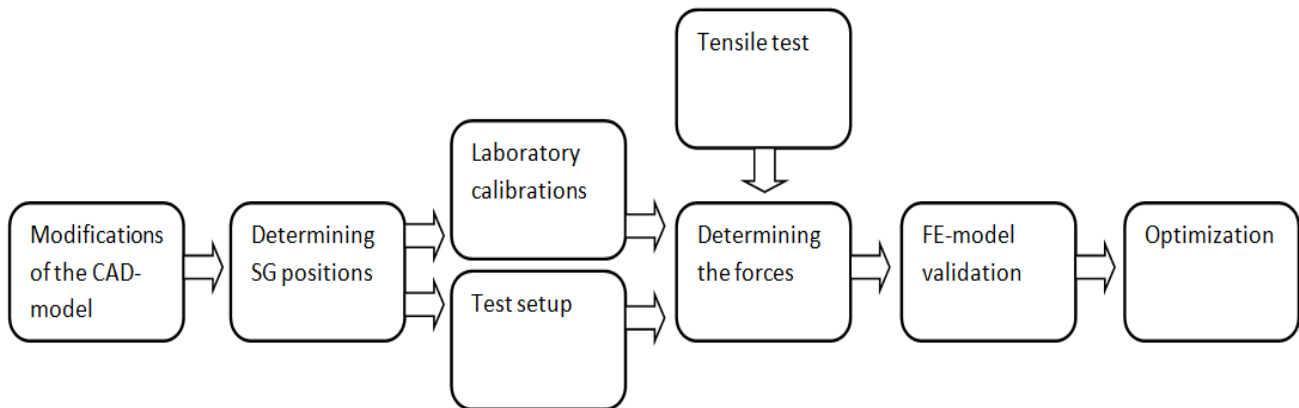


**Figure 4:** Flow chart of the steps in the method in order to determine the forces acting on the handbike, which in the end was used for optimization.

### 2.1.1 Modifications of the crankset

The crankarms from the acquired CAD-model were used, but new crankshaft, crankbox and pedals, were made, as the acquired CAD-model caused interferences, Figure 5. The simplified crankshaft and crankbox were considered adequate, as the rotational freedom between the parts and the thickness of the crankshaft and crankbox remained the same. The pedals and their connection to the crankarms were just considered a load transferring geometry. This meant that as long as the load was applied in the same distance from the crankarms, the forces on the rest of the structure would remain the same. Furthermore, a simplified tooth wheel and chain were made. The tooth wheel and chain were positioned, at the same distance to the crankbox on the crankshaft, and the modified tooth wheel had the same radius/length, as the original acquired tooth wheel. Again, the modified parts were seen, as load transferring geometries, and the strains in the modified tooth wheel and chain were not of interest. Only the lower part of the chain was modelled, as it is only the lower part of the chain, which transfers loads during cycling.

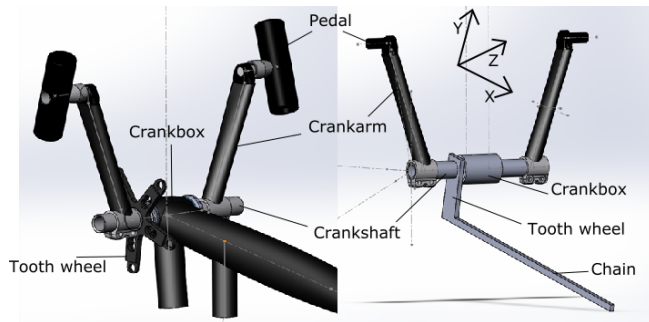


Figure 5: Acquired (left) and modified (right) CAD-model of the crankset.

### 2.1.2 Modifications of the front part

The front wheel and axle were simplified in order to reduce calculating time. The axle was represented by a tube and wheel was represented by beams attached to the tube/axle, Figure 6. The modified axle allowed for the same movements, as the original acquired axle, and the modified wheel, represented by beams, had the same length, as the radius of the original acquired wheel. Because of the same length and position on the axle, the modified wheel was not considered to alter the load transfer to the axle. In order to simulate the brake forces, at the front wheel, the middle beam was attached to the top tube, by a rod, which represented the brake pads, Figure 6. This attachment corresponded to where the brake pads are mounted on the real handbike, thus making the load transfer to the top tube realistic. Modifications were also made to the upper and lower front forks at the connection to the axle. The original

acquired parts between the upper and lower front forks at the axle, were replaced by a geometry that allowed load transfer between the adjacent parts. Further, modifications at the ends of the head tube were made, as they were not connected in the acquired CAD-model. The original acquired parts were replaced with tubes, which allowed for load transfer between the adjacent structures.

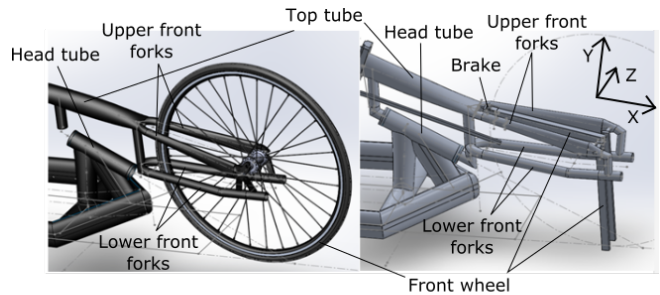


Figure 6: Acquired (left) and modified (right) CAD-model of the front part of the handbike.

## 2.2 Strain gauge positions

Free Body Diagram (FBD) and FEA were used to determine the positions of the SGs, needed to determine the forces applied to the handbike, in the three field test scenarios. FBD was used at the crank and rear wheel, and FEA was used at the front wheel.

### 2.2.1 Acceleration scenario

The force a human apply to the pedals can be split up into a tangential and a radial force, Figure 7, which is perpendicular and parallel to the crankarm, respectively. Further, a force pushing or pulling the pedals towards or away from each other is applied, which was however, neglected in this study, as it was assumed low. Therefore, the SGs were positioned, in order to determine the tangential and radial force.

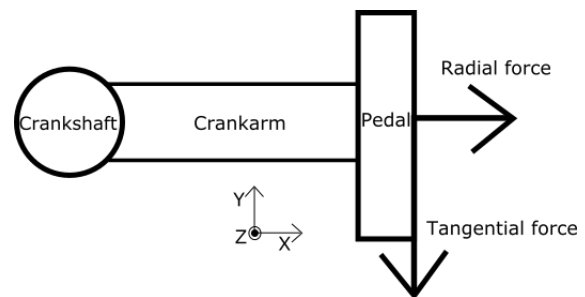
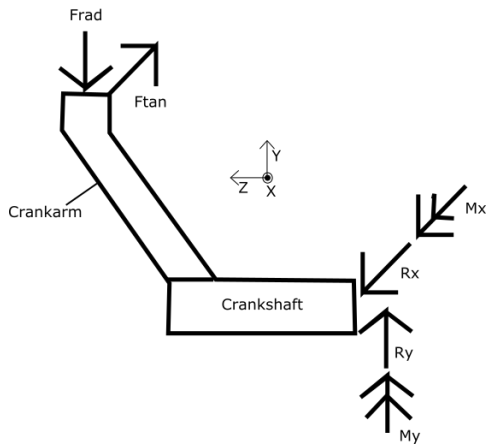


Figure 7: The direction of the tangential and radial force applied to the pedal during cycling.

A FBD analysis of the crankarm and crankshaft was used together with beam theory, to determine the position of the SGs used to measure the tangential force, Figure 8. The tangential force causes torsion of the crankshaft, while the radial force causes bending of the crankshaft around the X-axis.



**Figure 8:** FBD used to determine the position of SGs for measuring the tangential force.

To measure the torsional strains caused by the tangential force, two SGs were placed in a half bridge on the crankshaft, inside the crankbox, with a 45 degree angle to the longitudinal direction (Omega.com). From the view of the crankshaft and crankarm, Figure 9, the SG were placed on the middle of the crankshaft, illustrated by the dashed line. This was done in order to avoid measuring the normal strain caused by the radial force, as normal strain due to bending is zero on the dashed line on the crankshaft (Gere, Goodno 2013).

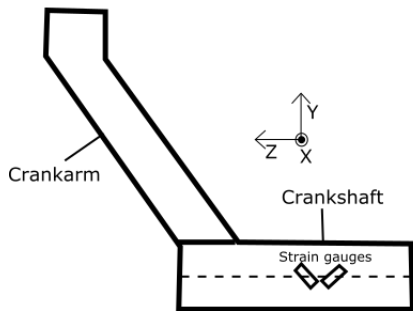


**Figure 9:** Position of the half bridge SGs on the crankshaft.

A FBD analysis of the crankarm was used to determine the position of the SG, used to measure the radial force, Figure 10. The tangential force causes bending around the Z-direction, while the radial force cause bending around the X-axis and compression/tension in the Y-direction of the crankarm, depending on where in the cycle the pedals are.

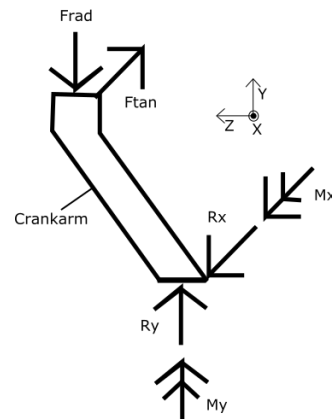


**Figure 10:** FBD used to determine the position of the SG for measuring the radial force.

To measure the strains caused by the radial force, one SG was placed in a quarter bridge on the middle of the surface pointing towards the crankbox, Figure 11, as the normal strain caused by the tangential force is zero at that location (Gere, Goodno 2013).

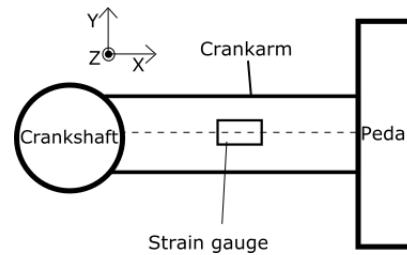


**Figure 11:** Position of the quarter bridge SG on the surface of the crankarm, which is pointing towards the crankbox.

### 2.2.2 Brake scenario

Brakes were only attached to the front wheel of the handbike. Therefore, the modified CAD-model of the handbike (from now on referred to as FE-model, due to the use in FEA), consisting of only the front part of the handbike, Figure 12, was used to determine the position of the SG needed to determine the forces applied by braking. The fixations and forces applied to the FE-model are illustrated by green and purple arrows, respectively.

A point on top of the right upper front fork, illustrated by the yellow mark, Figure 12, where the strains was more or less constant over an area, was chosen, as the position of the SG. This was chosen, as SGs are measuring mean strain over the area they are placed. Areas with large differences in strains, i.e. where geometry changes rapidly, is therefore unreliable. The distance from the axle of the front wheel to the chosen point was measured in the FE-model, and one SG was placed

in a quarter bridge, at the corresponding point on the handbike.

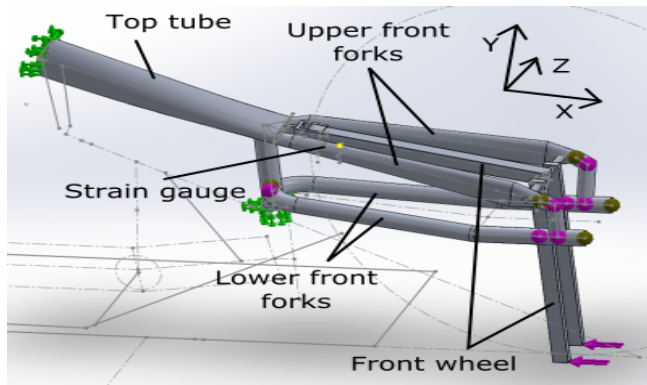


**Figure 12:** FE-model used for FEA to determine the SG position for the braking scenario. Green arrows=fixations and purple arrows=force.

### 2.2.3 Road irregularities scenario

Road irregularities applies loads, at both the front and rear wheels. At the front wheel the modified FE-model, used for the braking scenario, was also used to determine the position of the SG, used to determine the forces caused by road irregularities. However, in this scenario the brake pads were suppressed. The fixtures and forces are illustrated by green and purple arrows, respectively, Figure 13. The analysis revealed that the same SG used to determine brake force, could be used to determine the forces caused by road irregularities, as the same position had more or less constant strains over an area.

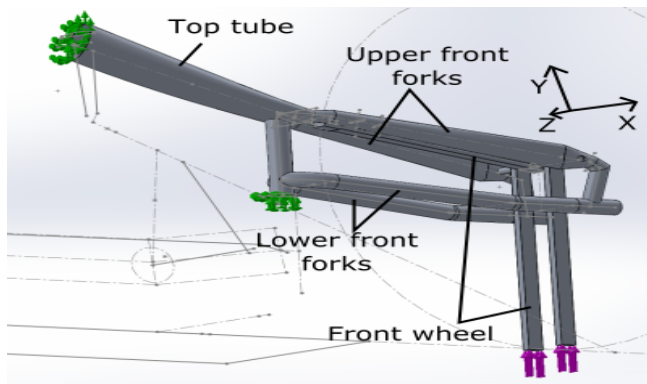


**Figure 13:** FE-model used for FEA to determine the SG position for the road irregularity scenario, at the front wheel. Green arrow= fixations and purple arrows=force.

It was assumed that the force applied, to each rear wheel would be the same. To determine the position of the SG, at the rear wheel, a FBD analysis was carried out, Figure 14. The forces in the X- and Z-direction were neglected, as the velocity of the handbike would be close to constant and that the wheels was attached to the axle with an angle of 90 degrees. Therefore just

one SG was positioned, in a quarter bridge, on top of the tube connecting the two rear wheels, as the force in the Y-direction can only cause bending around the X-axis.

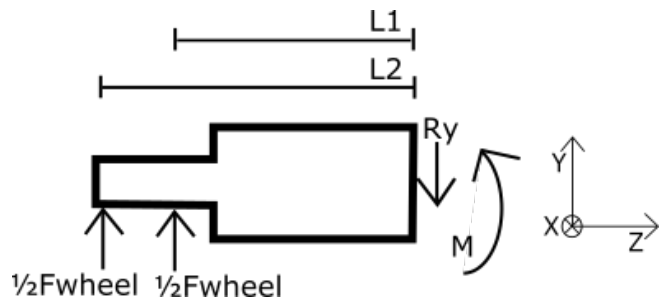


**Figure 14:** FBD of the rear wheel. L1 and L2 is the lengths from the spokes of the wheel to the SG.

### 2.3 Tensile test

A tensile test was carried out to determine the material properties of the material, used to manufacture the handbike. The procedure for the tensile test was in accordance to the standard ASTM E8/E8M, with a Zwick tensile tester and an attached extensometer (ASTM E8 / E8M-15a 2015). The speed up to yield point was 1.23 mm/min and from yield point to fracture the speed was 32.86 mm/min. The E-modulus and yield strength (0.2% offset) were calculated, which was applied to the FE-model.

### 2.4 Test setup

The subject, riding the handbike for the three scenarios, was a 25 year old male, who did weightlifting four times a week. The height and weight of the subject was 185 cm and 91 kg, respectively. The tire pressure of the 28" race wheels were 10 bar. The SGs attached to the handbike were 350 ohms (Micro-Measurements). The quarter and half bridges were attached to a bridge completion module (MR1-350-130, Micro Measurements), which were attached to the measuring system. The measuring system, for the breaking and road irregularity scenarios, consisted of a transmitter (V-link®-LXRS®, Lord Microstrain – Sensing systems) and a receiver (WSDA®-Base-101, Lord Microstrain – Sensing systems), which measured with a sampling frequency of 512 Hz. For the acceleration scenario a data acquisition device (DAQ) (NI USB-6008/6009DAQ USB Device, National Instruments) was attached to the receiver, as it enabled attachment of a wheel encoder. The DAQ enabled a total sampling frequency of 48000 Hz across all channels. The 48000 Hz was divided with four, as four channels were used in this scenario and thereby setting the sampling frequency to 12000 Hz per channel. The DAQ measured changes in volts, from where the strains could be derived. This was done by firstly transforming the volts

into bits, and then use a transformation formula from the measuring software to go from bits to strains. The wheel encoder had 500 impulses per pedal cycle, enabling determination of the crankarm position within 0.72 degrees.

#### 2.4.1 Test protocol

To determine the forces caused when accelerating, the handbike was mounted onto a home trainer (KICKR, Wahoo Fitness). The home trainer was controlled with the application "Wahoo Fitness" and the resistance was set to 40 percent of its maximum resistance, and the gear ratio was 2.5. Five trials of all-out acceleration, were performed for three pedal cycles, with a resting period of 1 min between trials, while strains and crank position were measured. The starting position of the crankarms were parallel to the floor and pointing towards the riders head.

The starting position was chosen from the subject's personal preference, as were he felt he could accelerate the fastest. To determine the forces occurring from braking, five trials of braking the handbike, as quickly as possible from a velocity of  $41.7 \pm 0.3$  km/h were performed, while the strains was measured. The velocity of  $41.7 \pm 0.3$  km/h were chosen, as it was the maximal velocity the subject could achieve within the equipment's measuring range. Further, the velocity was close to the average velocity used in high level competitive races. The velocity was measured with a bike computer (16.12 STS/CAD, Sigma), by the subject just before braking the handbike.

To determine the forces caused by road irregularities, five trials of riding the handbike, with a velocity of  $37.3 \pm 1.1$  km/h, over four wooden lists were performed, while strains, at the front and rear wheel, were measured. The wooden lists were fixed with a distance of 250 mm in between and had a height of 14 mm and a width of 64 mm. The wooden lists were used to simulate the peaks of riding across cobblestones in a standardized test scenario. The cobblestones peaks were found through a number of pilot tests.

To avoid influencing the strains measured, at the front and rear wheels, with forces occurring from applying loads in the pedals, the subject stopped pedaling just before riding across the wooden lists. The velocity of  $37.3 \pm 1.1$  km/h were chosen, as it was the maximal velocity the subject could achieve within the measuring range of the equipment. Further, the velocity was close to the average velocity used in high level competitive races. The velocity was measured with a bike computer (16.12 STS/CAD, Sigma), by the subject just before riding across the wooden lists.

## 2.5 Laboratory calibrations

Laboratory calibration tests were carried out in order to transform the measured strains, in the three field test

scenarios, into forces. A laboratory calibration test was carried out for the tangential, radial, brake and road irregularity at the front and rear wheel force.

In the laboratory calibration for the tangential and radial force, the crankbox and tooth wheel were fixed so the crankarms were completely horizontal and vertical, respectively. Loads of 0, 1, 2, 3, 4 and 5 kg were applied vertically to the pedals, while corresponding strains were measured, Figure 15 and 16.

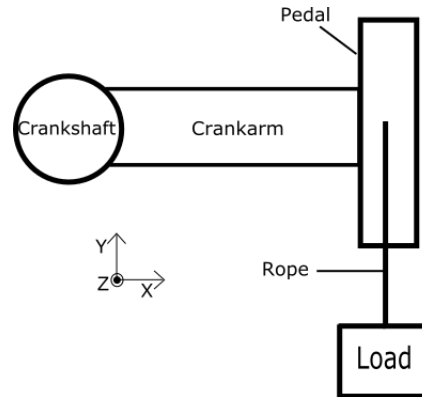


Figure 15: Test setup for the tangential laboratory force calibration.

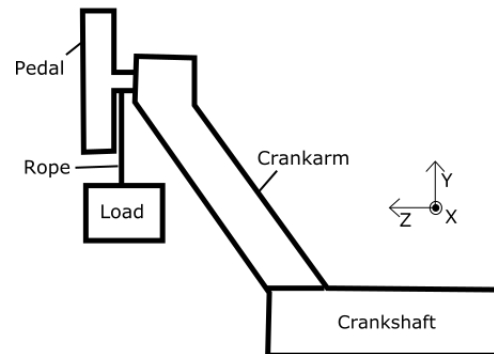
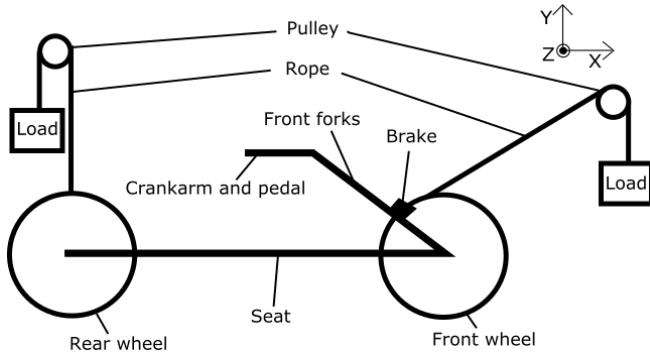


Figure 16: Test setup for the radial laboratory force calibration.

In the laboratory calibration for the brake force, the subject used for the three field test scenarios, was lying still in the handbike and the rotation of the front wheel was fixed, by blocking the brakes using a rope. Loads of 0, 5, 10, 15 and 20 kg were applied tangentially to the wheel, using a rope and a pulley, simulating the rotational force of the wheel, and the corresponding strains were measured, Figure 17.

In the laboratory calibrations for the the road irregularity forces, the subject used for the three field test scenarios, was lying still in the handbike. For both the front and rear wheel calibration the loads were applied vertically in the upward direction, to the wheel through a rope and pulley, Figure 17. Loads of 0, 5, 10, 15 and 20 kg were applied, while the corresponding strains were measured.



**Figure 17:** Test setup for the brake (right part of the handbike) and road irregularity (left part of the handbike) laboratory force calibrations.

Further, a FBD calibration for the road irregularities, at the rear wheel, was carried out, in order to validate the laboratory calibration. This was only done for the rear wheel, as the FBD analysis for this scenario was the easiest to carry out. The calibration was done using beam theory to calculate the total strain of the two applied forces from the spokes to the axle, Figure 14, Eq. 1.

$$\epsilon = \frac{1}{2} \frac{FL_1^3}{3EI} + \frac{1}{2} \frac{FL_2^3}{3EI} \quad (1)$$

Where  $\epsilon$  is strain,  $F$  is force in Newton,  $L$  is length in meters from the forces to the SG, Figure 13,  $E$  is the E-modulus in Pascal found in the tensile test and  $I$  is the moment of inertia for a hollow circular cross section. Calculations were carried out with  $F$  as the only variable. Values of 0 and 100 N was used as force and the corresponding strains was calculated.

## 2.6 Determining the forces

The applied forces and the corresponding strains measured in the laboratory calibration tests, were used for linear regressions, where the data was fitted to have no offset and thereby go through zero. This resulted in a slope for each of the five laboratory calibrations, which could be used in Eq. 2 to estimate the forces from the measured strains in the three field test scenarios.

$$F = slope \cdot \epsilon \quad (2)$$

The forces applied to the handbike, during the three field test scenarios, was estimated by inserting the measured strains from the different scenarios into the respective transformation formula.

## 2.7 FE-model validation

Calibration tests were carried out for the tangential, radial, brake and road irregularities, at the front wheel,

forces in SW, which were compared to the laboratory calibrations. This was done to validate the FE-model of the handbike. The modified crankset of the FE-model, Figure 5, was used to carry out the tangential and radial force calibrations in SW. One linear static study was done for the tangential and radial force, respectively. One study for each force was sufficient, as the strains is linearly correlated to the force applied in a linear static study. For both studies the tooth wheel and crankbox were fixated, and a load of 100 N were applied at the pedal in the tangential and radial direction, respectively, and the corresponding strains, at the SG position, were noted.

The same part of the FE-model used for determining the SG position, Figure 11 and 12, at the front wheel, were used for the SW calibrations of the brake and road irregularity forces. Further, the fixations and loads were applied to the same faces. One linear static study was done for both the brake and road irregularity scenario, by applying a load of 100 N and note the corresponding strains at the position of the SG. Again one study for each force was sufficient, as the strains is linearly correlated to the force applied in a linear static study.

The applied forces and corresponding strains were used for linear regression to find a slope, which could be used to determine the forces in the three field test scenarios, using Eq. 2. This allowed for comparison between the forces calculated with the laboratory and SW calibrations.

## 2.8 Optimization

An initial optimization was conducted in terms of stiffness and energy loss due to deflection. This was done by increasing the stiffness of different parts of the handbike, and investigating the energy loss due to deflection, compared to weight increase. The optimization was conducted on an FE-model of the upper front part of the handbike, Figure 18, where the green and purple arrows illustrates fixations and forces, respectively. The forces used as inputs were the maximal radial force, found in the field test acceleration scenario, and the corresponding tangential force at the same crankarm degree, calculated with the laboratory calibration. The crankarms in the FE-model were set in the same angle, as where the maximal radial force where found. The maximal radial and corresponding tangential forces were applied radially and tangentially to each pedal, respectively. The forces were applied to each pedal, as the acceleration forces found in the field tests were determined for just one pedal.

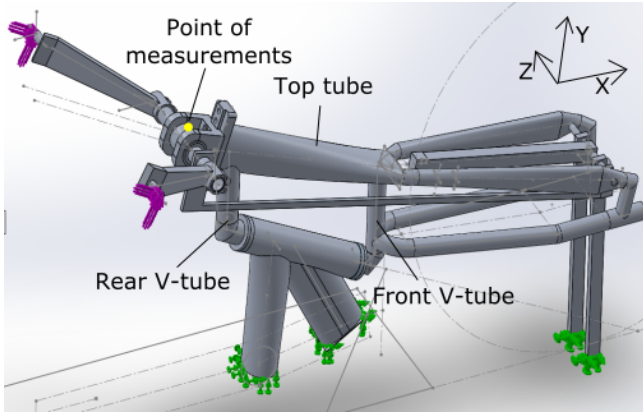


**Figure 18:** FE-model of the upper front part of the handbike used for optimization. Green arrows = fixations and purple arrows = force.

Five linear static studies were conducted, where one geometry was altered for each study, Table 1. The geometries that were altered, were chosen as they were subjected to the largest amounts of von Mises stress. This was because, the parts with highest von Mises stress are the ones causing most deflection. The weight increase, caused by alterations to the geometry, was found using the Mass Properties tool in SW. The deflection was measured on top of the crankbox, illustrated by the yellow dot, Figure 18, on the FE-model. The measured deflection was the total deflection in the X-, Y- and Z-direction, which is calculated with Eq. 3.

$$\text{Total deformation} = \sqrt{\mu_X^2 + \mu_Y^2 + \mu_Z^2} \quad (3)$$

Where  $\mu$  is the deflection in millimeters.

**Table 1:** The changed geometries for the five linear static studies. The highlighted text is the geometry that was altered to the given study. For the V-tubes the dimension 26.9 / 33.7 mm is the outer diameter and 3.2 / 4.0 mm is the wall thickness.

Study	Top tube	Front V-tube	Rear V-tube
1	1.25 shell thickness	26.9 x 3.2 mm	26.9 x 3.2 mm
2	<b>1.50 shell thickness</b>	26.9 x 3.2 mm	26.9 x 3.2 mm
3	<b>2.00 shell thickness</b>	26.9 x 3.2 mm	26.9 x 3.2 mm
4	1.25 shell thickness	<b>33.7 x 4.0 mm</b>	26.9 x 3.2 mm
5	1.25 shell thickness	26.9 x 3.2 mm	<b>33.7 x 4.0 mm</b>

The energy in Joule required to deflect the geometry by a given amount, was found by plotting the deflection to the force applied, and calculating the area under the curve to each of the five linear static studies, Eq. 4.

The energy is considered a 100 percent energy loss, as the deflected geometry is not considered to benefit the rider, in terms of energy return, when the geometry is unloaded.

$$\text{Energy loss}(J) = \frac{F_{total} \cdot \mu_{total}}{2} \quad (4)$$

Where energy loss is in Joule,  $F_{total}$  is the tangential and radial force combined in Newton and  $\mu_{total}$  is deflection in meters, calculated with Eq. 3.

## 3. Results

### 3.1 Tensile test

The stress-strain diagram of the tensile test conducted on the heat treated 7020 aluminum, Figure 19, was used to calculate the E-modulus and yield strength. The E-modulus was 76.2 GPa and the yield strength (0.2% offset) was 303.7 MPa.

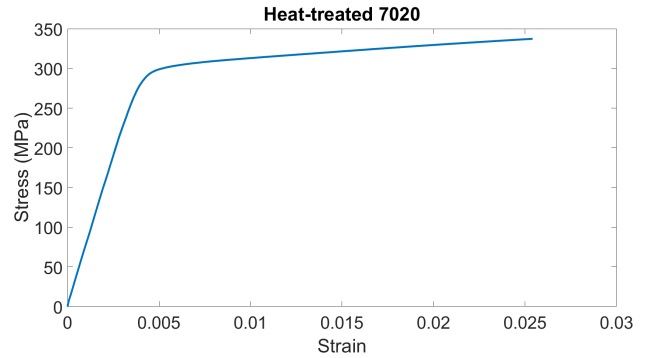


**Figure 19:** Stress-strain diagram for the heat treated 7020 aluminum.

### 3.2 Calibration tests

The transformation formulas of the fitted linear regression from the laboratory and SW/FBD calibrations, which were used to transform the measured micro strains into forces in Newton, are listed in Table 2.

**Table 2:** Transformation formulas, to calculate the forces (N) acting on the handbike, for the laboratory and SW/FBD calibrations.  $\epsilon$  is the measured strain from the three field test scenarios. The transformation formula marked with \* is from FBD and † is from SW.

Force	Transformation formula - Lab	Transformation formula - SW/FBD
Tangential	$F = 0.3963 \cdot \epsilon$	$F = 0.3166 \cdot \epsilon^\dagger$
Radial	$F = -0.4750 \cdot \epsilon$	$F = -0.5181 \cdot \epsilon^\dagger$
Brake	$F = -2.9093 \cdot \epsilon$	$F = -1.4815 \cdot \epsilon^\dagger$
Road irregularities front	$F = 23.2249 \cdot \epsilon$	$F = 1.6260 \cdot \epsilon^\dagger$
Road irregularities rear	$F = -35.1735 \cdot \epsilon$	$F = -32.2069 \cdot \epsilon^*$

### 3.3 Forces and FE-model validation

#### 3.3.1 Tangential force

The mean  $\pm$  standard deviation of the tangential force peak of the five field test trials, calculated with the laboratory and SW calibrations, were  $392.7 \pm 9.5$  N and  $313.7 \pm 7.6$  N, respectively. The maximal tangential force were found in trial 5, Figure 20, and were for the laboratory and SW calibrations  $407.6$  N and  $325.5$  N, respectively. The maximal tangential force, in trial 5, was found 28.8 degrees after starting position. The corresponding radial force at 28.8 degrees was  $236.8$  and  $258.3$  N for the laboratory and SW calibrations, respectively. The average tangential forces calculated with the laboratory calibration are 25.2 percent higher, than the forces calculated with the SW calibration.

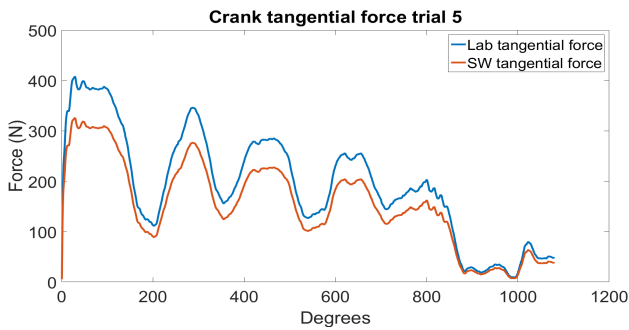


Figure 20: Calculated tangential force applied to the handbike in trial 5 for the laboratory and SW calibrations.

#### 3.3.2 Radial force

The mean  $\pm$  standard deviation of the radial force peak of the five field test trials, calculated with the laboratory and SW calibrations, were  $344.7 \pm 28.3$  N and  $376.1 \pm 30.9$  N, respectively. The maximal radial force were found in trial 5, Figure 21, and were for the laboratory and SW calibrations  $380.0$  N and  $414.6$  N, respectively. The maximal radial force, in trial 5, was found 12.2 degrees after starting position. The corresponding tangential force at 12.2 degrees was  $338.6$  and  $270.5$  N for the laboratory and SW calibrations, respectively. The average radial forces calculated with the laboratory calibration are 8.4 percent lower, than the forces calculated with the SW calibration.

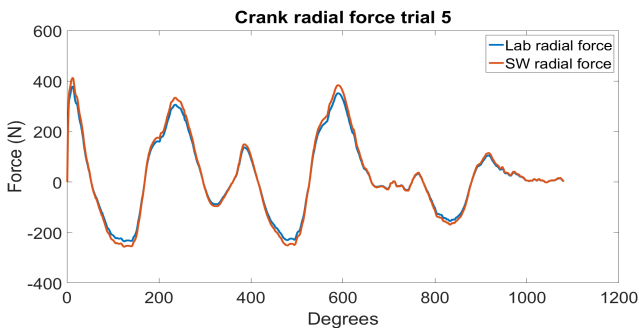


Figure 21: Calculated radial force applied to the handbike in trial 5 for the laboratory and SW calibrations.

#### 3.3.3 Brake force

The mean  $\pm$  standard deviation of the brake force peak of the five field test trials, calculated with the laboratory and SW calibrations, were  $1275.0 \pm 306.7$  N and  $649.2 \pm 156.2$  N, respectively. The maximal brake force were found in trial 1, Figure 22, and were for the laboratory and SW calibrations  $1571.1$  N and  $800.0$  N, respectively. The average brake forces calculated with the laboratory calibration are 96.4 percent higher, than the forces calculated with the SW calibration.

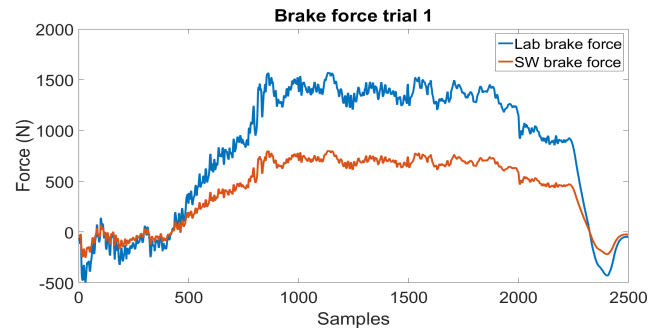


Figure 22: Calculated brake force applied to the handbike in trial 1 for the laboratory and SW calibrations.

#### 3.3.4 Road irregularities at the front wheel

The mean  $\pm$  standard deviation of the road irregularity force peak, at the front wheel, of the five field test trials, calculated with the laboratory and SW calibrations, were  $11807.8 \pm 713.6$  N and  $826.7 \pm 50.0$  N, respectively. The maximal road irregularity force, at the front wheel, were found in trial 1, Figure 23, and were for the laboratory and SW calibrations  $12952.4$  N and  $906.8$  N, respectively. The average road irregularity forces, at the front wheel, calculated with the laboratory calibration are 1328.3 percent higher, than the forces calculated with the SW calibration.

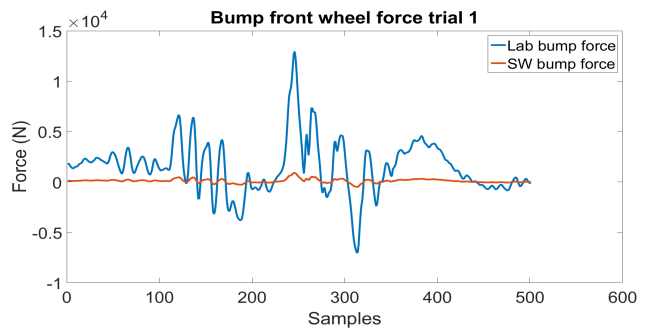
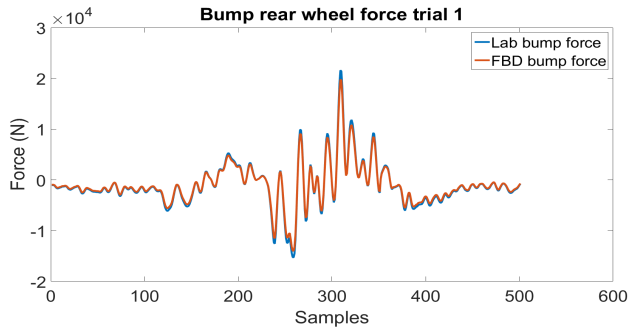


Figure 23: Calculated road irregularity force applied to the handbike, at the front wheel, in trial 1 for the laboratory and SW calibrations.

#### 3.3.5 Road irregularities at the rear wheel

The mean  $\pm$  standard deviation of the road irregularity force peak, at the rear wheel, of the five field test trials, calculated with the laboratory and FBD calibrations, were  $19770.4 \pm 1667.2$  N and  $18103.0 \pm 1526.6$  N, re-

spectively. The maximal road irregularity force, at the rear wheel, were found in trial 1, Figure 24, and were for the laboratory and FBD calibrations 21586.7 N and 20011.4 N, respectively. The average road irregularity forces, at the rear wheel, calculated with the laboratory calibration are 9.2 percent higher than, the forces calculated with the FBD calibration.



**Figure 24:** Calculated road irregularity force applied to the handbike, at the rear wheel, in trial 1 for the laboratory and SW calibrations.

### 3.4 Optimization

A maximal displacement of 0.899 mm was found in study 1, where no geometry changes were made, Table 3. This also had the highest energy loss of 0.579 J. The lowest displacement and energy loss was found in study 4, where the front V-tube was altered, with 0.494 mm and 0.318 J, respectively. Study 4 also had the highest energy saved per kg weight increase ratio.

## 4. Discussion

### 4.1 Forces acting on the handbike

A total force of 718.6 N (tangential+radial) was applied to the pedals, with the crankarms at 12.2 degrees after starting position, calculated with the laboratory calibrations in this study, Figure 21. To the authors knowledge no studies have determined the forces applied to a handbike during acceleration. However, if the total force is compared to the acceleration of a standard bicycle, it is about half the size (Soden, Millar et al. 1986), which was expected, as the lower extremities are stronger than the upper extremities (Izquierdo,

Häkkinen et al. 2002). The total force was found in the push phase of the pedal cycle. The movement in the push phase is similar to the movement in a standard bench-press exercise, and would correspond to a maximum applied force of approximately 140 kg to the bench-press rod. The subject's maximal bench-press strength was around 140-145 kg at the time the acceleration study was conducted, which was close to the forces found when accelerating. It is unlikely that the subject can apply the same amount of force to the pedals in an acceleration study, compared to a controlled maximal test in bench-press, indicating that the acceleration forces are slightly overestimated. However, joint angles in the acceleration scenario and bench-press exercise are different, making it not fully comparable.

The laboratory calibration resulted in an R-square value of 1 and 0.9998, Table 2, for the tangential and radial force, respectively. However, the laboratory calibration was conducted while only measuring the strains on the crankshaft for the tangential force, and on the crankarm for the radial force at a time, respectively. Additional laboratory calibrations should be done while measuring strains both on the crankshaft and crankarm simultaneously, while applying a tangential or radial force. This would reveal if the SG on the crankarm would pick up strains caused by the tangential force, and vice versa, which could lead to an overestimation of the forces.

In this study a maximal braking force of 1571.1 N was found, calculated with the laboratory calibration, Figure 22, which is about twice as high, compared to braking forces reported in studies on bicycles (800 N)(Maestrelli, Falsini 2008, Covill, Begg et al. 2014). Therefore, it seems that an upper limit for braking force have been found. Strains caused by pedaling and road irregularities could also be picked up by the SG as brake force. However, the field test was conducted on leveled tarmac and no pedaling was done while braking, why these factors can be assumed low. Further, as the laboratory calibration for the brake force had an R-square value of 0.9719, Table 2, the brake force in this study is considered valid and reliable.

**Table 3:** Displacement, energy loss, weight increase and energy saved per kg weight increase of the five linear static studies of the optimization.

Study	Displacement	Energy loss	Weight increase	Energy saved per kg weight increase
1	0.899 mm	0.579 J	0 g	0 J/kg
2	0.843 mm	0.543 J	35.8 g	1.01 J/kg
3	0.751 mm	0.484 J	107.2 g	0.89 J/kg
4	0.494 mm	0.318 J	51.6 g	5.06 J/kg
5	0.671 mm	0.432 J	47.9 g	3.07 J/kg

The maximal forces caused by road irregularities calculated with the laboratory calibrations in this study were 12952.4 N and 21586.7 N, for the front and rear wheel respectively, Figure 23 and 24. When compared to another study, which found values of 2210 N and 3683 N at the front and rear hubs, respectively (DeLorenzo, Hull 1999), during off-road bicycling, the road irregularity forces in the present study are high. However, the study by DeLorenzo and Hull used lower speeds (24-32 km/h), had a different type of bicycle, an average rider weight of 75 kg and rode across different types of bumps, making the study not fully comparable. However, the maximal forces for the rear wheels in this study were 21586.7 N for each wheel, which are much higher than the 3683 N. Therefore, the road irregularity forces in this study are considered too high and not valid.

For the brake and road irregularity calibration the subject was lying in the handbike, which could result in imprecise results, if the subject slightly moved in between the readings, while more load was applied to the handbike. To avoid this, weights could have been placed in the seat instead of the subject. However, this would result in a mismatch between the calibration tests and the test scenarios. In addition the squared R-values found were close to 1, Table 2, making the calibrations tests reliable, which is backed up by the corresponding FBD calibration, at the rear wheel. A mismatch between the laboratory and FBD calibrations, and the field test, could be a reasonable explanation for the high force values. For the calibrations only one force was applied at the wheel, while the subject was lying still. In the field test the subject bounced up and down in the seat, and thereby applying more force to the seat than in the calibration, which caused strains the SG could pick up. Further, forces caused by road irregularities in the field test were applied to both rear wheels, creating additional strains at the opposite wheel, which the SG might have picked up.

#### 4.2 Tensile test

For the tensile test only one specimen was tested. It would have been desirable to have carried out the tensile test for more specimens and calculated the mean E-modulus and yield strength to be certain that the results were correct. However, the E-modulus of 76.2 GPa and yield strength of 303.7 MPa found in the tensile test corresponded well to the literature (Dudzik 2011, Norton 2006). Therefore the use of the results, as input for the FE-model gives a more valid output of the simulations than if one of the standard aluminum alloys in SolidWorks had been used.

#### 4.3 FE-model validation

The acceleration forces calculated with the laboratory and SW calibrations corresponded, with a maximal tangential and radial force of 25.2 percent higher and 8.4 percent lower, respectively, for the laboratory calibration compared to the SW calibration. The difference is likely due to geometric difference between the real crankarm and crankshaft, and the FE-model. This is especially likely for the crankarm, as it is manufactured by rolling an aluminum tube, which gives it a complex geometry, making it hard to measure and create accurately as a FE-model. As the SG measuring the radial force was positioned on the surface of the crankarm, any potential difference of the geometry could result in the difference between the two calibration types. To see how sensitive the SG was to geometry changes, an estimated calculation was done for a hollow eclipse, which represented the crankarm geometry. This was done by making the width and height of eclipse five percent wider and narrower, respectively, and comparing it to its original dimensions. This resulted in a force difference of approximately 10 percent, which could explain the difference found between the laboratory and SW calibrations. In respect to the tangential force the SG was positioned on the surface of a hollow tube, which is easy to measure and create as a FE-model. Because of this it was surprising there was a 25.2 percent difference in maximal force between the calibration types. As the laboratory calibration for the tangential force resulted in a R-square value of 1, Table 2, the laboratory calibration is reliable, and is therefore not considered the reason for the difference found. The difference must be assigned to a mismatch in constraints between the laboratory and SW calibrations.

The maximal brake force was 96.4 percent higher, when calculated with the laboratory calibration, compared to the SW calibration. As the maximal brake force was higher for the laboratory calibration, it means that to a given brake force, more strain was measured at the SG position on the FE-model, than on the handbike. As simplifications was made, at the connection between the top tube and upper front forks, less force might have been transferred to the top tube, which would result in more force at the upper front forks. The laboratory calibration design was considered valid in order to only determine the brake force, and as the R-square value was 0.9719, Table 2, it is also considered reliable. Because of this the laboratory calibration is not considered the reason for the difference in maximal force. To get better results, a more accurate FE-model, at and around the brake pads, are therefore suggested being the best solution.

The road irregularity force, at the front wheel, was 1328.3 percent higher, when calculated with the laboratory calibration, compared to the SW calibration. As

the difference was so big, some important factor must have been wrong. In this scenario the force had to go through the most complex geometry before reaching the SG position, why the largest differences was expected for this scenario. Like at the brake force, a reason for the difference might be because less force is transferred to other geometries, i.e. the lower front forks. Another explanation could be that the fixations are too close to where the force is applied, and where the SG is positioned. Both contributions are however unknown, and further work for this scenario is required.

#### 4.4 Test protocol

The choice of using a subject with no experience in handbiking, was because all trials were less than 30 seconds of riding, where fatigue was not an issue. Further, the push and pull phase in the pedal cycle could be compared to weightlifting scenarios, in which the subject was trained. Because of this, the choice of subject was considered adequate. However, to precisely quantify the acceleration forces in handbiking, several competitive handbike riders should be tested.

The choice of riding the handbike at close to 40 km/h, was due to this being an average velocity at high level competitions, as well as the upper limit the subject could accelerate the handbike up to within the measuring range of the equipment. More extreme scenarios can always be thought of, however the velocity in this study is still considered high enough, as more extreme scenarios is taken into account by designing a handbike with a factor of safety.

#### 4.5 Optimization

With a total force of 718.6 N (tangential + radial) applied to each pedal, the lowest deflection and energy loss was 0.494 mm and 0.318 J, respectively, found in study 4, where the front V-tube was altered to have a larger diameter and wall thickness. This deflection and energy loss was close to half of the deflection and energy loss of study 1. When looking at the energy loss to weight increase ratio, Table 3, study 4 also had the highest ratio, making it the most beneficial structure to optimize, compared to the top tube and rear V-tube.

An energy loss of 0.579 J was found in study 1, which is the energy loss for just the push phase, in one pedal cycle. Energy loss would also be present in the pull phase, how much is however not tested. A rough assumption could be that the same amount of deflection would also occur in the pull phase of the pedal cycle, and that the rider applies the same amount of force, as the maximal force found in this study during a whole sprint. If that was the case the effect lost due to deflection would be 1.93 W and 1.06 W, for study 1 and 4, respectively, calculated with a cadence of 100 rpm.

Of course the extra weight would also result in a necessary increase in effort to maintain the same velocity, depending on the amount of vertical meters the rider would have to climb, making it a tradeoff between weight and stiffness of the frame. If a rider climbs 500 vertical meters in an hour, the extra weight of 51.6 g of the front V-tube would result in an average increased effort of 0.07 W spent on climbing. The rough calculations show that it would be beneficial to increase the dimensions of the front V-tube.

As this is just an initial optimization study, more work would be required in order to include factors like strength and more complex geometry changes. Further, this optimization study only focused on the acceleration forces on the upper front part of the handbike. More work incorporating brake and road irregularity forces on the whole handbike, should be done in order to optimize the frame stiffness, of different parts on the handbike.

### 5. Conclusion

A total acceleration force of 718.6 N (tangential+radial) was found in this study calculated with the laboratory calibration. This force is considered slightly overestimated and further validation is necessary. A maximal brake force of 1571.1 N was found, calculated with the laboratory calibration, which is considered valid, as no other factors were thought to influence the brake force measurement. Road irregularity forces of 12952.4 N and 21586.7 N, at the front and rear wheel, respectively, was found calculated with the laboratory calibration. However, the forces are not considered valid, as they are much higher compared to other studies conducted on standard bicycles.

The forces calculated with the FE-model calibrations did not correspond to the forces calculated with the laboratory calibrations. The smallest difference was found at the acceleration scenario, with a 25.2 and 8.4 percent difference for the tangential and radial force, respectively. For the brake and road irregularity forces, at the front wheel, the differences was 96.4 and 1328.3 percent, respectively. As disagreement between the results of the FE-model and laboratory calibration were present, the FE-model cannot be fully trusted for FEA, especially in regard to brake and road irregularity forces.

The initial optimization study revealed that the highest stiffness by least weight increase was obtained by thickening the frontal V-tube.

### Acknowledgement

The authors would like to thank Wolturnus A/S for supplying the handbike and the SolidWorks CAD-model used in this study.

---

## 6. References

1. ASTM E8 / E8M-15A, 2015. Standard Test Methods for Tension Testing of Metallic Materials. West Conshohocken: ASTM International.
2. CALFEEDDESIGN.COM, , Calfeedesign.com. Available: <http://calfeedesign.com/tech-papers/technical-white-paper/> [5/23, 2016].
3. COVILL, D., BEGG, S., ELTON, E., MILNE, M., MORRIS, R. and KATZ, T., 2014. Parametric Finite Element Analysis of Bicycle Frame Geometries. *Procedia Engineering*, 72, pp. 441-446.
4. DALLMEIJER, A.J., ZENTGRAAFF, I.D., ZIJP, N.I. and VAN DER WOUDE, L.H., 2004. Sub-maximal physical strain and peak performance in handcycling versus handrim wheelchair propulsion. *Spinal cord*, 42(2), pp. 91-98.
5. DELORENZO, D.S. and HULL, M.L., 1999. Structural Loading and Fatigue Failure Analysis of Off-Road Bicycle Components. *Fatigue and Fracture Mechanics: 29th Volume*. ASTM International, .
6. DUDZIK, K., 2011. Mechanical properties of 5083, 5059 and 7020 aluminium alloys and their joints welded by MIG. *Journal of KONES*, 18, pp. 73-77.
7. GERE, J.M. and GOODNO, B.J., 2013. 5. STRESSES IN BEAMS. *Mechanics of Materials*. Eighth edn. Stamford: Cengage Learning.
8. HETTINGA, F.J., VALENT, L., GROEN, W., VAN DRONGELEN, S., DE GROOT, S. and VAN DER WOUDE, L.H., 2010. Hand-cycling: an active form of wheeled mobility, recreation, and sports. *Physical Medicine and Rehabilitation Clinics of North America*, 21(1), pp. 127-140.
9. IZQUIERDO, M., HÄKKINEN, K., GONZALEZ-BADILLO, J.J., IBANEZ, J. and GOROSTIAGA, E.M., 2002. Effects of long-term training specificity on maximal strength and power of the upper and lower extremities in athletes from different sports. *European journal of applied physiology*, 87(3), pp. 264-271.
10. LE PINE, J., CHAMPOUX, Y. and DROUET, J., 2015. The relative contribution of road bicycle components on vibration induced to the cyclist. *Sports Engineering*, 18(2), pp. 79-91.
11. MAESTRELLI, L. and FALSINI, A., 2008. Bicycle frame optimization by means of an advanced Gradient Method Algorithm.
12. NORTON, R.L., 2006. Appendix A. Machine Design, An Integrated Approach. Third edn. London: Pearson Education, Inc.
13. OMEGA.COM, , Positioning Strain Gages to Monitor Bending, Axial, Shear, and Torsional Loads. Available: <http://www.omega.com/faq/pressure/pdf/positioning.pdf> [5/23, 2016].
14. SODEN, P., MILLAR, M., ADEYEFA, B. and WONG, Y., 1986. Loads, stresses, and deflections in bicycle frames. *The Journal of Strain Analysis for Engineering Design*, 21(4), pp. 185-195.
15. SPERLICH, B., KLEINOEDER, H., DE MARÉES, M., QUARZ, D., LINVILLE, J., HAEGELE, M. and MESTER, J., 2009. Physiological and perceptual responses of adding vibration to cycling. *Journal of Exercise Physiology online*, 12, pp. 40-46.
16. VANWALLEGHEM, J., 2009. Study of the damping and vibration behaviour of flax-carbon composite bicycle racing frames. Master's Thesis, Ghent University, 2010.
17. WILSON, D.G., 2004. *Bicycling Science*. Third edn. Cambridge: MIT Press.

# Workpapers

# Contents

1. Method .....	4
1.1 Tensile test.....	4
1.1.1 Tensile test protocol .....	4
1.1.2 Finding the E-modulus and yield strength.....	5
1.1.3 Tensile test results.....	6
1.2 Modifications of the CAD-model .....	7
1.2.1 Crankset.....	8
1.2.2 Front part.....	8
1.3 Determining strain gauge position .....	9
1.3.1 Rear wheel.....	9
1.3.2 Crank.....	12
1.3.3 Brake and road irregularities .....	14
1.4 Laboratory calibration .....	16
1.4.1 Overall laboratory calibration test protocol.....	16
1.4.2 Rear wheel.....	16
1.4.3 Tangential and radial force.....	18
1.4.4 Brake and road irregularities .....	20
1.5 Test protocol.....	21
1.5.1 Measurement equipment and calculations .....	21
1.5.2 Test procedure.....	22
1.6 FE-model validation .....	24
1.7 Optimization .....	26
1.8 Initial process of this study .....	27
2. References .....	28
3. Appendix.....	29
3.1 Protocol for attaching the strain gauges .....	29
3.2 Wiring diagrams for attached strain gauges .....	30
3.3 Technical drawing.....	31
3.4 Initial plan of SG position and force determination .....	32
3.4.1 Crank.....	32
3.4.2 Front wheel.....	34
3.5 Force data plots .....	39
3.6 MatLab script.....	42

3.6.1 Tensile Test .....	42
3.6.2 Calibrations and force determination .....	46
3.6.3 Optimization .....	60

# 1. Method

## 1.1 Tensile test

In order to determine the yield strength and modulus of elasticity of the 7020 aluminum used to manufacture the frames of the handbike, tensile tests were conducted. This was done, as the aluminum used for the handbike frames are heat-treated (HT), which changes the properties of the aluminum. This changes the standard values listed from the manufacturer of the specific type of aluminum, which gives wrong inputs to the FE model, causing imprecise outputs. Other types of aluminum both HT and non-treated (NT) were desired tested, in order to see if other aluminum types behaved better in terms of yield strength and modulus of elasticity than the material used to manufacture the handbike. However, just one other material was tested, which did not benefit from HT, due to limitations in manufacturing the test specimens.

To make the tension tests two types of aluminum sheets were acquired: 7020 aluminum with 6 mm thickness and 5005 with 3 mm thickness. The 5005 was tested NT, while the 7020 was tested both as NT and HT.

A drawing of the specimen were made in SolidWorks with the desired dimensions according to the standard ASTM E8/E8M - Standard Test Methods for Tension Testing of Metallic Materials. The technical drawing of the test specimens, Appendix 2.3, were send to the workshop at Aalborg University, where they were manufactured.

### 1.1.1 Tensile test protocol

The test protocol is written in accordance with the standard ASTM E8/E8M. The speed of the Zwick tensile tester up to yield point was found by multiplying 0.015 mm/min with the reduced section of the specimen (82.15 mm), giving a speed of 1.23 mm/min. After yield point a speed of 32.86 mm/min was used, found by multiplying 0.4 mm/min with the reduced section of the specimen (82.15 mm). The elongation of the specimens were measured using an attached extensometer.

#### **Materials and equipment**

- One specimen of type 7020 aluminum
- One specimen of type 7020 aluminum – heat-treated
- Four specimens of type 5005 aluminum
- Zwick tensile tester
- Extensometer
- Two specimen grips

## Test procedure

Test procedure step by step for each specimen. The first two specimens of type 5005 aluminum (non-treated) functions as pilot-tests to make sure everything works as desired.

1. Mount the specimen grips in the Zwick tensile tester
2. Warm up the test machine
3. Measure dimensions of the test specimen
4. Mark the gage length of the test specimen
5. Mount the test specimen in the Zwick tensile tester
6. Zero the test machine
7. Setup the Zwick tensile tester with inputs of the dimensions of the specimens
8. Setup the Zwick tensile tester to have a speed of 1.23 mm/min up to yield point and a speed of 32.86 mm/min after yield point
9. Attach the extensometer
10. Elongate the specimen up to yield point
11. Remove the extensometer
12. Elongate the specimen until fracture
13. Remove the test specimen and save the data
14. Repeat steps 3-12 for the remaining specimens

### 1.1.2 Finding the E-modulus and yield strength

In order to find the E-modules of the tested specimens, the elongation and equivalent force measured in the tensile test is needed. The elongation is used to calculate the strain with equation (1).

$$\varepsilon = \frac{\delta}{L} \quad (1)$$

Where  $\varepsilon$  is strain,  $\delta$  is elongation measured and  $L$  is the gage length of the extensometer (20mm). The measured force is used to calculate the stress. Stress is the applied force over area, and as the cross sectional area of the test specimens are known it is possible to calculate the stress with equation (2).

$$\sigma = \frac{F}{A} \quad (2)$$

Where  $\sigma$  is the stress,  $F$  is the force in Newton and  $A$  is the cross sectional area in  $\text{m}^2$ . Now it is possible to make the stress-strain diagram, Figure 1. When the stress-strain diagram visually is examined a linear and curved part is seen. The linear part is, where the E-modulus is found, which is the slope of this part and it is

an expression for the stiffness of the material. Where the graph changes from linear to curved is where the material starts to yield and is where the yield strength can be found.

To find the slope and thereby the E-modulus the correlation between stress and strain is used, equation (3).

$$E = \frac{\sigma}{\varepsilon} \quad (3)$$

Where  $E$  is the E-modulus and can be found by linear regression of the data points of the linear part of the diagram.

Now the yield strength can be determined, according to the standard ASTM E8/E8M, by drawing a line with a slope equal to the E-modulus with an offset of 0.2 percent. The yield strength is where the offset line and stress-strain curve intersect.

### 1.1.3 Tensile test results

The stress-strain diagram with the 0.2 percent offset line for all materials is shown on Figure 1. NT 5005 was tested twice, as two specimens were left after the pilot tests. An error occurred half way through the test of the NT 7020 but it was still possible to determine the E-modulus, as data for the linear part was collected. However the yield strength could not be determined.

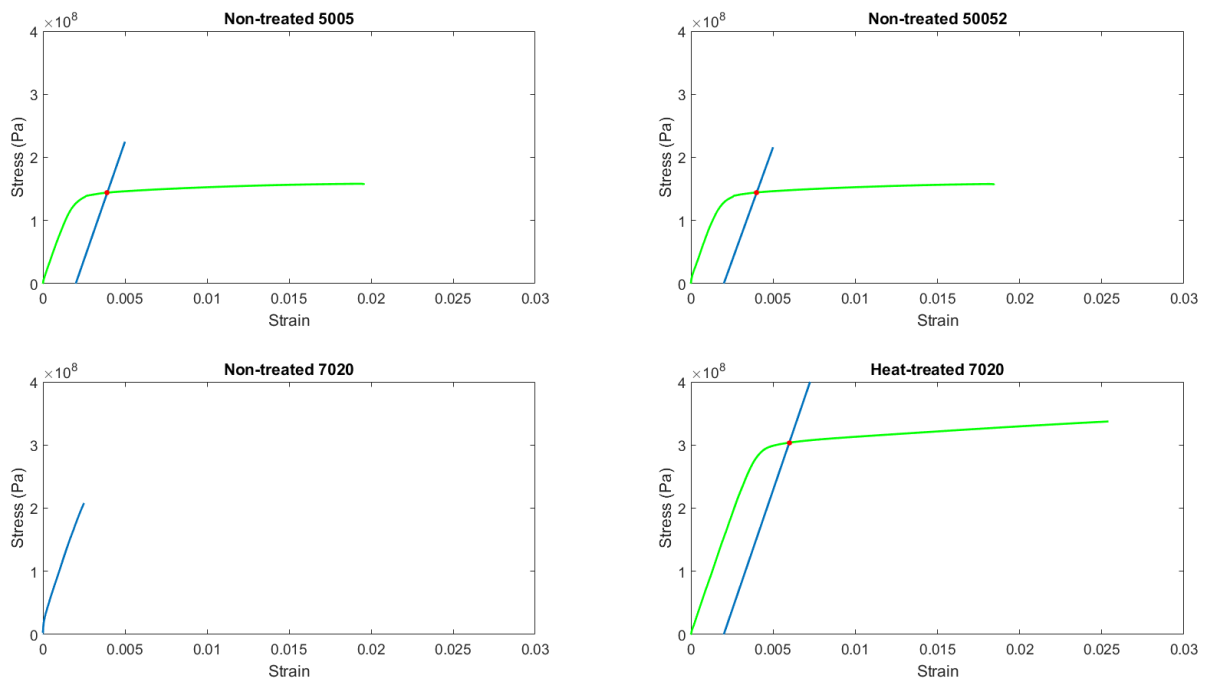


Figure 1 – Stress-strain diagrams with the 0.2 percent offset line for the tensile tests.

To determine the E-modulus for the tensile test the curve fitting tool in Matlab was used to carry out the linear regression. Figure 2 show the selected data and the fitted curved. The fitted curve represent the data precisely, as the R-square value is close to 1 for all plots.

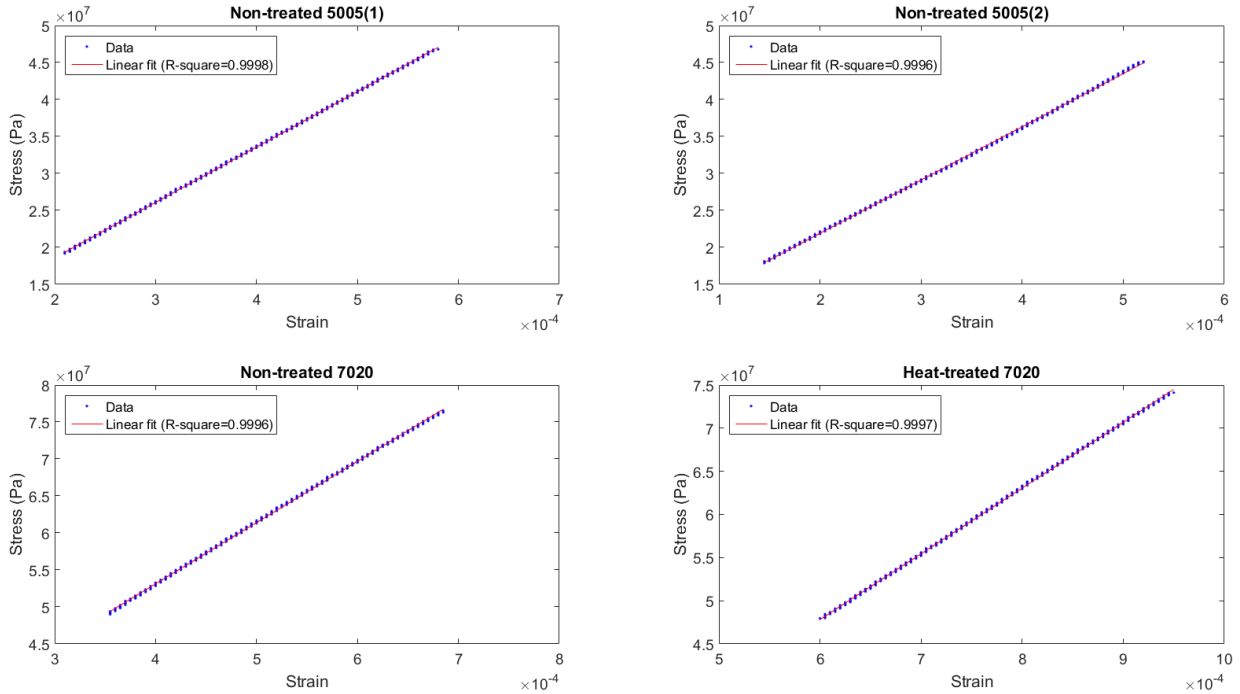


Figure 2 – Regression plots of the selected data used to find the E-modulus.

The E-modulus and yield strength are generally higher for 7020 than 5005 aluminum, Table 1. The NT 7020 has a higher E-modulus than the HT 7020, which was unexpected, as the heat treatment should make the material stiffer.

Table 1 – E-modulus and yield strength of the materials.

Material	NT 5005(1)	NT 5005(2)	NT 7020	HT 7020
E-modulus	74.9 GPa	72.0 GPa	82.8 GPa	76.2 GPa
Yield strength	144.1 MPa	144.4 MPa	Unknown	303.7 MPa

### 1.2 Modifications of the CAD-model

Wolturnus A/S supplied a SolidWorks made CAD-model of the handbike. However, this was only used for technical drawings and not simulations, why modifications and repairs of the CAD-model was required in order to run simulations.

The dimensioning of the CAD-model did not correspond to the dimensions of the handbike, as the CAD-model was a model of the overall design and not the exact handbike acquired. Therefore length

measurements were made on the real handbike and the dimensions of the CAD-model were corrected. In order to use the CAD-model to run a simulation study, repairs and simplifications had to be made, as several components interfered or were not properly connected. The dimensions of the components, which interfered was repaired, thus making the dimensions of the different components fit each other. Simplifications were made for the crank set, wheels, brake pads, connection parts at the head tube and the front forks connection with the axle of the front wheel. In addition a 7050 aluminum from the SW repository was altered, with the E-modulus and yield strength values found in the tensile test, and applied to the model.

### 1.2.1 Crankset

The crankset consisted of many small components, which interfered with each other, which was not easily repaired and the fastening of the crankbox did not correspond between the real handbike and the CAD-model. The actual fastening structure was acquired and applied to the model. Further, a simplified crankset, consisting of a crankshaft, crankbox and pedals were made instead, Figure 3. Furthermore the tooth wheel and the chain were simplified, as a square and a long thin beam, respectively.

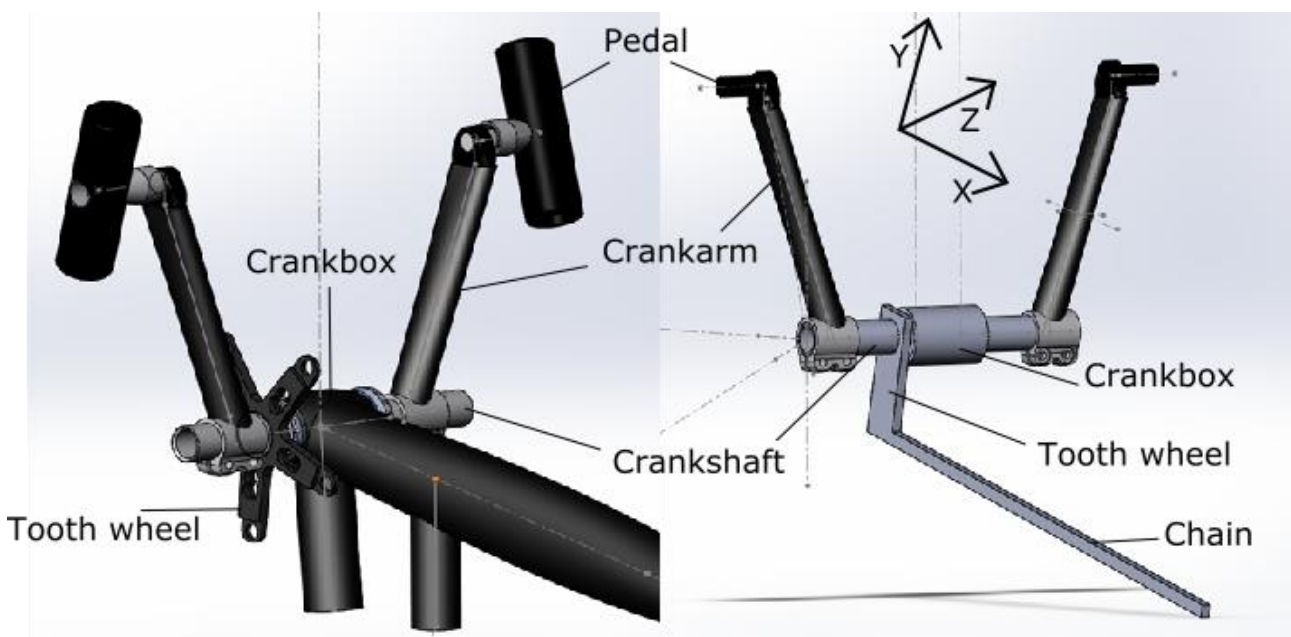


Figure 3 - CAD-models of the original (left) and new (right) crank set.

### 1.2.2 Front part

In order to minimize calculation time of the simulations, the wheels were simplified, Figure 4, as they are complex structures, which takes a lot of calculating power. A simple circular rod was used, as the axle instead of the more complex geometry seen on the real handbike. The wheel and tire itself was simplified, as a beam attached to the axle. The middle beam was attached to the oval top tube, by a rod, which represented the brake pads.

Modifications were also made to the upper and lower front forks at the connection to the axle. The original parts between the upper and lower front forks and the axle were replaced by a geometry that allowed load transfer between the parts. Further, modifications at the ends of the head tube were made. The original parts were replaced with tubes, which allowed for a load transfer between the structures, as they were not connected in the original model.

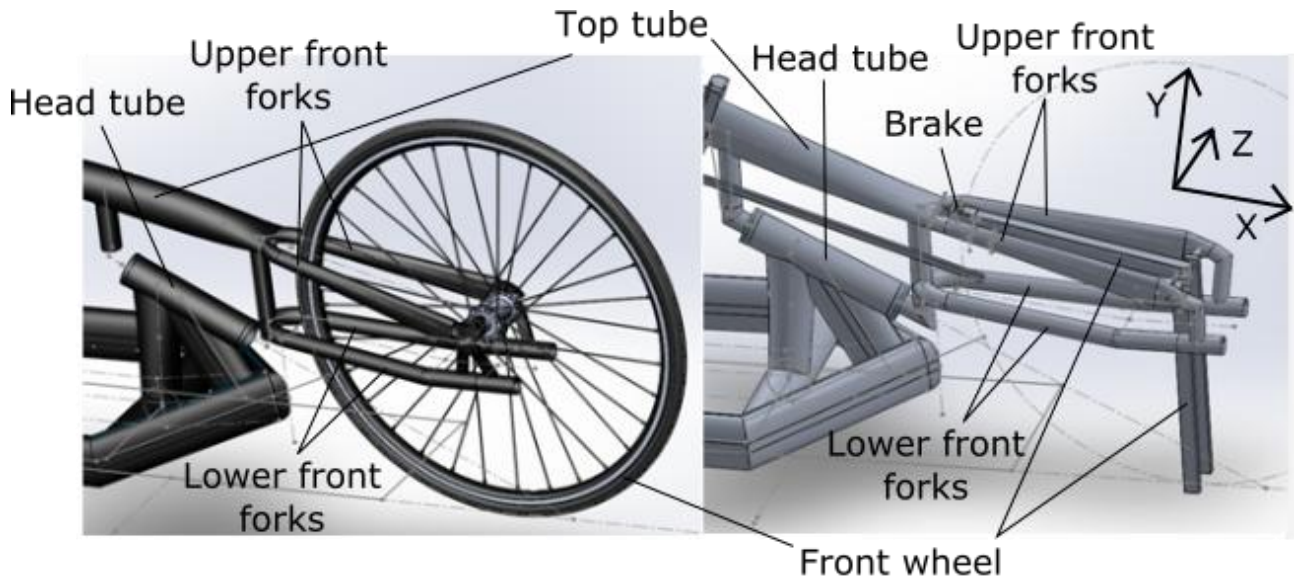


Figure 4 - Front part of the handbike before (left) and after (right) modifications.

### 1.3 Determining strain gauge position

#### 1.3.1 Rear wheel

In order to determine the SG position and the forces applied to the rear wheels, caused by road irregularities, a Free Body Diagram (FBD) analysis was conducted.

It was assumed that the forces acting on the rear wheels were the same on both wheels. Furthermore it was assumed that the forces transferred from the spokes to the axle, could be split into two equally big forces, as the spokes are attached to the axel two places. First the scenario is sketched, Figure 5.

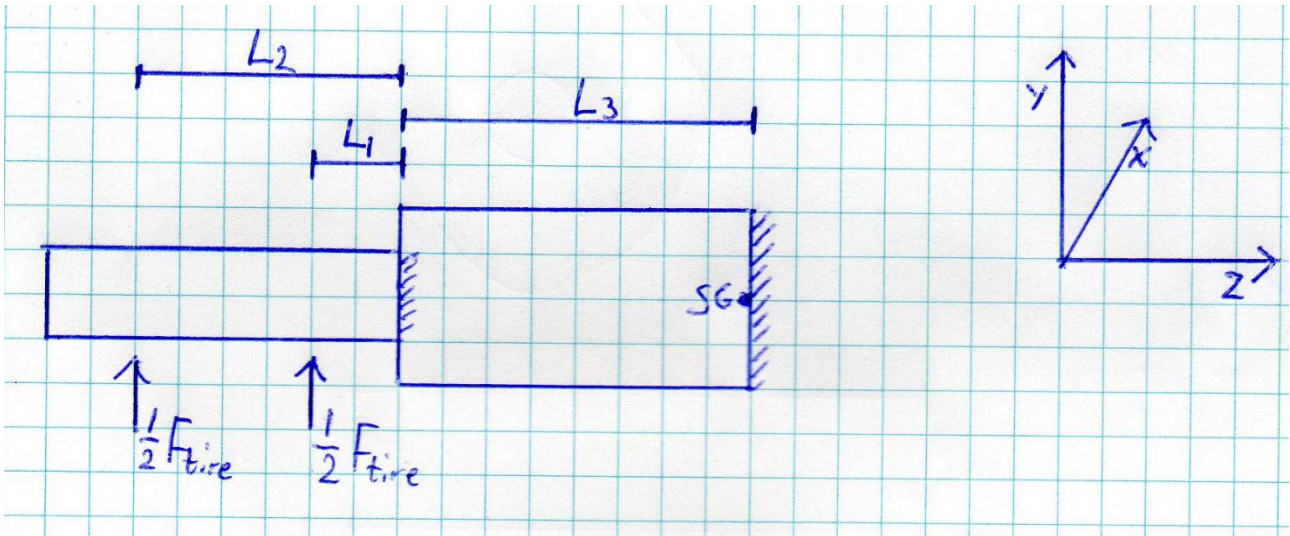


Figure 5 – Sketch of the rear wheel scenario.

$L_1$  and  $L_2$  are the two lengths to the forces applied to the axel from the road irregularities and  $L_3$  is the length from the fixation point of the axel on the tube to the point SG. A FBD, Figure 6, were made for the scenario where the forces in the X- and Z-directions were assumed to be zero, when the handbike is ridden with constant velocity and as the angle of the wheel is 90 degrees to the axel, respectively. Therefore the equilibrium is set up for the forces in the Y-direction and for the moment in point (a), where the axle is fixed with the tube.

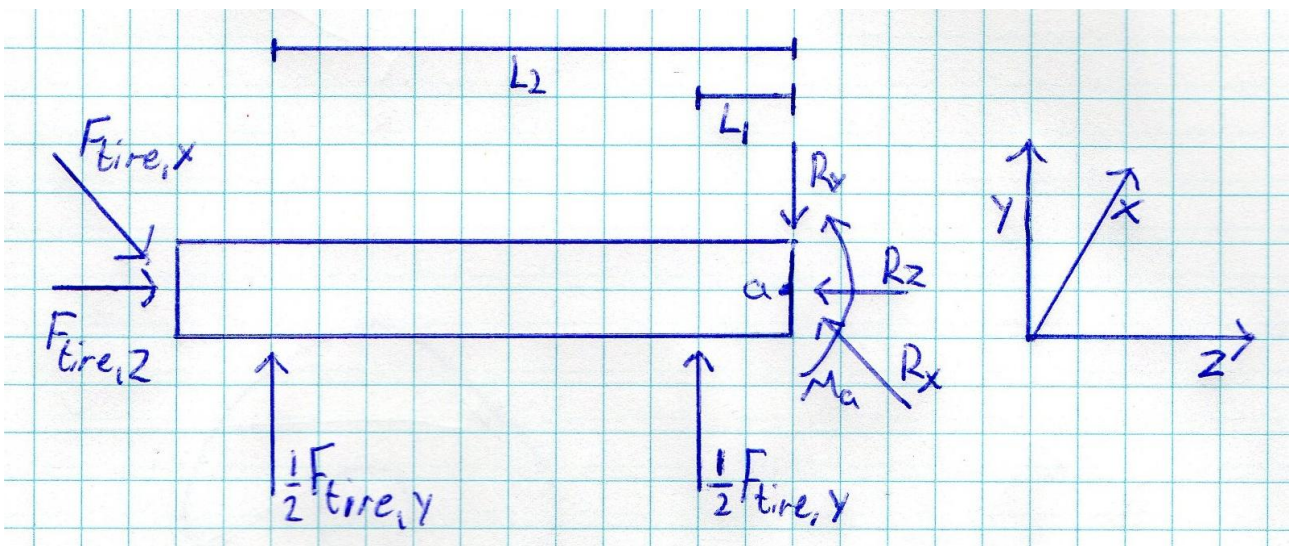


Figure 6 – FBD of the axel at the rear wheels.

$$\sum F_y = \frac{1}{2}F_{tire} + \frac{1}{2}F_{tire} - R_y = 0 \leftrightarrow \frac{1}{2}F_{tire} + \frac{1}{2}F_{tire} = R_y$$

$$\sum M_a = \frac{1}{2}F_{tire,y}L_2 + \frac{1}{2}F_{tire,y}L_1 - M_a = 0 \leftrightarrow M_a = \frac{1}{2}F_{tire,y}L_2 + \frac{1}{2}F_{tire,y}L_1$$

As it is not possible to measure the strain on the axle, due to the lack of space, the strain will be measured at the tube, which has another dimension than the axle, therefore a FBD was drawn for the tube, Figure 7. All the force is transferred to the tube, as the axle is fixed onto the tube and the structure does not yield. The forces in the X- and Z-directions were already set to be zero at the axle, so only the forces in the Y-direction was looked upon. The moment  $M_a$  is transferred to the tube. A FBD was drawn for the tube and the equilibrium equations were set up, where the moment equilibrium equation was taken in point (SG).

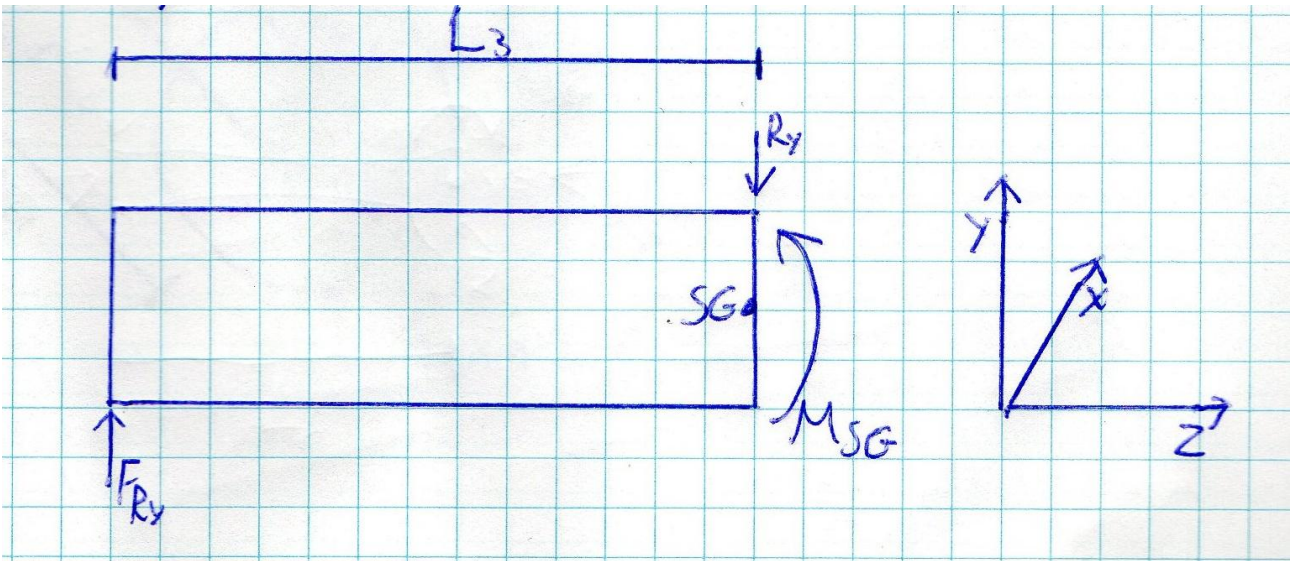


Figure 7 – FBD of the tube, where the axle is fixed upon, at the rear wheels.

$$\sum F_y = F_{Ry} - R_y = 0 \leftrightarrow F_{Ry} = R_y$$

$$\sum M_{(SG)} = F_{Ry}L_3 + M_a - M_{SG} = 0 \leftrightarrow M_{SG} = F_{Ry}L_3 + M_a$$

The forces acting on the axle can only cause bending around the X-axis therefore one SG placed in a quarter bridge on top of the tube, between the back wheels, will be sufficient, Figure 8. It was assumed that no or little strain was transferred from the opposite rear wheel.



Figure 8 - Position of the quarter bridge SG at the rear wheel.

### 1.3.2 Crank

The applied force of a human to the crank can be split up into three forces. A tangential and radial force, Figure 9, which is perpendicular and parallel to the crankarm, respectively, and a force pushing or pulling the pedals towards or away from each other. The last force is however neglected in this study, as it is assumed that the athlete apply minimal force in that direction. Therefore, the mounting of SGs for this scenario will be in the interest of determining the tangential and radial force.

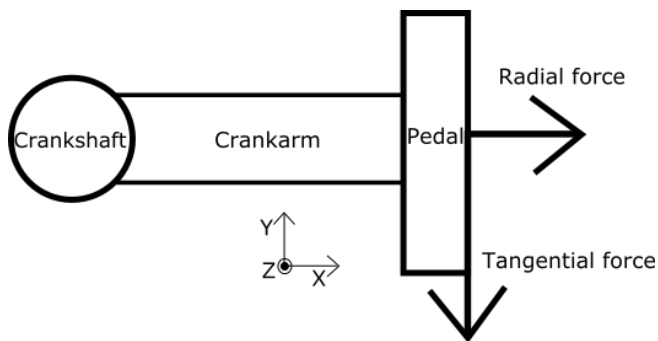


Figure 9 - Tangential and radial force directions.

A FBD analysis of the crankarm and crankshaft was used to determine the position of the SGs used to measure the tangential force, Figure 10. The tangential force causes torsion of the crankshaft, while the radial force causes bending of the crankshaft around the Z-axis. To measure the torsional strain caused by the tangential force, two SGs were placed in a half bridge on the crankshaft, inside the crankbox, with a 45 degree angle to the longitudinal direction (Omega.com). From the view of the crankshaft and crankarm, Figure 11, the SG were placed on the middle of the crankshaft, illustrated by the dashed line. This was done in order to avoid measuring the strain caused by the radial force, as the strain caused by bending is zero in the middle of the crankshaft (Gere, Goodno 2013).

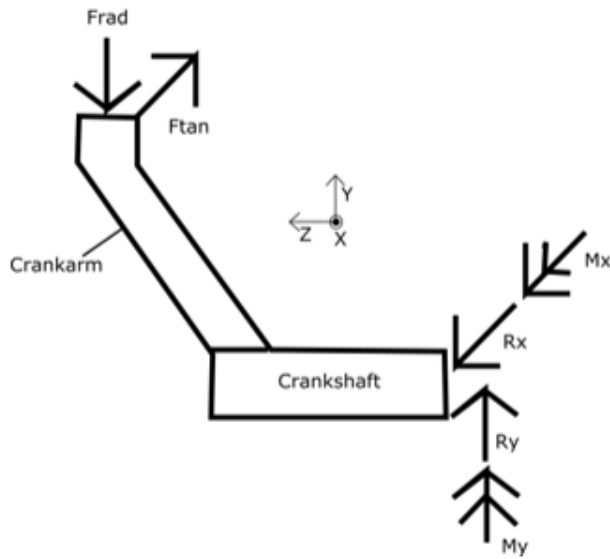


Figure 10 - Free Body Diagram used to determine the positions of SGs for measuring the tangential force.

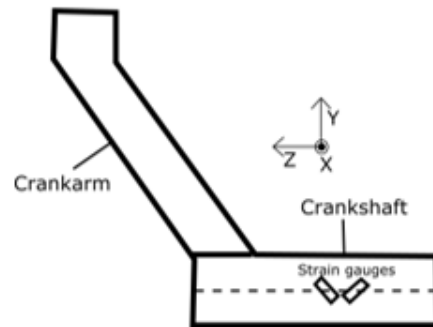


Figure 11 - Position of the SGs on the crankshaft.

A free body diagram (FBD) analysis of the crankarm was used to determine the position of the SG used to measure the radial force, Figure 12. The tangential force causes bending around the Z-axis, while the radial force cause bending around the X-axis and compression/tension in the Y-direction, depending on where in the cycle the pedals are. To measure the strain caused by the radial force, one SG was placed in a quarter bridge on the middle of the surface pointing towards the crankbox, as the strain caused by the tangential force is zero at that location (Gere, Goodno 2013).

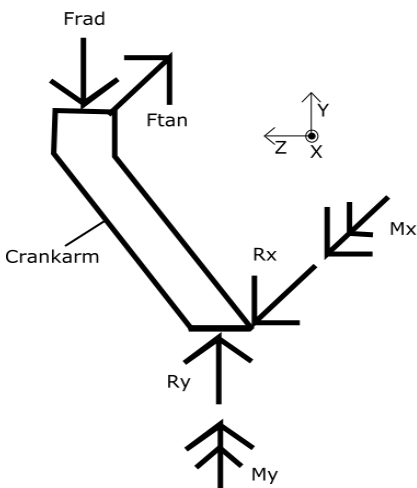


Figure 12 – Free Body Diagram used to determine the positions of SGs for measuring the radial force.

The position of where the SGs where mounted at the crankshaft and crankarm can be seen on Figure 13 and 14, respectively.



Figure 13 – Strain gauges position on the crankshaft.

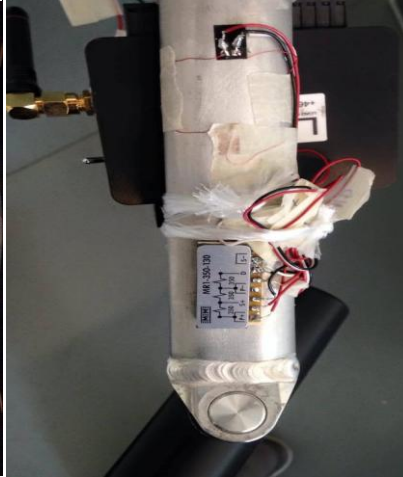


Figure 14 – Strain gauge position on the crankarm.

### 1.3.3 Brake and road irregularities

The position of the SG used to measure brake force and road irregularities, at the front wheel, were determined using FEA on the front part of the modified CAD-model acquired from Wolturnus A/S. Furthermore parts, which had no influence on the behavior of the handbike caused by braking or road irregularities, was suppressed, Figure 4.

Before conducting the FEA, it was necessary to apply material, contact points, a mesh, fixtures and loads. The material applied was a 7050 aluminum modified with the E-modulus and yield strength found in the tensile test. A no penetration contact was made between the modified front forks and axle. In order to mesh the model the mesh had to be a fine curvature based mesh. The fixtures and loads applied, as indicated on Figure 15, by green and purple arrows, respectively, depended on the scenario simulated. For the braking scenario the force was applied horizontally at the beams simulating the wheel, as that is where the wheel is stopped by the friction on the ground. The middle beam was attached to the oval top tube, by a rod, which is where the brake pads are mounted.

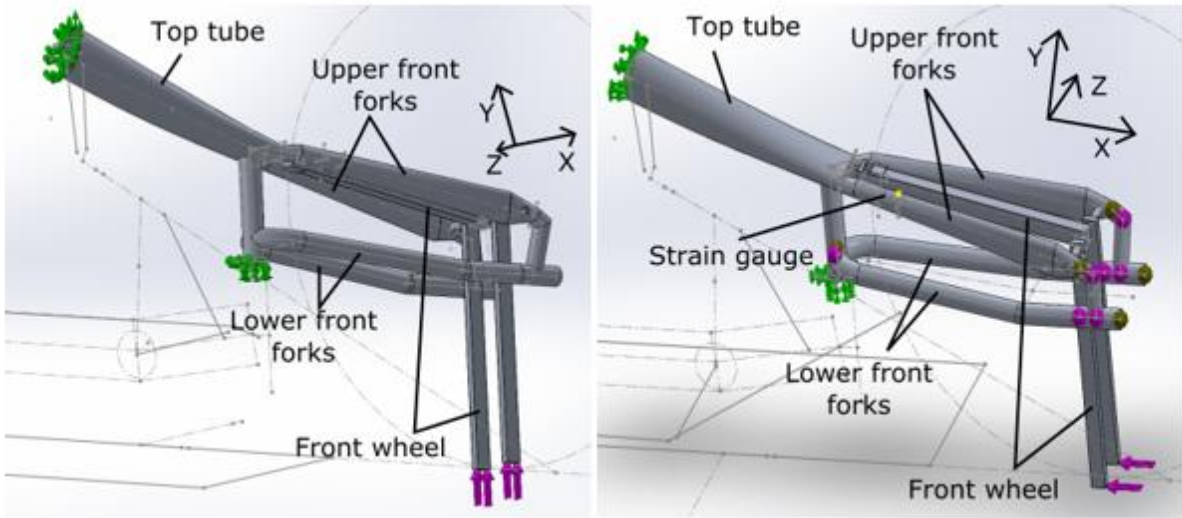


Figure 15 - CAD-models used for road irregularities (left) and brake force (right) simulations. Green arrows=fixations and purple arrows=force.

The FEA was conducted and the plot for normal strain in the X-direction of a local coordinate system was chosen. The local coordinate systems X-axis was aligned with the longitudinal direction of the right front fork. The position of the SG was chosen from the criteria that the strain had to more or less constant over an area. Furthermore it had to be a distance away from fixtures and geometry changes to get reliable results. A point on top of the right fork was chosen and the distance to that point was measured in the CAD-model. One SG was then placed, in a quarter bridge, according to that distance on the handbike, Figure 16.



Figure 16 - Position of the quarter bridge SG at the front wheel.

## 1.4 Laboratory calibration

Laboratory calibration tests were carried out in order to transform the measured strain, in the three field test scenarios, into forces. A calibration test were carried out for the tangential, radial, brake and road irregularities, at the front and rear wheel, force.

### 1.4.1 Overall laboratory calibration test protocol

The overall test protocol for the laboratory calibration were as follows:

1. Open Node Commander on a laptop and establish communication with the gateway and node. For calibration of the crankset, open LabVIEW as well.
2. Configure the node to select the desired SG.
3. Configure the SG to have the following settings:
  - Conversion Coefficients, Class: Strain
  - Conversion Coefficients, Units:  $\mu$ Strain
  - PGA Settings, Input Range: +/- 2.5 mV [569] (which is the gain setting)
  - PGA Setting: Low scale or Midscale depending on the SG
4. Select Use the Strain Measurement Wizard and set it to have the following settings:
  - Number of active gauges: 1 or 2 depending on the SG (quarter or half bridge)
  - Gauge factor: 2
  - Gauge resistance: 350 ohms.
  - Shunt Resistance: 499000 ohms.
5. Click calibrate and apply the changes.
6. Press auto-balance (to assign this sensor value as a no-load measurement)
7. Note the slope found using Strain Measurement Wizard (for later use at the three field test scenarios)
8. Measure and note the strain/volt (depending on using Node Commander or LabVIEW) to the desired weights applied.

### 1.4.2 Rear wheel

In order to determine the force acting on the handbike at the rear wheel, both a FBD and Laboratory calibration were made. The laboratory calibration was used to calculate the measured strain from the field test into force, whereas the FBD calibration was used, as a validation of the laboratory calibration. For the FBD calibration, a prismatic beam model was considered, equation (4).

$$\varepsilon = \frac{FL^3}{3EI} \quad (4)$$

Where  $F$  is the force,  $L$  is the length from the force to the SG,  $E$  is the E-modulus of the material and  $I$  is the moment of inertia, which, for a hollow circular cross-section, can be found with equation (5).

$$I = \frac{\pi}{4} (r_2^4 - r_1^4) \quad (5)$$

Where  $r_2$  and  $r_1$  are the outer and inner radius of the circle, respectively. If the axle do not yield, which it is expected not to, all the force acting on the axle will be transmitted to the tube. We can use equation (6) to calculate to total strain at the SG, as it is assumed that the force is split into two equally big forces at two different distances from the SG.

$$\varepsilon = \frac{1}{2} \frac{FL_1^3}{3EI} + \frac{1}{2} \frac{FL_2^3}{3EI} \quad (6)$$

Equation (6) was used to calculate the corresponding strain to 0 N and 100 N of force applied, which was used for linear regression.

For the laboratory calibration the subject used for the three field test scenarios was lying still in the handbike. Weights of 0, 5, 10, 15 and 20 kg was applied vertically using a rope and a pulley, Figure 17, while



Figure 17 – Calibration setup for the rear wheel.

the corresponding strains were measured. This data was used for linear regression.

The Linear regressions were carried out using the CurveFittingTool in MatLab and resulted in transformation formulas, Figure 18. The forces applied to the handbike from the road irregularities, at the

rear wheel, were determined by inserting the measured strains into the transformation formula found in the FBD and laboratory calibration.

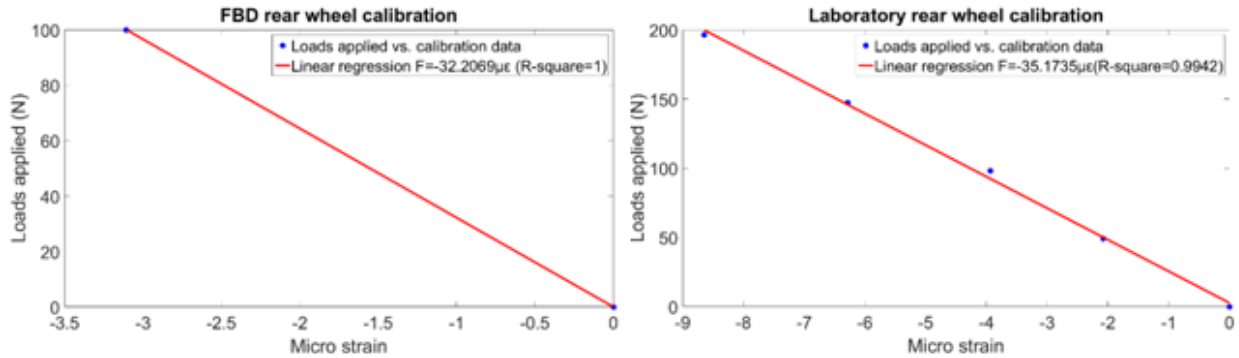


Figure 18 – Linear regressions for FBD and laboratory calibrations of road irregularities forces at the rear wheel.

#### 1.4.3 Tangential and radial force

For the laboratory calibration of the tangential and radial force, the crankbox was fixed in a vices and the tooth wheel were fixed with a clamp. The tooth wheel were fixed so the crankarms were completely horizontal or vertical, respectively, Figure 19. Weights of 0, 1, 2, 3, 4 and 5 kilograms were applied and the corresponding strain was measured, which was used for linear regression. Only weights up to 5 kilograms were applied, due to difficulty in fixating the crank set properly. Ideally, weights of up to what the crankset is actually subjected to in a field accelerating study should have been applied. However, as the R-square value is almost 1, Figure 20, this was considered sufficient.



Figure 19 - Laboratory crank set calibration for the tangential (left) and radial (right) force.

The Linear regressions were carried out using the CurveFittingTool in MatLab and resulted in equations used to calculate the tangential and radial forces applied to the handbike, Figure 20.

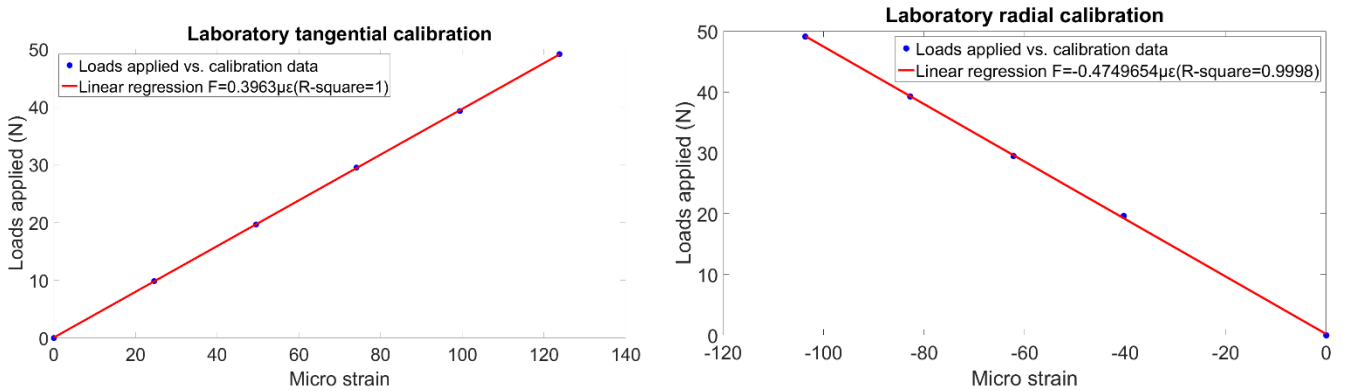


Figure 20 - Linear regressions for the laboratory calibrations of tangential (left) and radial (right) force at the crank set.

### 1.4.4 Brake and road irregularities

In order to determine the braking and road irregularities forces acting on the handbike at the front wheel, laboratory calibration were made.

For the laboratory calibration of the brake force the subject used for the three field test scenarios was lying still in the handbike and the rotation of the front wheel was fixed by blocking the brakes, using a rope. Weights of 0, 5, 10, 15 and 20 kg was applied tangentially to the front wheel using a rope and a pulley, Figure 21, while the corresponding strains were measured.

For the road irregularities forces the subject used for the three field test scenarios was lying still in the handbike. Weights of 0, 5, 10, 15 and 20 kg was applied vertically using a rope and a pulley, Figure 21, while the corresponding strains were measured. The data was used for linear regression.

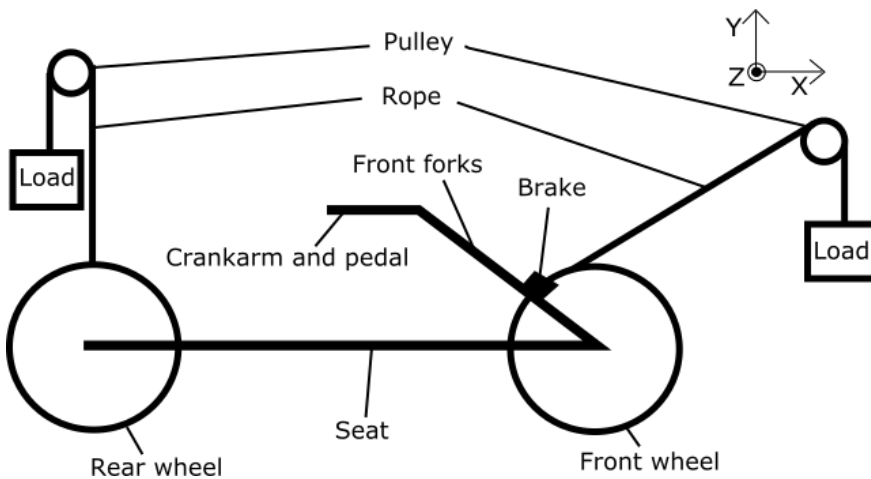


Figure 21 - Test setup for the road irregularities (left) and brake force calibrations (right).

The Linear regressions were carried out using the CurveFittingTool in MatLab and resulted in equations used to calculate the forces acting on the handbike, due to brake force and road irregularities, at the front wheel, Figure 22.

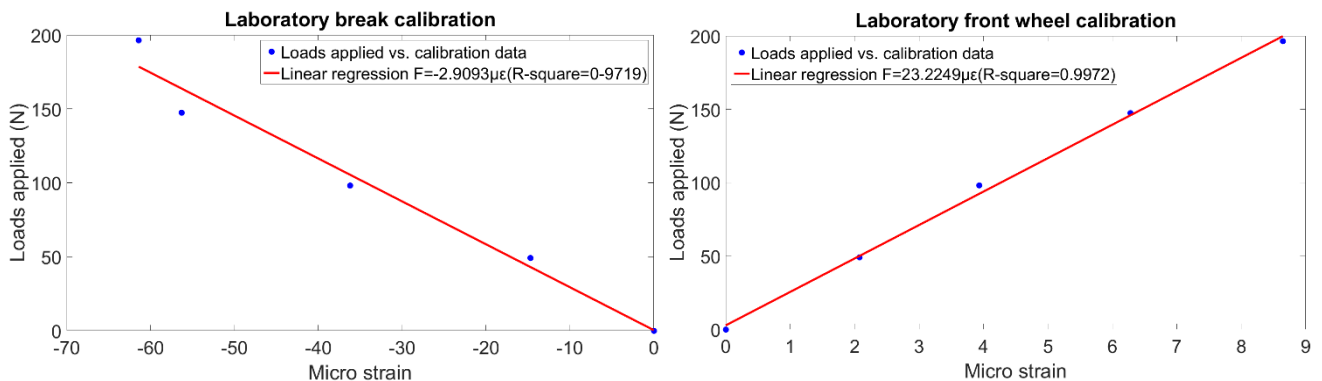


Figure 22 – Linear regressions for the laboratory calibrations of brake (left) and the road irregularities (right) force at the crankset.

## 1.5 Test protocol

In order to get SG measurements when using the handbike, realistic scenarios were determined and tested in a field test. The tests included upper limit scenarios the handbike might be subjected to. The scenarios include brake force, road irregularities and accelerating the handbike. The tires used for all test scenarios were 28" race tires, with a tire pressure of 10 bar. The crank position were adjusted to the user's personal preference. The velocity of the handbike was measured with a bike computer (16.12 ST/CAD, Sigma), by the subject just before braking the handbike and riding across the wooden lists.

Prior to the actual test procedure, a pilot study was conducted for all test scenarios to make sure everything functioned as desired.

### 1.5.1 Measurement equipment and calculations

The measurement equipment was a LORD MicroStrain® Wireless Sensor Network system which in a short term is a sensor data acquisition and a sensor networking system. It consists of a wireless sensor node called V-Link and a data collecting gateway called WSDA-Base. The software program Node Commander is used to control, configure and acquire data from the node and gateway. Some of the things you can change when you configure a node using Node Commander is gain, offset scale and calibration, which all will be explained further in the following section.

Gain is usually a measure of how many times you amplify the input signal to the output signal. This is done by adding energy from a power supply to the signal. I.e. if a sensor has a listed signal range of 0-50 mV but the node input range is between 0-3 V, then if the sensor signal is not amplified, it gives a very bad resolution as that is a very small part of the node input range. This is because there are more digital counts available to measure the signal when more of the range is used. The digital counts are the bits that correspond to the voltage measurement. For example the V-Link has a full scale bit range of 4096, as it is a 12-bit node, which corresponds to the 0-3 V node input. The more bit range there is, the more digital counts are available to convert the analog signal to digital – leading to a higher resolution.

The V-Link has several different gain settings available. To calculate if a gain setting is good, you multiply the upper signal range of the sensor, with a given gain, equation (7). The calculated voltage should be close but below 3 volts which is the maximum node input range.

$$50 \text{ mV (upper signal range)} * 21 \text{ (gain)} = 1.05 \text{ V} \quad (7)$$

Three different types of offset scales are available with the V-Link: high scale, midscale and low scale. The offset scales are where the no-loads measurements are positioned in the 0-3 V range of the node input, for the sensor. The low scale is positioned at 750 mV and is used for signals that are mostly positive. The

midscale is at 1.5 V and is used for both positive and negative sensor measurements. The high scale is at 2.25 V and is used for mostly negative sensor measurements.

The offset scale has to be accounted for when calculating the gain, by adding the voltage of the used offset scale to equation (7). So if a midscale offset is used with the same gain and sensor input as with equation (7), the maximum sensor input to the node would be found with equation (8).

$$50 \text{ mV (upper signal range)} * 21 \text{ (gain)} + 1.5 \text{ V (offset scale)} = 2.55 \text{ V} \quad (8)$$

To calibrate each SG Node Commander can be used by entering the Strain Wizard. In the Strain Wizard the number of active gauges is entered, which is one for a quarter bridge two for a half bridge and four for a full bridge. Also gauge factor and gauge resistance is entered, which are specifications for the SG used. Shunt Resistance should be set to 499000 ohms, which is a standard value. The Strain Wizard then calculates a slope, an offset value and a formula used to convert the signal measurement to engineering units like micro-strain. The same calculated slope for each SG found in the Strain Wizard calibration, is then used every time data is acquired for the respective SG.

### 1.5.2 Test procedure

#### Material list

1. Custom made handbike with attached SGs at the rear wheel and front fork
2. Laptop with Node Commander and LabVIEW software
3. V-Link - wireless sensor node
4. WSDA-base – data collecting gateway
5. Digital to analog converter (DAC)
6. Handbike with SGs at the crankarm and crankshaft
7. Home trainer to mount the handbike in
8. Device like a smartphone with Wahoo Fitness app that controls the home trainer installed

#### Determining braking loads.

1. Position the handbike at a 150+ meter flat tarmac road.
2. Open Node Commander on a laptop and establish communication with the gateway and node.
3. Configure the node to select the SG at the front fork.
4. Configure the SG to have the following settings:
  - Conversion Coefficients, Class: Strain
  - Conversion Coefficients, Units:  $\mu$ Strain

- PGA Settings, Input Range: +/- 2.5 mV [569] (which is the gain setting)
  - PGA Setting: Low scale (as the brake force only creates a positive-going strain signal).
5. Apply the calculated slope found using Strain Wizard at the laboratory calibration to the SG channel
  6. Have the rider mount the handbike.
  7. Press auto-balance (to assign this sensor value as a no-load measurement)
  8. Start a sample stream in Node Commander.
  9. Accelerate the handbike up to 40-45 km/h.
  10. After a few seconds of sampling brake as quickly as possible while still sampling.
  11. When the velocity of the handbike is 0 km/h, stop sampling and save the data.
  12. If the speed of the handbike was not within 40-45 km/h, discard the data and do a new trial.
  13. Repeat step 1-12 for a total of five successful trials.

#### **Determining the loads acquiring from load irregularities**

1. Position the handbike 100+ meters before a 20+ meter flat cobblestone road
2. Open Node Commander on a laptop and establish communication with the gateway and node.
3. Configure the node to select the SGs at the front fork and back wheel.
4. Configure the SGs to have the following settings:
  - Conversion Coefficients, Class: Strain
  - Conversion Coefficients, Units:  $\mu$ Strain
  - PGA Settings, Input Range: +/- 2.5 mV [569] (which is the gain setting)
  - PGA Setting: Low scale (as the road irregularities only create a positive going signal).
5. Have the rider mount the handbike
6. Apply the calculated slopes found using Strain Wizard at the laboratory calibration to each SG channel
7. Press auto-balance (to assign this sensor value as a no-load measurement)
8. Start a sample stream in Node Commander.
9. Accelerate the handbike up to 35-40 km/h before reaching the cobblestones.
10. When the rider has rode across the cobblestones, then stop the handbike, stop sampling and save the data.
11. If the speed of the handbike was not within 35-40 km/h, discard the data and do a new trial.
12. Repeat step 1-11 for a total of five successful trials.

When the signals are processed then create a more controlled experiment which replicates the signal and strains achieved riding on the cobblestones. This is done by riding across four wooden planks with a

distance of 250 mm between them at  $37 \pm 1.5$  km/h. Several different thicknesses of wooden planks are used until a signal similar to the cobblestones are found.

When the correct plank thickness is found which replicates the desired signal then do five trials using the same steps and settings as on the cobblestones but riding across the planks instead.

### **Determining the loads during acceleration**

1. Open Node Commander on a laptop and establish communication with the gateway and node.
2. Configure the node to select the SGs at the crankshaft and at the crankarm.
3. Configure the SGs to have the following settings:
  - Conversion Coefficients, Class: Strain
  - Conversion Coefficients, Units:  $\mu$ Strain
  - PGA Settings, Input Range:  $\pm 2.5$  mV [569] (which is the gain setting)
  - PGA Setting: Low scale for the SG on the crankshaft (as the tangential force only creates a positive-going signal). Midscale for the SG at the crankarm (as the radial forces creates both a positive and negative-going strain signal).
4. Have the rider mount the handbike.
5. Apply the calculated slopes found using Strain Wizard at the laboratory calibration to each SG channel
6. Set the resistance in the Wahoo Fitness app to 40 %.
7. Press auto-balance (to assign this sensor value as a no-load measurement)
8. Open LabVIEW and establish connection with Node Commander so that the measured strains are transferred to LabVIEW, and synchronized with the wheel encoder.
9. Start sampling in both Node Commander and LabVIEW and tell the rider to accelerate as fast as possible.
10. After doing three all-out pedal cycles tell the rider to stop pedaling, then stop sampling and save the data.
11. Repeat step 1-10 for a total of five trials.

### **1.6 FE-model validation**

Calibration tests were carried out for the tangential, radial, brake and road irregularities at the front wheel forces in SolidWorks, which were compared to the laboratory calibrations. This was done to validate the FE-model of the handbike.

The modified crankset of the FE-model, Figure 23, was used to carry out the tangential and radial force calibrations in SW. One linear static study was done for the tangential and radial force, respectively. One study for each force was sufficient, as the strain is linearly correlated to the force applied in a linear static study. For both studies the tooth wheel and crankbox were fixated, and a load of 100 N were applied at the pedal in the tangential and radial direction, respectively, and the corresponding strain at the SG position were noted.

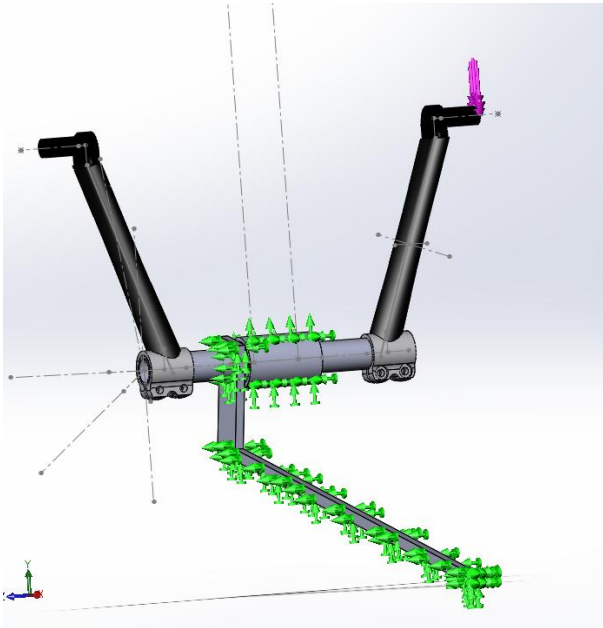


Figure 23 - Crank set validation in SolidWorks.

The same part of the FE-model used for determining the SG position, Figure 15, at the front wheel were used for the SW calibrations of the brake and road irregularities forces. Further the fixations and loads were applied to the same faces. One linear static study were done for both the brake and road irregularities scenario, by applying a load of 100 N and note the corresponding strains at the position of the SG. Again one study for each force was sufficient, as the strain is linearly correlated to the force applied in a linear static study.

The Linear regressions for the SW validations of the tangential and radial, brake and front wheel road irregularities were carried out using the CurveFittingTool in MatLab and is seen on Figure 24 and 25 , respectively.

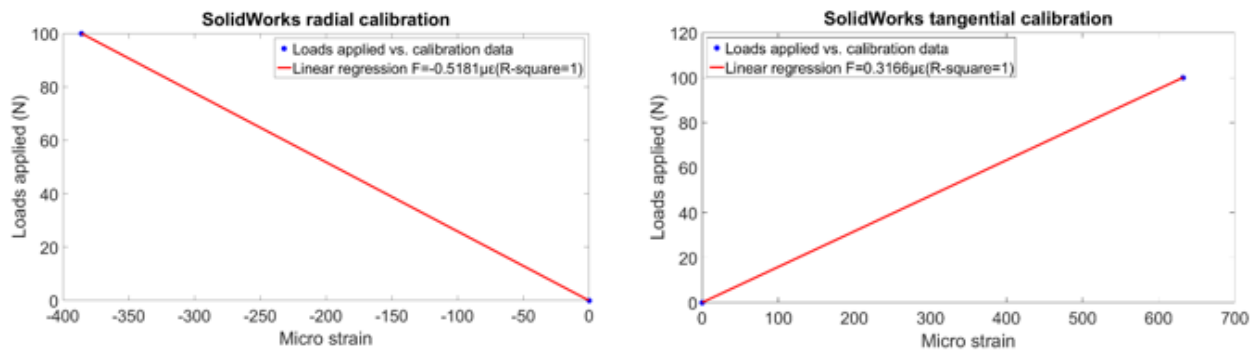


Figure 24 - SolidWorks regression equations for the validation of the radial (left) and tangential (right) force.

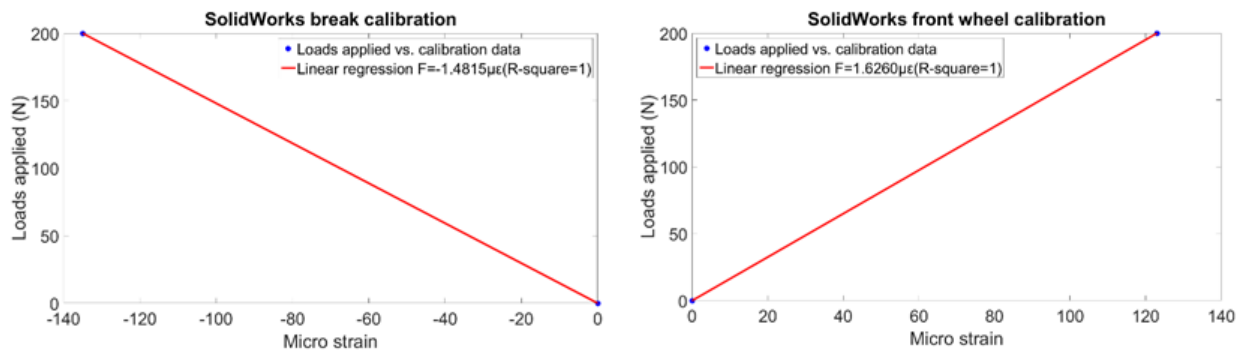


Figure 25 - SolidWorks regression equations for the validation of the brake force (left) and road irregularities of the front wheel (right).

## 1.7 Optimization

The geometries that were altered were chosen because they were subjected to the largest amount of von Mises stress on the frame of the handbike. This was found by visually examining a von Mises stress plot of the FE-model used for optimization, where no geometries were altered, Figure 26.

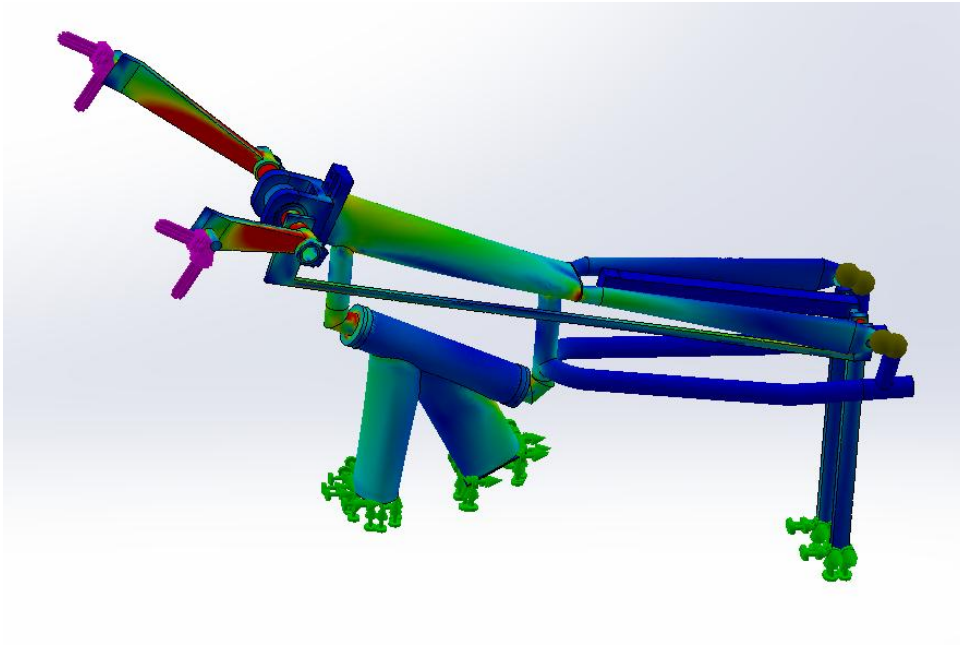


Figure 26 – Von Mises stress plot of the upper front part of the handbike, used for optimization.

### 1.8 Initial process of this study

Initially in the start of this study, the SG positions was meant to be found by only doing FBD analysis and no SW simulation. However, the SG positions for braking and road irregularities, at the front wheel, were in the end instead found by doing SW simulations. This meant that in the end only the SG position of the acceleration and road irregularities, at the rear wheel, were found using FBD analysis. A large amount of time and effort was done in order to determine all forces using FBDs, which ended up being disregarded. To determine the acceleration force, the initial plan was to mount SGs on top of the top tube, to measure both the tangential and radial force. However, the top tube on the acquired handbike had a shorter top tube than expected, meaning the SGs had to be mounted too close to structural changes. Further, difficulty in determining the crankarm position to a given strain lead to a change of plans in regard to determining the acceleration forces.

To find the brake and road irregularities forces, at the front wheel, the initial plan was to mount SGs on both on the upper and lower front forks. However, the use of FBDs was assumed to be too imprecise, as too many simplification had to be made. This was especially due to the fact that a 2D FBD analysis was considered too simple, as the upper and lower front forks changed in all 3 dimensions. Because of this the use of SW analysis was chosen instead.

Some of the initial work in determining SG position for the acceleration, brake and road irregularities at the front wheel using FBDs can be seen in Appendix 3.4.

## 2. References

GERE, J.M. and GOODNO, B.J., 2013. 5. STRESSES IN BEAMS. *Mechanics of Materials*. Eighth edn. Stamford: Cengage Learning.

OMEGA.COM, Positioning Strain Gages to Monitor Bending, Axial, Shear, and Torsional Loads. Available: <http://www.omega.com/faq/pressure/pdf/positioning.pdf> [5/23, 2016].

## 3. Appendix

### 3.1 Protocol for attaching the strain gauges

The SGs were attached following a standard from the Vishay Precision Group, as seen below.

Basic Surface Preparation and Installation with M-Bond 200 Adhesive.

1. Degrease
2. Wet abrade with MCA-1 conditioner
3. Mark out
4. Scrub with MCA-1 conditioner
5. Wipe dry from centre to edge
6. Repeat 4 and 5 until a fresh cotton bud is clean
7. Scrub with MN5A-1 neutraliser
8. Wipe dry from centre to edge
9. Prepare clean area on gauge box with MN5A-1 neutraliser
10. Clean tweezers with MN5A-1 neutraliser
11. Position gauge on box and pick up gauge with tape
12. Position gauge on specimen
13. Peel back tape (shallow angle)
14. Apply catalyst and wait 30 seconds)
15. Apply adhesive
16. Spread adhesive through and apply thumb pressure (1 minute)
17. Wait 2 minutes then peel away tape (roll back over itself)

### 3.2 Wiring diagrams for attached strain gauges

Figure 27 and 28, show the wiring between the SG and the bridge completion module and the wiring between the bridge completion module and the V-Link transmitter, for a half and quarter bridge circuit, respectively.

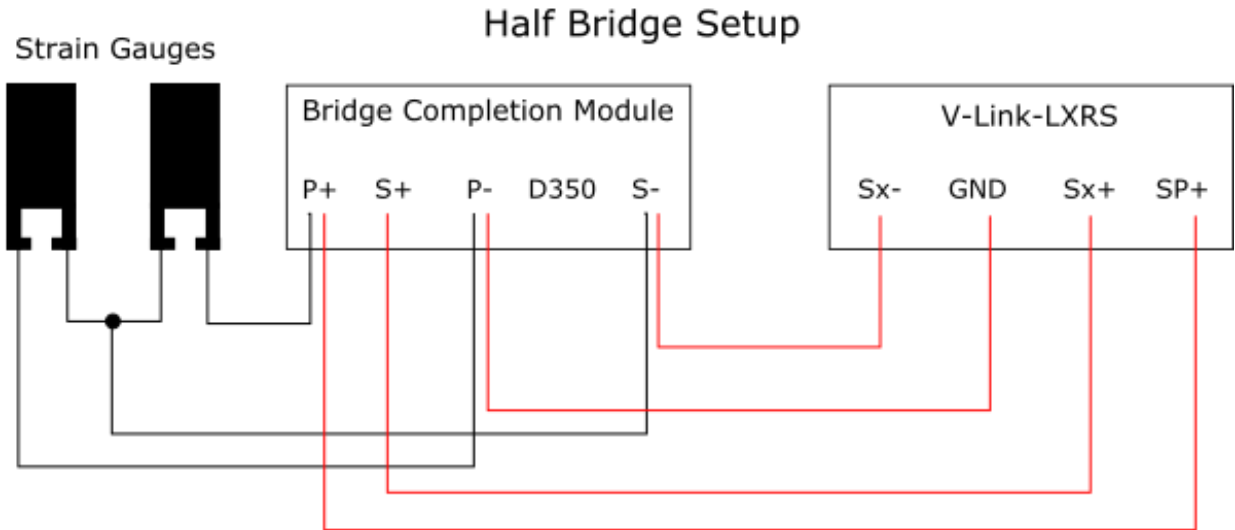


Figure 27 – The wiring between strain gauges and bridge completion module (black lines) and wiring between bridge completion module and V-Link transmitter (red lines), in a half bridge circuit.

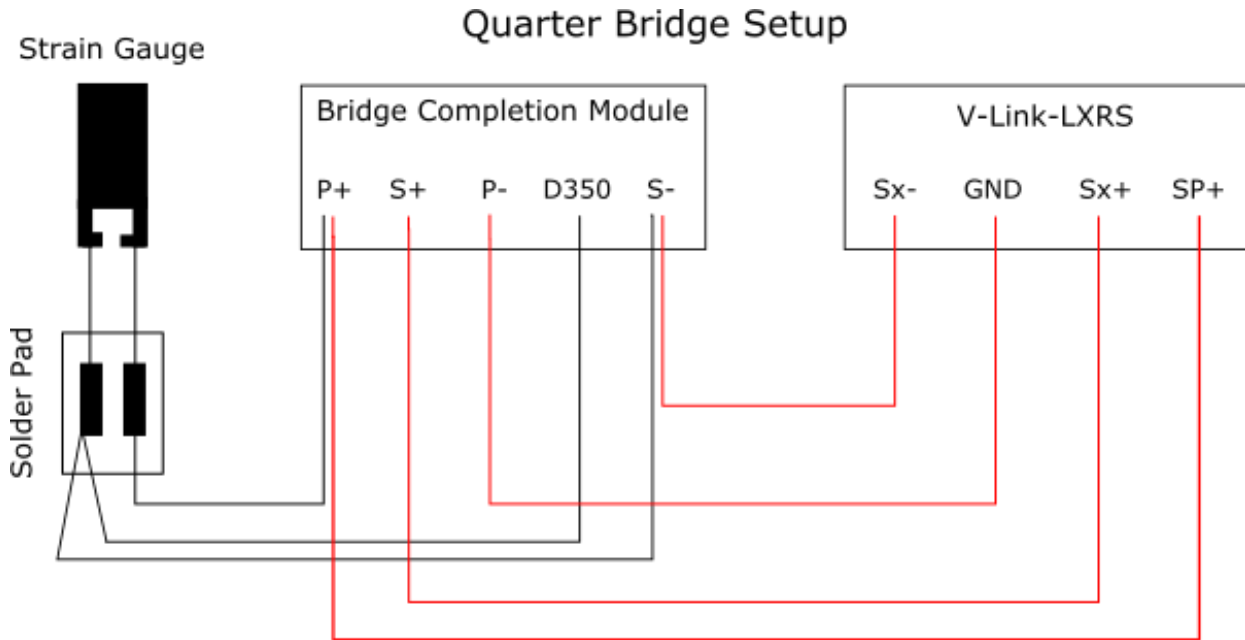


Figure 28 – The wiring between strain gauge and bridge completion module (black lines) and wiring between bridge completion module and V-Link transmitter (red lines), in a quarter bridge circuit.

### 3.3 Technical drawing

Figure 29, show the technical drawing made of the specimens for tensile tests. The technical drawing was used by the workshop to manufacture the specimens.

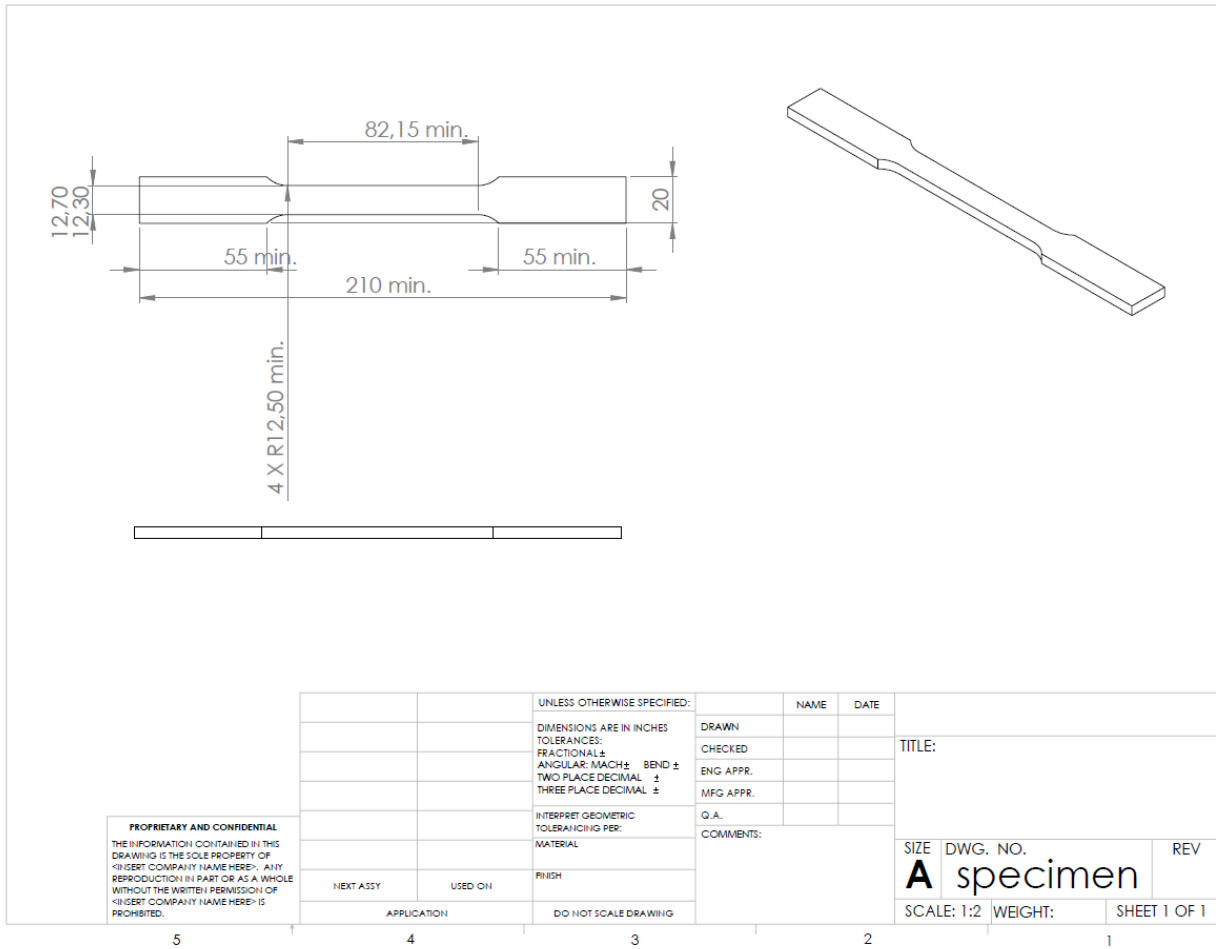


Figure 29 – Technical drawing of specimens for the tensile tests.

### 3.4 Initial plan of SG position and force determination

The initial plan of the SG position and force determination for the acceleration, brake and road irregularities forces at the front wheel, was by using FBD. The following section covers some of the initial work and thought process. This was in the end however not how the forces were found.

#### 3.4.1 Crank

The force applied to the pedals by the human, can be split into a tangential force  $F_{\text{tangiel}}$  and a radial force  $F_{\text{radial}}$ . The tangential force is the force generating the propulsion and is perpendicular to the crankarm and radial force. The radial force is parallel to the crankarm and is not generating propulsion. If we take a look at the sketch of the crank, Figure 30, which is a static problem meaning that the sum of forces in all directions should be zero. When looking at the radial force, there must be an equally big corresponding reaction force  $R_{\text{radial}}$ , acting the opposite way. The tangential force creates a moment in the crank, which pulls the chain with the reaction force  $F_{\text{chain}}$ .

The radial force creates bending, compression and tension forces on the top tube, depending on where the pedals are in the cycle. Therefore we want to place two SGs, Figure 30, which enables us to determine the amount of force applied and if it are bending, compression or tension forces. SG 1 will measure the strain of bending around the Z-axis, while SG 2 will help determining the compression and tension force. To avoid moving the coordinate system of the SGs, which would happen if they were placed on the crankarm, the SGs are placed on the nearest fixed structure.

This is in 2D, as we neglect the forces acting in the Z-direction, as the pedal type is synchronic and thereby the lateral torsion is zero or at least very low.

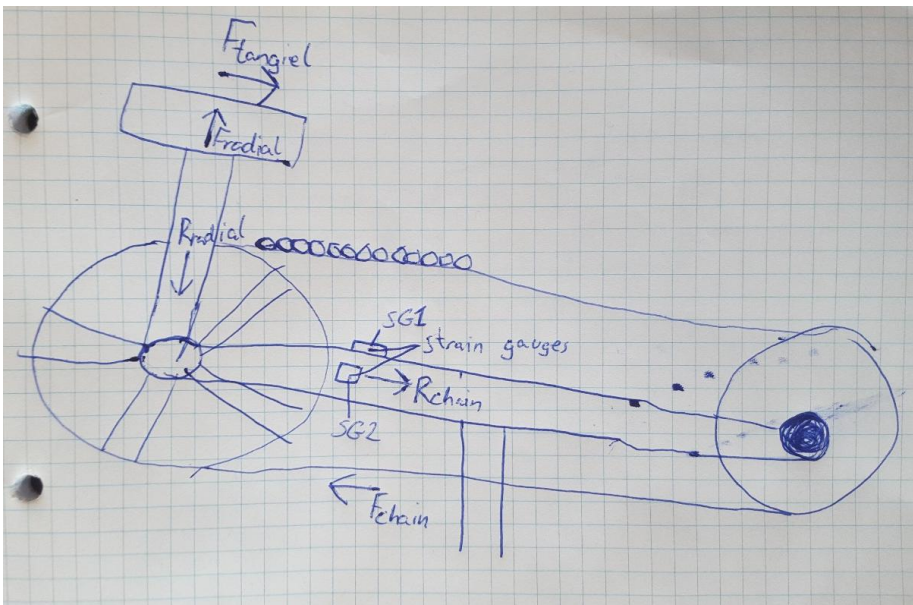


Figure 30 - Crank scenario.

We set up our equilibrium equations. Again the forces in the Z-direction is neglected and the tangential force is equal to the chain force, so we are left with the radial force and the radial reaction force. The scenario depends where in the cycle the pedals are and thereby the angle ( $\theta$ ) between the crankarm and top tube. Following is applicable:

$$\text{if } \theta = 90 \text{ or } 270 \sum F_x = 0 \text{ and if } \theta = 0 \text{ or } 180 \sum F_y = 0$$

For all other angles the radial force are split into a X and Y component by simple trigonometry. The equilibrium equations will be:

$$\sum F_x = F_{rad} * \cos(\theta) - R_{rad} * \cos(\theta) = 0$$

$$F_{rad,x} = R_{rad,x}$$

$$\sum F_y = F_{rad} * \sin(\theta) - R_{rad} * \sin(\theta)$$

$$F_{rad,y} = R_{rad,y}$$

$$\sum M_{SG} = F_{rad} * \sin(\theta) * L - R_{rad} * L = 0$$

$$F_{rad} * \sin(\theta) * L = R_{rad} * L$$

The  $F_x$  component will cause compression or tension in the tube and the  $F_y$  component will cause bending around the Z-axis. We need two SGs in this scenario to be able to distinguish the type of force applied. SG1 will measure both compression/tension and bending and SG2 will only be able to measure compression/tension, as it is placed in the center on the side of the tube. By subtracting the strain measure with SG2 from the strain measured with SG1 we know the size of the force in both the X- and Y-direction.

When we have the compression/tension strain we are able to calculate  $F_{rad,x}$  by first calculating stress in the tube with formula (9).

$$\sigma = E\varepsilon \text{ (9)}$$

We know that stress equals force over area, and we can isolate force in the equation, formula (10).

$$\sigma = \frac{F}{A} \leftrightarrow F = \sigma A \text{ (10)}$$

Where A is the cross sectional area, which for a hollow ellipse can be found with formula (11).

$$A = \frac{\pi}{4}(ba - b_1a_1) \text{ (11)}$$

Where  $b$  and  $b_1$  is the outer and inner width of the narrower direction of the ellipse, respectively, and  $a_1$  is the outer and inner width of the wider direction of the ellipse, respectively.

Now we know  $F_{rad,x}$ , so now we need to find the  $F_{rad,y}$ , which is done by looking at a beam model. As we only have one force causing bending, we can use formula (12) and isolate  $F$ , formula (13).

$$\varepsilon = \frac{FL^3}{3EI} \quad (12)$$

$$F = \frac{3\varepsilon EI}{L^3} \quad (13)$$

The moment of inertia is however different this time, as it is not a hollow circle, but a hollow ellipse.

Moment of inertia for a hollow ellipse can be found with formula (14).

$$I = \frac{\pi}{64}(ba^3 - b_1a_1^3) \quad (14)$$

Now we know the size and direction of the force applied to the pedals.

### 3.4.2 Front wheel

To establish the forces during braking, the front wheel must be considered, as that is the only wheel with brakes on. The forward motion of the handbike is stopped by braking the rotation of the front wheel, which creates additional friction on the ground surface, thereby stopping the handbike. This creates a braking force  $F_B$  in the X-direction, which acts at the center of the wheel. As the forces has to be in equilibrium, reaction forces of equal size occur in the opposite direction. As there is little room for SGs at the center of the wheel, and because the SGs would rotate if they were attached at the wheel axel, this position was disregarded. The two rods left of the wheel center was chosen instead, as the brake force travels through the structure and can be measured there instead.

The brake force creates compression in the X-direction and bending around the Z-axis, at the two rods. SGs are positioned, Figure 31, where SG1 and SG3 measures bending around the Z-axis and SG2 and SG4 measures compression in the X-direction. As the drawing is only in 2D, the exact same thing happens on the other side of the wheel, where two other pipes are connected to the center of the wheel, creating two more reactions forces,  $R_3$  and  $R_4$ . As that is however, a mirrored situation there is only positioned SGs to measure  $R_1$  and  $R_2$ , as the  $R_3$  and  $R_4$  are equal in size.

The forces occurring between the wheel and the road irregularities creates a force in the Y-direction,  $F_R$ , which acts at the center of the wheel. This force travels through the structure to the two rods left of the

wheel center, creating bending around the Z-axis. This bending is measured with SG1 and SG3. As with the brake forces, this is also a mirrored situation, where the same thing happens on the other side of the wheel.

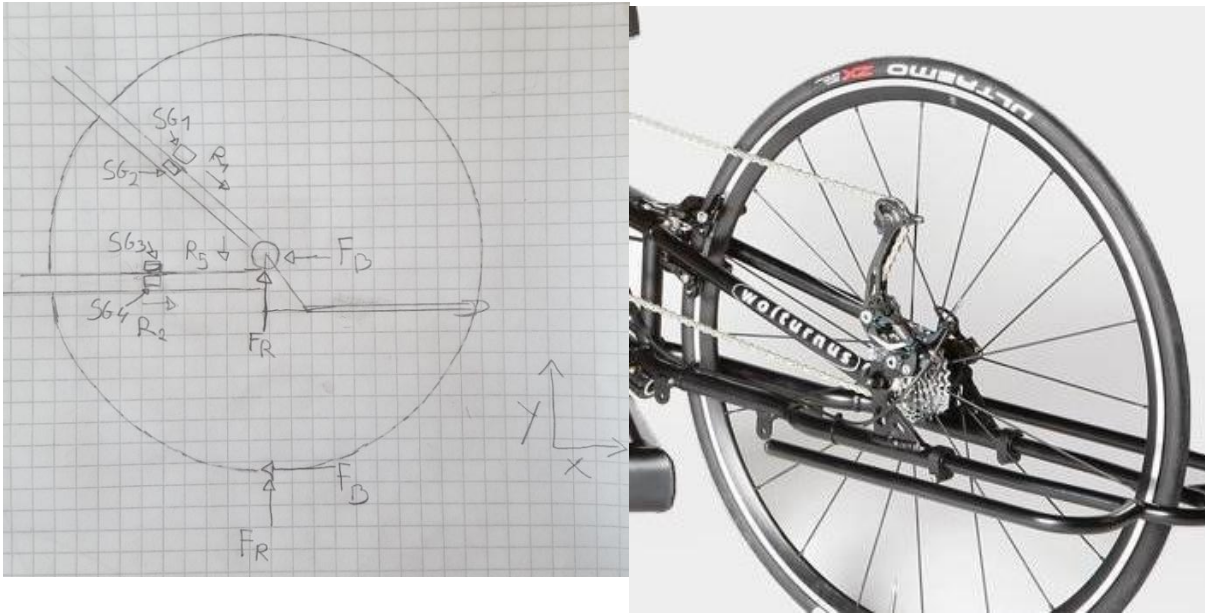


Figure 31 - Front wheel scenario.

### Brake scenario

If we look at the first scenario with the brake force, we set up equilibrium equations.

As the brake force comes in with an angle to the upper rod, the force is split in an X- and Y-component. The X-component is what causes compression of the rod, which is strain measured with SG2 and the Y-component caused bending, which strain is measured with SG1.

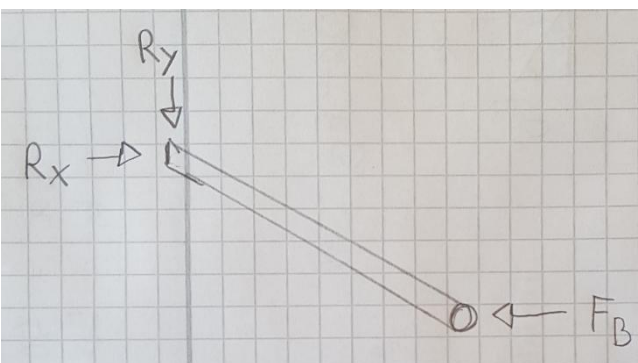


Figure 32 - FBD of the upper front fork.

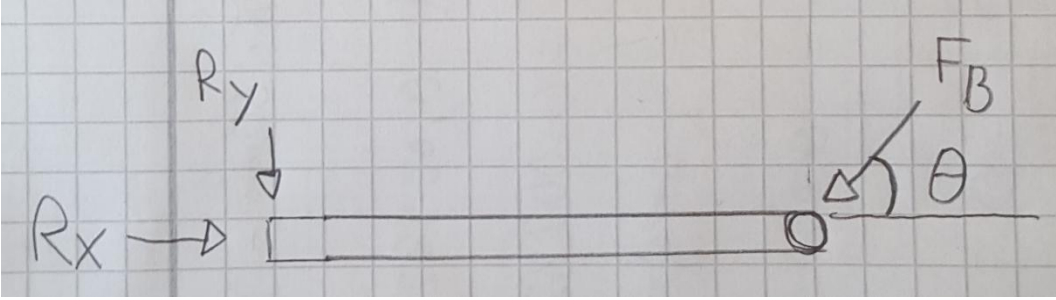


Figure 33 - FBD of the upper front fork.

For the upper rod:

$$\sum F_x = F_B * \cos(\theta) - R_x = 0 \rightarrow F_B * \cos(\theta) = R_x$$

$$\sum F_y = F_B * \sin(\theta) - R_y = 0 \rightarrow F_B * \sin(\theta) = R_y$$

$$\sum M_{SG} = F_B * \sin(\theta) * L - R_y * L = 0$$

$$F_B * \sin(\theta) * L = R_y * L$$

To find the force from the strain in the X-direction, we use formula (9), which gives us the stress. From that stress, we can calculate the force in the X-direction using formula (10), as we know the cross sectional area of the rod, which for a hollow tube is calculated with formula (15).

$$A = \pi r_2^2 - \pi r_1^2 \quad (15)$$

Where  $r_2$  and  $r_1$  is the outer and inner radius of the hollow tube, respectively.

To find the force in the Y-direction we look at a simple beam model where the force is applied vertically at the tip, formula (16).

$$\varepsilon = \frac{FL^3}{3EI} \quad (16)$$

Where the moment of inertia is for a hollow circle, formula (17).

$$I = \frac{\pi}{4}(r_2^4 - r_1^4) \quad (17)$$

As force is the unknown, we isolate F in formula (16) and with the strain input from SG1 we can now calculate the force in the Y-direction with formula (18)

$$F_y = \frac{3\varepsilon EI}{L^3} \quad (18)$$

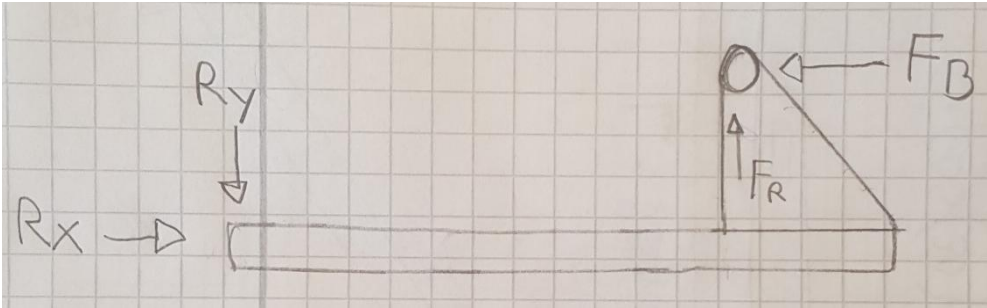


Figure 34 - FBD of the lower front fork.

For the lower rod.

$$\sum F_x = F_B - R_x = 0 \rightarrow F_B = R_x$$

The force in the lower rod can be found by the same way as the X-component in the top rod. By going from strains to stress using formula (9) and then go to force using formula (10).

*Road irregularities at the front wheel*

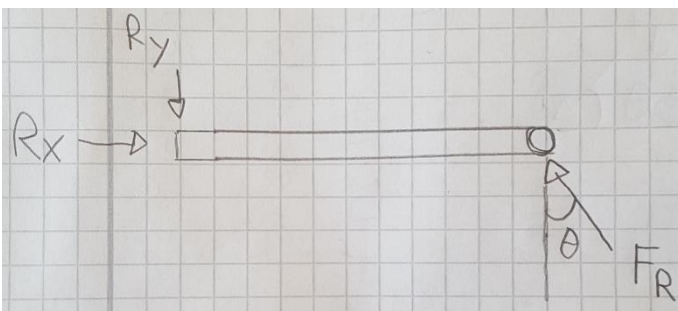


Figure 35 - FBD of the upper front fork.

To calculate the forces from the road irregularities a much similar scenario occurs to the top rod, as that with the brake force. As the road irregularity force comes in with an angle to the upper rod, the force is split in an X- and Y-component. The X-component is what causes compression of the rod, which is strain measured with SG2 and the Y-component causes bending, which strain is measured with SG1.

$$\sum F_x = F_R * \sin(\theta) - R_x = 0 \rightarrow F_R * \sin(\theta) = R_x$$

$$\sum F_y = F_R * \cos(\theta) - R_y = 0 \rightarrow F_R * \cos(\theta) = R_y$$

$$\sum M_{SG} = F_R * \cos(\theta) * L - R_y * L = 0$$

$$F_R * \cos(\theta) * L = R_y * L$$

To find the force from the strain in the X-direction, we use formula (9), which gives us the stress. From that stress, we can calculate the force in the X-direction using formula (10), as we know the cross sectional area of the rod, which for a hollow tube is calculated with formula (15).

To find the force in the Y-direction we do the same, as with the brake force scenario using formula (13) with the moment of inertia for a hollow circle, formula (17).

For the lower rod, the road irregularities creates bending around the Z-axis, which strain is measured from SG3.

$$\sum F_y = F_R - R_y = 0 \rightarrow F_R = R_y$$

The force is calculated with formula (18) with the moment of inertia of a hollow circle.

### 3.5 Force data plots

Figure 36 to 40, show the force plots for the five trials of each scenario. The force is calculated with both the laboratory and SW/FBD calibrations.

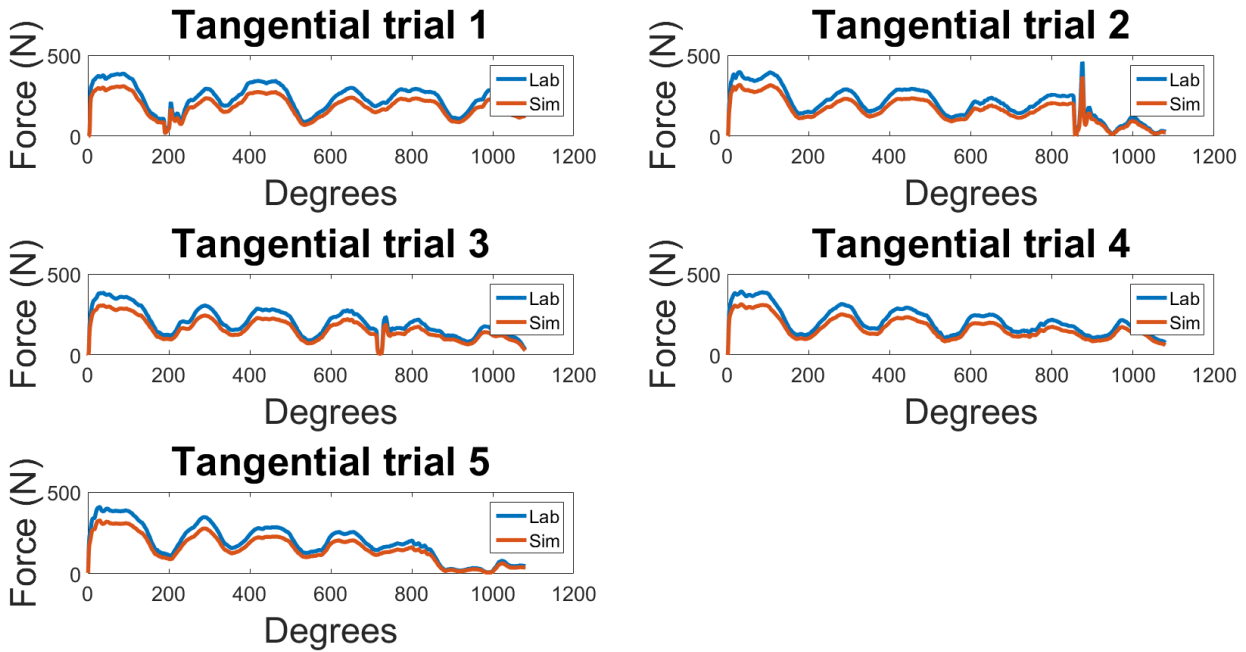


Figure 36 – Laboratory and SW calibration calculated tangential forces.

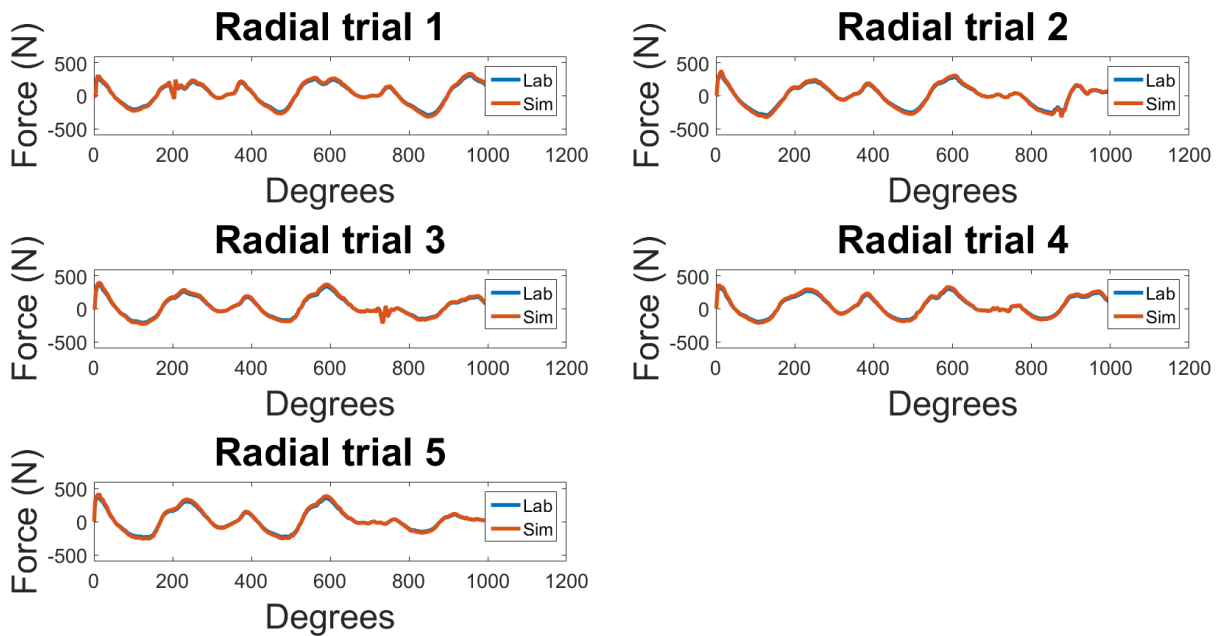


Figure 37 – Laboratory and SW calibration calculated radial forces.

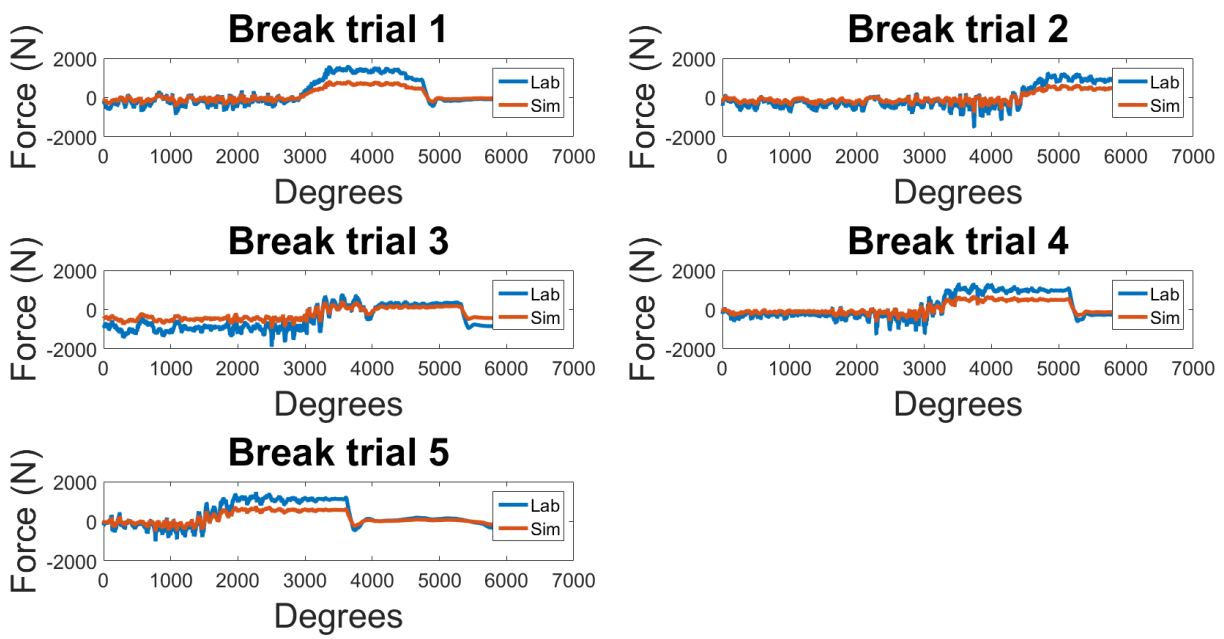


Figure 38 – Laboratory and SW calibration calculated brake forces.

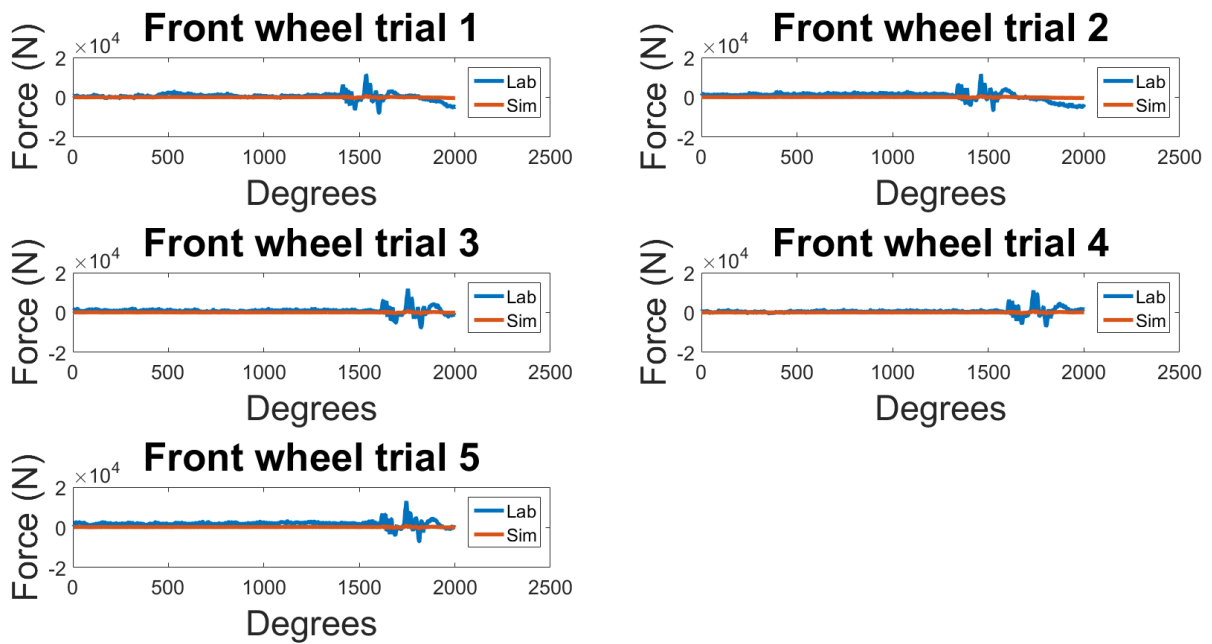


Figure 39 – Laboratory and SW calibration calculated road irregularities forces at the front wheel.

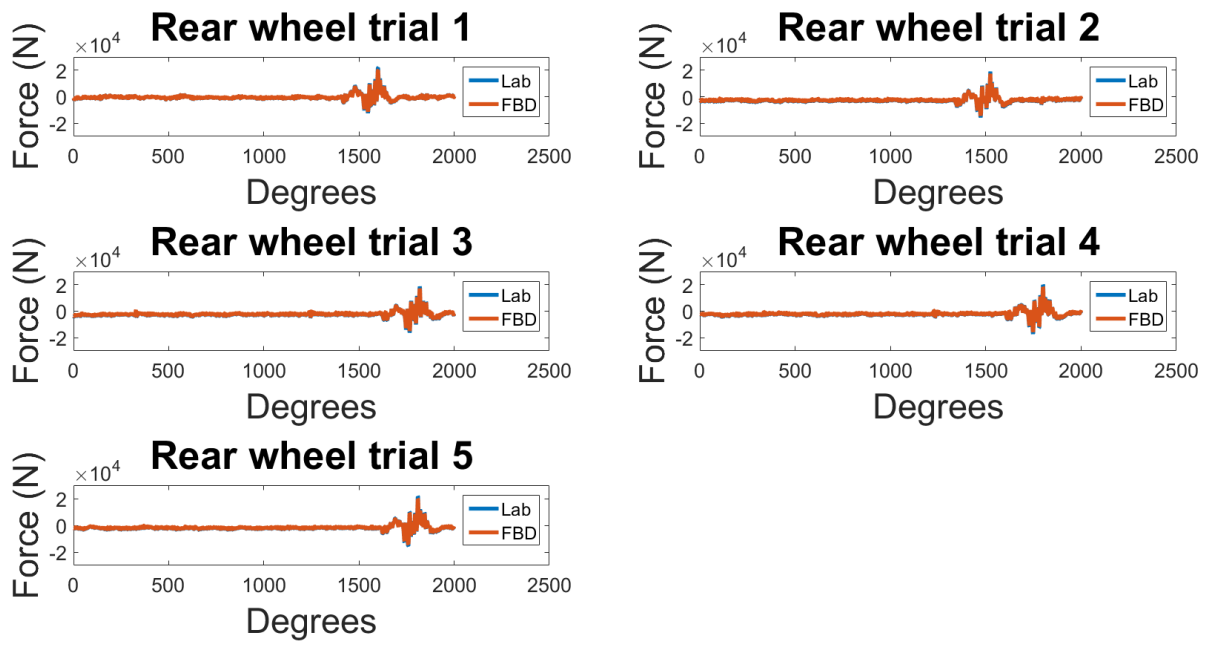


Figure 40 – Laboratory and SW calibration calculated road irregularities forces at the rear wheel.

## 3.6 MatLab script

### 3.6.1 Tensile Test

```
%% Clears Workspace
clear all

%% Loading data
load 'HT7020'
load 'NT7020'
load 'NT5005'
load 'NT50052'

%% Calculating stress and strain for the tensile tests
SNT5005=NT5005(:,2)/0.0000375;
ENT5005=(NT5005(:,1)/1000)/0.02;
SNT50052=NT50052(:,2)/0.0000375;
ENT50052=(NT50052(:,1)/1000)/0.02;
SNT7020=NT7020(:,2)/0.000075;
ENT7020=(NT7020(:,1)/1000)/0.02;
SHT7020=HT7020(:,2)/0.000075;
EHT7020=(HT7020(:,1)/1000)/0.02;

%% Creating subplot for stress-strain diagrams for the tensile tests
figure3 = figure('Color',[1 1 1]);
subplot1 = subplot(2,2,1,'Parent',figure3);
xlim(subplot1,[0 0.03]);
ylim(subplot1,[0 400000000]);
box(subplot1,'on');
set(subplot1,'FontSize',14);
hold(subplot1,'all');
plot1=plot(ENT5005,SNT5005,'LineWidth',2);
xlabel({'Strain'},'FontSize',16);
ylabel({'Stress (Pa)'},'FontSize',16);
title({'Non-treated 5005(1)'},'FontSize',16);
subplot2 = subplot(2,2,2,'Parent',figure3);
xlim(subplot2,[0 0.03]);
ylim(subplot2,[0 400000000]);
box(subplot2,'on');
set(subplot2,'FontSize',14);
hold(subplot2,'all');
plot2=plot(ENT50052,SNT50052,'LineWidth',2);
xlabel({'Strain'},'FontSize',16);
ylabel({'Stress (Pa)'},'FontSize',16);
title({'Non-treated 5005(2)'},'FontSize',16);
subplot3 = subplot(2,2,3,'Parent',figure3);
xlim(subplot3,[0 0.03]);
ylim(subplot3,[0 400000000]);
box(subplot3,'on');
set(subplot3,'FontSize',14);
hold(subplot3,'all');
plot3=plot(ENT7020,SNT7020,'LineWidth',2);
xlabel({'Strain'},'FontSize',16);
ylabel({'Stress (Pa)'},'FontSize',16);
title({'Non-treated 7020'},'FontSize',16);
subplot4 = subplot(2,2,4,'Parent',figure3);
xlim(subplot4,[0 0.03]);
ylim(subplot4,[0 400000000]);
box(subplot4,'on');
```

```

set(subplot4,'FontSize',14);
hold(subplot4,'all');
plot4=plot(EHT7020,SHT7020,'LineWidth',2);
xlabel({'Strain'},'FontSize',16);
ylabel({'Stress (Pa)'},'FontSize',16);
title({'Heat-treated 7020'},'FontSize',16);

%% Linear regression
% Selecting data for the linear regression
CFSNT5005(:,1)=SNT5005(600:1300);
CFENT5005(:,1)=ENT5005(600:1300);
CFSNT50052(:,1)=SNT50052(600:1300);
CFENT50052(:,1)=ENT50052(600:1300);
CFSNT7020(:,1)=SNT7020(2000:2700);
CFENT7020(:,1)=ENT7020(2000:2700);
CFSHT7020(:,1)=SHT7020(2000:2700);
CFEHT7020(:,1)=EHT7020(2000:2700);

% Creating fitting results for the subplot
ft = fittype( 'poly1' );
[fitresult1, gof] = fit( CFENT5005, CFSNT5005, ft );
ft = fittype( 'poly1' );
[fitresult2, gof] = fit( CFENT50052, CFSNT50052, ft );
ft = fittype( 'poly1' );
[fitresult3, gof] = fit( CFENT7020, CFSNT7020, ft );
ft = fittype( 'poly1' );
[fitresult4, gof] = fit( CFEHT7020, CFSHT7020, ft );

% Creating subplot of curve fittings
figure1 = figure('Color',[1 1 1]);
subplot1 = subplot(2,2,1,'Parent',figure1);
xlim(subplot1,[0.0002 0.0007]);
box(subplot1,'on');
set(subplot1,'FontSize',14);
hold(subplot1,'all');
plot1=plot( fitresult1, CFENT5005, CFSNT5005 );
legend( plot1, 'Data', 'Linear fit (R-square=0.9998)', 'Location', 'NorthWest' );
xlabel({'Strain'},'FontSize',16);
ylabel({'Stress (Pa)'},'FontSize',16);
title({'Non-treated 5005(1)'},'FontSize',16);
subplot2 = subplot(2,2,2,'Parent',figure1);
xlim(subplot2,[0.0001 0.0006]);
box(subplot2,'on');
set(subplot2,'FontSize',14);
hold(subplot2,'all');
plot2=plot( fitresult2, CFENT50052, CFSNT50052 );
legend( plot2, 'Data', 'Linear fit (R-square=0.9996)', 'Location', 'NorthWest' );
xlabel({'Strain'},'FontSize',16);
ylabel({'Stress (Pa)'},'FontSize',16);
title({'Non-treated 5005(2)'},'FontSize',16);
subplot3 = subplot(2,2,3,'Parent',figure1);
xlim(subplot3,[0.0003 0.0008]);
box(subplot3,'on');
set(subplot3,'FontSize',14);
hold(subplot3,'all');
plot3=plot( fitresult3, CFENT7020, CFSNT7020 );

```

```

legend( plot3, 'Data', 'Linear fit (R-square=0.9996)', 'Location', 'NorthWest'
);
xlabel({'Strain'},'FontSize',16);
ylabel({'Stress (Pa)'},'FontSize',16);
title({'Non-treated 7020'},'FontSize',16);
subplot4 = subplot(2,2,4,'Parent',figure1);
xlim(subplot4,[0.0005 0.0010]);
box(subplot4,'on');
set(subplot4,'FontSize',14);
hold(subplot4,'all');
plot4=plot( fitresult4, CFEHT7020, CFSHT7020 );
legend( plot4, 'Data', 'Linear fit (R-square=0.9997)', 'Location', 'NorthWest'
);
xlabel({'Strain'},'FontSize',16);
ylabel({'Stress (Pa)'},'FontSize',16);
title({'Heat-treated 7020'},'FontSize',16);

% E-modulus NT5005 = 7.494e+10
% E-modulus NT50052 = 7.202e+10
% E-modulus NT7020 = 8.282e+10
% E-modulus HT7020 = 7.62e+10

%% Determining yield strength
x=0.002:0.00005:0.0075; % Creating the x data points

% Setting the slope and finding the y-axis intersection
NT5005a=7.494e+10;
NT5005b=-7.494e+10*0.002;
NT50052a=7.202e+10;
NT50052b=-7.202e+10*0.002;
HT7020a=7.62e+10;
HT7020b=-7.62e+10*0.002;

% Creating the y data points
NT5005y=NT5005a*x(:,1:61)+NT5005b;
NT50052y=NT50052a*x(:,1:61)+NT50052b;
HT7020y=HT7020a*x+HT7020b;

% Determining the intersections between original and 2 percent offset curve
[xout(1,1),yout(1,1)] = intersections(x(:,1:61),NT5005y,ENT5005,SNT5005,1);
[xout(2,1),yout(2,1)] = intersections(x(:,1:61),NT50052y,ENT50052,SNT50052,1);
[xout(3,1),yout(3,1)] = intersections(x,HT7020y,EHT7020,SHT7020,1);

% Creating subplot of yield strength determination
figure2 = figure('Color',[1 1 1]);
subplot1 = subplot(2,2,1,'Parent',figure2);
xlim(subplot1,[0 0.03]);
ylim(subplot1,[0 4e+8]);
box(subplot1,'on');
set(subplot1,'FontSize',14);
hold(subplot1,'all');
plot(x(:,1:61),NT5005y,'linewidth',2)
hold on
plot(ENT5005,SNT5005,'g','linewidth',2)
plot(xout(1,1),yout(1,1),'r.','markersize',18)
xlabel({'Strain'},'FontSize',16);
ylabel({'Stress (Pa)'},'FontSize',16);
title({'Non-treated 5005'},'FontSize',16);

```

```

subplot2 = subplot(2,2,2,'Parent',figure2);
xlim(subplot2,[0 0.03]);
ylim(subplot2,[0 4e+8]);
box(subplot2,'on');
set(subplot2,'FontSize',14);
hold(subplot2,'all');
plot(x(:,1:61),NT50052y,'linewidth',2)
hold on
plot(ENT50052,SNT50052,'g','linewidth',2)
plot(xout(2,1),yout(2,1),'r.','markersize',18)
xlabel({'Strain'},'FontSize',16);
ylabel({'Stress (Pa)'},'FontSize',16);
title({'Non-treated 50052'},'FontSize',16);
subplot3 = subplot(2,2,3,'Parent',figure2);
xlim(subplot3,[0 0.03]);
ylim(subplot3,[0 4e+8]);
box(subplot3,'on');
set(subplot3,'FontSize',14);
hold(subplot3,'all');
plot(x,HT7020y,'linewidth',2)
hold on
plot(EHT7020,SHT7020,'g','linewidth',2)
plot(xout(3,1),yout(3,1),'r.','markersize',18)
xlabel({'Strain'},'FontSize',16);
ylabel({'Stress (Pa)'},'FontSize',16);
title({'Heat-treated 7020'},'FontSize',16);

%% Creating subplot for stress-strain diagrams for the tensile tests
figure4 = figure('Color',[1 1 1]);
subplot1 = subplot(2,2,1,'Parent',figure4);
xlim(subplot1,[0 0.03]);
ylim(subplot1,[0 4e+8]);
box(subplot1,'on');
set(subplot1,'FontSize',14);
hold(subplot1,'all');
plot(x(:,1:61),NT5005y,'linewidth',2)
hold on
plot(ENT5005,SNT5005,'g','linewidth',2)
plot(xout(1,1),yout(1,1),'r.','markersize',18)
xlabel({'Strain'},'FontSize',16);
ylabel({'Stress (Pa)'},'FontSize',16);
title({'Non-treated 5005'},'FontSize',16);
subplot2 = subplot(2,2,2,'Parent',figure4);
xlim(subplot2,[0 0.03]);
ylim(subplot2,[0 4e+8]);
box(subplot2,'on');
set(subplot2,'FontSize',14);
hold(subplot2,'all');
plot(x(:,1:61),NT50052y,'linewidth',2)
hold on
plot(ENT50052,SNT50052,'g','linewidth',2)
plot(xout(2,1),yout(2,1),'r.','markersize',18)
xlabel({'Strain'},'FontSize',16);
ylabel({'Stress (Pa)'},'FontSize',16);
title({'Non-treated 50052'},'FontSize',16);
subplot3 = subplot(2,2,3,'Parent',figure4);
xlim(subplot3,[0 0.03]);
ylim(subplot3,[0 400000000]);
box(subplot3,'on');

```

```

set(subplot3,'FontSize',14);
hold(subplot3,'all');
plot3=plot(ENT7020,SNT7020,'LineWidth',2);
xlabel({'Strain'},'FontSize',16);
ylabel({'Stress (Pa)'},'FontSize',16);
title({'Non-treated 7020'},'FontSize',16);
subplot4 = subplot(2,2,4,'Parent',figure4);
xlim(subplot4,[0 0.03]);
ylim(subplot4,[0 4e+8]);
box(subplot4,'on');
set(subplot4,'FontSize',14);
hold(subplot4,'all');
plot(x,HT7020y,'linewidth',2)
hold on
plot(EHT7020,SHT7020,'g','linewidth',2)
plot(xout(3,1),yout(3,1),'r','markersize',18)
xlabel({'Strain'},'FontSize',16);
ylabel({'Stress (Pa)'},'FontSize',16);
title({'Heat-treated 7020'},'FontSize',16);

% Creating plot for article
figure5=figure('Color',[1 1 1]);
axes1 = axes('Parent',figure5);
plot(EHT7020,SHT7020/10^6,'LineWidth',4)
ylim([0 350]);
xlabel({'Strain'},'FontSize',35);
ylabel({'Stress (MPa)'},'FontSize',35);
title({'Heat-treated 7020'},'FontSize',40);
set(axes1,'FontSize',35);

```

### 3.6.2 Calibrations and force determination

```

%% Clears Workspace
clear all

%% Laboratory calibrations
% Load data
load 'TanTwoMV'
load 'RadTwoMV'
load 'BreakTwoMV'
load 'BumpFTwoMV'
load 'BumpRTwoMV'

% Transforming volt data into micro strain data
TanTwoMVS=0.561167*TanTwoMV*4096/3-468.5744-135;
RadTwoMVS=0.842441*RadTwoMV*4096/3-1778.392;

% Calculating the mean of the output for each applied load
for i=1:6
    TanCaliData(:,i)=mean(TanTwoMVS(1:15000,i))-mean(TanTwoMVS(1:15000,1));
end
for i=1:5
    RadCaliData(:,i)=(mean(RadTwoMVS(1:35000,i))-mean(RadTwoMVS(1:35000,1)));
    BreakCaliData(:,i)=mean(BreakTwoMV(1:12000,i))-mean(BreakTwoMV(1:12000,1));
    BumpFCaliData(:,i)=mean(BumpFTwoMV(1:11000,i))-mean(BumpFTwoMV(1:11000,1));
    BumpRCaliData(:,i)=mean(BumpRTwoMV(1:12000,i))-mean(BumpRTwoMV(1:12000,1));
end

```

```

% Generating arrays of load applied in the calibrations
Kilo=[0 1 2 3 4 5]*9.82;
Kilo2=[0 2 3 4 5]*9.82;
Kilo3=[0 5 10 15 20]*9.82;

% Performing linear regression of Lab calibrations
Slope(1,1)=TanCaliData'\Kilo';
Slope(2,1)=RadCaliData'\Kilo2';
Slope(3,1)=BreakCaliData'\Kilo3';
Slope(4,1)=BumpFCaliData'\Kilo3';
Slope(5,1)=BumpRCaliData'\Kilo3';

% Finding R-square value
Rsq(1,1)=1-sum((Kilo-TanCaliData*Slope(1,1)).^2)/sum((Kilo-mean(Kilo)).^2);
Rsq(2,1)=1-sum((Kilo2-RadCaliData*Slope(2,1)).^2)/sum((Kilo2-mean(Kilo2)).^2);
Rsq(3,1)=1-sum((Kilo3-BreakCaliData*Slope(3,1)).^2)/sum((Kilo3-mean(Kilo3)).^2);
Rsq(4,1)=1-sum((Kilo3-BumpFCaliData*Slope(4,1)).^2)/sum((Kilo3-mean(Kilo3)).^2);
Rsq(5,1)=1-sum((Kilo3-BumpRCaliData*Slope(5,1)).^2)/sum((Kilo3-mean(Kilo3)).^2);

%% Solid Works and Free Body Diagram calibrations
% FBD at rear tire
I=pi/4*(0.035^4-0.0335^4); % calculating the moment of inertia
E=76.2*10^9; % E-modulus found in tensile test
L1=0.132; % Length from outer spokes to SG
L2=0.073; % Length from inner spokes to SG
F=[0 100]; % Force array
S=(0.5*F*L1^3/(3*E*I)+0.5*F*L2^3/(3*E*I))*10^6*-1; % Calculating strain
corresponding to F

% SW at front tire
Kilo4=[0 200]; % Applied load at front wheel in SW

% Break
SimBreakCaliData=[0 1.35E-04]*10^6*-1;

% Bump
SimBumpFCaliData=[0 -1.23E-04]*10^6*-1; % Data from SW
SimBumpRCaliData=[0 -1.39E-04]*10^6; % Data from SW

% SW at crank
% Tangential
SimTanCaliData=[0 6.318E-04]*10^6; % Data from SW

% Radial
SimRadCaliData=[0 3.86E-04]*10^6*-1; % Data from SW

% Performing linear regression of Lab calibrations
Slope(1,2)=SimTanCaliData'\Kilo4';
Slope(2,2)=SimRadCaliData'\Kilo4';
Slope(3,2)=SimBreakCaliData'\Kilo4';
Slope(4,2)=SimBumpFCaliData'\Kilo4';
% Slope(5,2)=SimBumpRCaliData'\Kilo4'; % SW
Slope(5,2)=S'\F'; % FBD

% Finding R-square value

```

```

Rsq(1,2)=1-sum((Kilo5-SimTanCaliData*Slope(1,2)).^2)/sum((Kilo5-mean(Kilo5)).^2);
Rsq(2,2)=1-sum((Kilo5-SimRadCaliData*Slope(2,2)).^2)/sum((Kilo5-mean(Kilo5)).^2);
Rsq(3,2)=1-sum((Kilo4-SimBreakCaliData*Slope(3,2)).^2)/sum((Kilo4-mean(Kilo4)).^2);
Rsq(4,2)=1-sum((Kilo4-SimBumpFCaliData*Slope(4,2)).^2)/sum((Kilo4-mean(Kilo4)).^2);
% Rsq(5,2)=1-sum((Kilo4-SimBumpRCaliData*Slope(5,2)).^2)/sum((Kilo4-mean(Kilo4)).^2); % SW
Rsq(5,2)=1-sum((F-S*Slope(5,2)).^2)/sum((F-mean(F)).^2); % FBD

% Calculating the percent difference between lab and simulate calibrations
for i=1:5
    Diff(i,1)=(Slope(i,1)-Slope(i,2))/Slope(i,2);
end

%% Crank force
% Load Data
load 'AccOne'
load 'AccTwo'
load 'AccThree'
load 'AccFour'
load 'AccFive'

% Elongate arrays to fit into a matrix
AccTwo(55001:100000,1:3)=100000;
AccThree(75001:100000,1:3)=100000;
AccFour(60001:100000,1:3)=100000;
AccFive(60001:100000,1:3)=100000;

% Transforming volts measured into strains
AccOneS(:,1)=0.561167*AccOne(:,2)*4096/3-468.5744-135;
AccOneS(:,2)=0.842441*AccOne(:,3)*4096/3-1778.392;
AccTwoS(:,1)=0.561167*AccTwo(:,2)*4096/3-468.5744-135;
AccTwoS(:,2)=0.842441*AccTwo(:,3)*4096/3-1778.392;
AccThreeS(:,1)=0.561167*AccThree(:,2)*4096/3-468.5744-135;
AccThreeS(:,2)=0.842441*AccThree(:,3)*4096/3-1778.392;
AccFourS(:,1)=0.561167*AccFour(:,2)*4096/3-468.5744-135;
AccFourS(:,2)=0.842441*AccFour(:,3)*4096/3-1778.392;
AccFiveS(:,1)=0.561167*AccFive(:,2)*4096/3-468.5744-135;
AccFiveS(:,2)=0.842441*AccFive(:,3)*4096/3-1778.392;

% Create cycles matrix
CyclesData(:,1)=AccOne(:,1);
CyclesData(:,2)=AccTwo(:,1);
CyclesData(:,3)=AccThree(:,1);
CyclesData(:,4)=AccFour(:,1);
CyclesData(:,5)=AccFive(:,1);

% Create tangential force matrix
LabTanForce(:,1)=(AccOneS(:,1)-AccOneS(1,1))*Slope(1,1);
LabTanForce(:,2)=(AccTwoS(:,1)-AccTwoS(1,1))*Slope(1,1);
LabTanForce(:,3)=(AccThreeS(:,1)-AccThreeS(1,1))*Slope(1,1);
LabTanForce(:,4)=(AccFourS(:,1)-AccFourS(1,1))*Slope(1,1);
LabTanForce(:,5)=(AccFiveS(:,1)-AccFiveS(1,1))*Slope(1,1);
SimTanForce(:,1)=(AccOneS(:,1)-AccOneS(1,1))*Slope(1,2);
SimTanForce(:,2)=(AccTwoS(:,1)-AccTwoS(1,1))*Slope(1,2);

```

```

SimTanForce(:,3)=(AccThreeS(:,1)-AccThreeS(1,1))*Slope(1,2);
SimTanForce(:,4)=(AccFourS(:,1)-AccFourS(1,1))*Slope(1,2);
SimTanForce(:,5)=(AccFiveS(:,1)-AccFiveS(1,1))*Slope(1,2);

% Create radial force matrix
LabRadForce(:,1)=(AccOneS(:,2)-AccOneS(1,2))*Slope(2,1);
LabRadForce(:,2)=(AccTwoS(:,2)-AccTwoS(1,2))*Slope(2,1);
LabRadForce(:,3)=(AccThreeS(:,2)-AccThreeS(1,2))*Slope(2,1);
LabRadForce(:,4)=(AccFourS(:,2)-AccFourS(1,2))*Slope(2,1);
LabRadForce(:,5)=(AccFiveS(:,2)-AccFiveS(1,2))*Slope(2,1);
SimRadForce(:,1)=(AccOneS(:,2)-AccOneS(1,2))*Slope(2,2);
SimRadForce(:,2)=(AccTwoS(:,2)-AccTwoS(1,2))*Slope(2,2);
SimRadForce(:,3)=(AccThreeS(:,2)-AccThreeS(1,2))*Slope(2,2);
SimRadForce(:,4)=(AccFourS(:,2)-AccFourS(1,2))*Slope(2,2);
SimRadForce(:,5)=(AccFiveS(:,2)-AccFiveS(1,2))*Slope(2,2);

% Find the tangential and radial force for 3 cycles
for i=1:5
    Cycles(:,i)=CyclesData(:,i)-CyclesData(1,i)+1;
    for p=1:1500
        LabTan(p,i)=mean(LabTanForce(find(Cycles(:,i)<p+1 & Cycles(:,i)>p-
1),i));
        LabRad(p,i)=mean(LabRadForce(find(Cycles(:,i)<p+1 & Cycles(:,i)>p-
1),i));
        SimTan(p,i)=mean(SimTanForce(find(Cycles(:,i)<p+1 & Cycles(:,i)>p-
1),i));
        SimRad(p,i)=mean(SimRadForce(find(Cycles(:,i)<p+1 & Cycles(:,i)>p-
1),i));
        Degrees(p,1)=p*360/500;
    end
end

% Find the maximal tangential and radial force
LabTanPeak(:,1)=max(LabTan(1:500,:));
SimTanPeak(:,1)=max(SimTan(1:500,:));
LabRadPeak(:,1)=max(LabRad);
SimRadPeak(:,1)=max(SimRad);

MeanLabTanPeak=mean(LabTanPeak);
MeanLabRadPeak=mean(LabRadPeak);
STDLabTanPeak=std(LabTanPeak);
STDLabRadPeak=std(LabRadPeak);
MeanSimTanPeak=mean(SimTanPeak);
MeanSimRadPeak=mean(SimRadPeak);
STDSimTanPeak=std(SimTanPeak);
STDSimRadPeak=std(SimRadPeak);

% Find the position of the crank to the force peaks in degrees
for i=1:5
    PosTan(:,i)=find(LabTan(1:500,i)>LabTanPeak(i,1)-0.0001)*0.72;
    PosRad(:,i)=find(LabRad(:,i)>LabRadPeak(i,1)-0.0001)*0.72;
end

%% Break Force
% Load Data
load 'BreakData'

```

```

% Create break force matrix
for i=1:6
    LabBreakForce(:,i)=(BreakData(:,i)-BreakData(1,i))*Slope(3,1);
    SimBreakForce(:,i)=(BreakData(:,i)-BreakData(1,i))*Slope(3,2);
end
% Find the break force peak
BreakForcePeak(:,1)=max(LabBreakForce(:,2:6));
BreakForcePeak(:,2)=max(SimBreakForce(:,2:6));

% Calculate the mean of the break force peak
MeanBreakForcePeak=mean(BreakForcePeak);
STDBreakForcePeak=std(BreakForcePeak);

%% Road irregularities
% Load Data
load 'BumpFData'
load 'BumpRData'

% Create bump force matrixs
for i=1:6
    LabBumpFForce(:,i)=(BumpFData(:,i)-BumpFData(1,i))*Slope(4,1);
    LabBumpRForce(:,i)=(BumpRData(:,i)-BumpRData(1,i))*Slope(5,1);
    SimBumpFForce(:,i)=(BumpFData(:,i)-BumpFData(1,i))*Slope(4,2);
    SimBumpRForce(:,i)=(BumpRData(:,i)-BumpRData(1,i))*Slope(5,2);
end

% Find the bump force peak
BumpFForcePeak(:,1)=max(LabBumpFForce(:,,:));
BumpRForcePeak(:,1)=max(LabBumpRForce(:,,:));
BumpFForcePeak(:,2)=max(SimBumpFForce(:,,:));
BumpRForcePeak(:,2)=max(SimBumpRForce(:,,:));

% Calculate the mean of the break force peak
MeanBumpFForcePeak=mean(BumpFForcePeak);
MeanBumpRForcePeak=mean(BumpRForcePeak);
STDBumpFForcePeak=std(BumpFForcePeak);
STDBumpRForcePeak=std(BumpRForcePeak);

%% Plots of max trials for article
o=40; % Font size for marker and title
p=4; % Font size for linewidth
q=35; % Font size for axes and label
r=20; % Font size for axes on subplots

% Max trial (5) for tangential force
figure2 = figure('Color',[1 1 1]);
axes1 = axes('Parent',figure2);
hold(axes1,'on');
plot1=plot(Degrees,LabTan(:,5),Degrees,SimTan(:,5));
set(plot1(1),'LineWidth',p);
set(plot1(2),'LineWidth',p);
legend(plot1, 'Lab tangential force', 'SW tangential force', 'Location',
'NorthEast' );
xlabel({'Degrees'},'FontSize',q);
ylabel({'Force (N)'},'FontSize',q);
title({'Crank tangential force trial 5'},'FontSize',o);
box(axes1,'on');

```

```

set(axes1, 'FontSize', q);

% Max trial (5) for radial force
figure17 = figure('Color', [1 1 1]);
axes1 = axes('Parent', figure17);
hold(axes1, 'on');
plot1=plot(Degrees, LabRad(:,5), Degrees, SimRad(:,5));
set(plot1(1), 'LineWidth', p);
set(plot1(2), 'LineWidth', p);
legend( plot1, 'Lab radial force', 'SW radial force', 'Location', 'NorthEast' );
xlabel({'Degrees'}, 'FontSize', q);
ylabel({'Force (N)'}, 'FontSize', q);
title({'Crank radial force trial 5'}, 'FontSize', o);
box(axes1, 'on');
set(axes1, 'FontSize', q);

Samples(:,1)=1:1:2500; % Creating array for plot
% Max trial (1) for break force
figure3 = figure('Color', [1 1 1]);
axes1 = axes('Parent', figure3);
hold(axes1, 'on');
plot1=plot(Samples, LabBreakForce(16501:19000,2), Samples, SimBreakForce(16501:19000,2));
set(plot1(1), 'LineWidth', p);
set(plot1(2), 'LineWidth', p);
legend( plot1, 'Lab break force', 'SW break force', 'Location', 'NorthEast' );
xlabel({'Samples'}, 'FontSize', q);
ylabel({'Force (N)'}, 'FontSize', q);
title({'Break force trial 1'}, 'FontSize', o);
box(axes1, 'on');
set(axes1, 'FontSize', q);

Samples2(:,1)=1:1:501; % Creating array for plot
% Max trial (5) for road irregularities front tire force
figure18 = figure('Color', [1 1 1]);
axes1 = axes('Parent', figure18);
hold(axes1, 'on');
plot1=plot(Samples2, LabBumpFForce(14250:14750,6), Samples2, SimBumpFForce(14250:14750,6));
set(plot1(1), 'LineWidth', p);
set(plot1(2), 'LineWidth', p);
legend( plot1, 'Lab bump force', 'SW bump force', 'Location', 'NorthEast' );
xlabel({'Samples'}, 'FontSize', q);
ylabel({'Force (N)'}, 'FontSize', q);
title({'Bump front wheel force trial 1'}, 'FontSize', o);
box(axes1, 'on');
set(axes1, 'FontSize', q);

% Max trial (5) for road irregularities rear tire force
figure18 = figure('Color', [1 1 1]);
axes1 = axes('Parent', figure18);
hold(axes1, 'on');
plot1=plot(Samples2, LabBumpRForce(14250:14750,6), Samples2, SimBumpRForce(14250:14750,6));
set(plot1(1), 'LineWidth', p);
set(plot1(2), 'LineWidth', p);
legend( plot1, 'Lab bump force', 'FBD bump force', 'Location', 'NorthEast' );
xlabel({'Samples'}, 'FontSize', q);

```

```

ylabel({'Force (N)'},'FontSize',q);
title({'Bump rear wheel force trial 1'},'FontSize',o);
box(axes1,'on');
set(axes1,'FontSize',q);

%% Regression plots
% Laboratory tangential linear regression
[xData, yData] = prepareCurveData( TanCaliData,Kilo );
ft = fittype( 'poly1' );
[fitresult, gof] = fit( xData, yData, ft );
figure5=figure('Color',[1 1 1]);
axes1 = axes('Parent',figure5);
hold(axes1,'on');
h = plot( fitresult, xData, yData);
set(h(1),'Marker','.', 'MarkerSize',o);
set(h(2),'LineWidth',p);
legend( h, 'Loads applied vs. calibration data', 'Linear regression
F=0.3963??(R-square=1)', 'Location', 'NorthWest' );
xlabel('Micro strain','FontSize',q);
ylabel('Loads applied (N)','FontSize',q);
title('Laboratory tangential calibration','FontSize',o);
box(axes1,'on');
set(axes1,'FontSize',q);

% SolidWorks tangential linear regression
[xData, yData] = prepareCurveData( SimTanCaliData,F );
ft = fittype( 'poly1' );
[fitresult, gof] = fit( xData, yData, ft );
figure10=figure('Color',[1 1 1]);
axes1 = axes('Parent',figure10);
hold(axes1,'on');
h = plot( fitresult, xData, yData);
set(h(1),'Marker','.', 'MarkerSize',o);
set(h(2),'LineWidth',p);
legend( h, 'Loads applied vs. calibration data', 'Linear regression
F=0.3166??(R-square=1)', 'Location', 'NorthWest' );
xlabel('Micro strain','FontSize',q);
ylabel('Loads applied (N)','FontSize',q);
title('SolidWorks tangential calibration','FontSize',o);
box(axes1,'on');
set(axes1,'FontSize',q);

% Laboratory radial linear regression
[xData, yData] = prepareCurveData( RadCaliData,Kilo2 );
ft = fittype( 'poly1' );
[fitresult, gof] = fit( xData, yData, ft );
figure6=figure('Color',[1 1 1]);
axes1 = axes('Parent',figure6);
hold(axes1,'on');
h = plot( fitresult, xData, yData);
set(h(1),'Marker','.', 'MarkerSize',o);
set(h(2),'LineWidth',p);
legend( h, 'Loads applied vs. calibration data', 'Linear regression F=-
0.4749654??(R-square=0.9998)', 'Location', 'NorthEast' );
xlabel('Micro strain','FontSize',q);
ylabel('Loads applied (N)','FontSize',q);
title('Laboratory radial calibration','FontSize',o);
box(axes1,'on');

```

```

set(axes1,'FontSize',q);

% SolidWorks radial linear regression
[xData, yData] = prepareCurveData( SimRadCaliData,F );
ft = fittype( 'poly1' );
[fitresult, gof] = fit( xData, yData, ft );
figure11=figure('Color',[1 1 1]);
axes1 = axes('Parent',figure11);
hold(axes1,'on');
h = plot( fitresult, xData, yData);
set(h(1),'Marker','.', 'MarkerSize',o);
set(h(2),'LineWidth',p);
legend( h, 'Loads applied vs. calibration data', 'Linear regression F=-
0.5181??(R-square=1)', 'Location', 'NorthEast' );
xlabel('Micro strain','FontSize',q);
ylabel('Loads applied (N)','FontSize',q);
title('SolidWorks radial calibration','FontSize',o);
box(axes1,'on');
set(axes1,'FontSize',q);

% Laboratory break linear regression
[xData, yData] = prepareCurveData( BreakCaliData, Kilo3 );
ft = fittype( 'poly1' );
[fitresult, gof] = fit( xData, yData, ft );
figure7=figure('Color',[1 1 1]);
axes1 = axes('Parent',figure7);
hold(axes1,'on');
h = plot( fitresult, xData, yData);
set(h(1),'Marker','.', 'MarkerSize',o);
set(h(2),'LineWidth',p);
legend( h, 'Loads applied vs. calibration data', 'Linear regression F=-
2.9093??(R-square=0-9719)', 'Location', 'NorthEast' );
xlabel('Micro strain','FontSize',q);
ylabel('Loads applied (N)','FontSize',q);
title('Laboratory break calibration','FontSize',o);
box(axes1,'on');
set(axes1,'FontSize',q);

% SolidWorks break linear regression
[xData, yData] = prepareCurveData( SimBreakCaliData, Kilo4 );
ft = fittype( 'poly1' );
[fitresult, gof] = fit( xData, yData, ft );
figure14=figure('Color',[1 1 1]);
axes1 = axes('Parent',figure14);
hold(axes1,'on');
h = plot( fitresult, xData, yData);
set(h(1),'Marker','.', 'MarkerSize',o);
set(h(2),'LineWidth',p);
legend( h, 'Loads applied vs. calibration data', 'Linear regression F=-
1.4815??(R-square=1)', 'Location', 'NorthEast' );
xlabel('Micro strain','FontSize',q);
ylabel('Loads applied (N)','FontSize',q);
title('SolidWorks break calibration','FontSize',o);
box(axes1,'on');
set(axes1,'FontSize',q);

% Laboratory Front wheel linear regression
[xData, yData] = prepareCurveData( BumpFCaliData, Kilo3 );

```

```

ft = fittype( 'poly1' );
[fitresult, gof] = fit( xData, yData, ft );
figure8=figure('Color',[1 1 1]);
axes1 = axes('Parent',figure8);
hold(axes1,'on');
h = plot( fitresult, xData, yData);
set(h(1),'Marker','.', 'MarkerSize',o);
set(h(2),'LineWidth',p);
legend( h, 'Loads applied vs. calibration data', 'Linear regression
F=23.2249??(R-square=0.9972)', 'Location', 'NorthWest' );
xlabel('Micro strain','FontSize',q);
ylabel('Loads applied (N)','FontSize',q);
title('Laboratory front wheel calibration','FontSize',o);
box(axes1,'on');
set(axes1,'FontSize',q);

% SolidWorks front wheel linear regression
[xData, yData] = prepareCurveData( SimBumpFCaliData,Kilo4 );
ft = fittype( 'poly1' );
[fitresult, gof] = fit( xData, yData, ft );
figure12=figure('Color',[1 1 1]);
axes1 = axes('Parent',figure12);
hold(axes1,'on');
h = plot( fitresult, xData, yData);
set(h(1),'Marker','.', 'MarkerSize',o);
set(h(2),'LineWidth',p);
legend( h, 'Loads applied vs. calibration data', 'Linear regression
F=1.6260??(R-square=1)', 'Location', 'NorthWest' );
xlabel('Micro strain','FontSize',q);
ylabel('Loads applied (N)','FontSize',q);
title('SolidWorks front wheel calibration','FontSize',o);
box(axes1,'on');
set(axes1,'FontSize',q);

% Laboratory rear wheel linear regression
[xData, yData] = prepareCurveData( BumpFCaliData*-1, Kilo3 );
ft = fittype( 'poly1' );
[fitresult, gof] = fit( xData, yData, ft );
figure9=figure('Color',[1 1 1]);
axes1 = axes('Parent',figure9);
hold(axes1,'on');
h = plot( fitresult, xData, yData);
set(h(1),'Marker','.', 'MarkerSize',o);
set(h(2),'LineWidth',p);
legend( h, 'Loads applied vs. calibration data', 'Linear regression F=-
35.1735??(R-square=0.9942)', 'Location', 'NorthEast' );
xlabel('Micro strain','FontSize',q);
ylabel('Loads applied (N)','FontSize',q);
title('Laboratory rear wheel calibration','FontSize',o);
box(axes1,'on');
set(axes1,'FontSize',q);

% Free Body Diagram rear wheel linear regression
[xData, yData] = prepareCurveData( S,F );
ft = fittype( 'poly1' );
[fitresult, gof] = fit( xData, yData, ft );
figure13=figure('Color',[1 1 1]);
axes1 = axes('Parent',figure13);

```

```

hold(axes1,'on');
h = plot( fitresult, xData, yData);
set(h(1),'Marker','.', 'MarkerSize',o);
set(h(2), 'LineWidth',p);
legend( h, 'Loads applied vs. calibration data', 'Linear regression F=-
32.2069??(R-square=1)', 'Location', 'NorthEast' );
xlabel('Micro strain','FontSize',q);
ylabel('Loads applied (N)','FontSize',q);
title('FBD rear wheel calibration','FontSize',o);
box(axes1,'on');
set(axes1,'FontSize',q);

%% Force data plots - Appendix
% Tangential
figure19 = figure('Color',[1 1 1]);
subplot1 = subplot(3,2,1,'Parent',figure19);
ylim(subplot1,[0 500]);
box(subplot1,'on');
set(subplot1,'FontSize',r);
hold(subplot1,'all');
plot1=plot(Degrees,LabTan(:,1),Degrees,SimTan(:,1));
set(plot1(1), 'LineWidth',p);
set(plot1(2), 'LineWidth',p);
legend( plot1, 'Lab', 'Sim', 'Location', 'NorthEast' );
xlabel({'Degrees'}, 'FontSize',q);
ylabel({'Force (N)'}, 'FontSize',q);
title({'Tangential trial 1'}, 'FontSize',o);
subplot2 = subplot(3,2,2,'Parent',figure19);
ylim(subplot2,[0 500]);
box(subplot2,'on');
set(subplot2,'FontSize',r);
hold(subplot2,'all');
plot1=plot(Degrees,LabTan(:,2),Degrees,SimTan(:,2));
set(plot1(1), 'LineWidth',p);
set(plot1(2), 'LineWidth',p);
legend( plot1, 'Lab', 'Sim', 'Location', 'NorthEast' );
xlabel({'Degrees'}, 'FontSize',q);
ylabel({'Force (N)'}, 'FontSize',q);
title({'Tangential trial 2'}, 'FontSize',o);
subplot3 = subplot(3,2,3,'Parent',figure19);
ylim(subplot3,[0 500]);
box(subplot3,'on');
set(subplot3,'FontSize',r);
hold(subplot3,'all');
plot1=plot(Degrees,LabTan(:,3),Degrees,SimTan(:,3));
set(plot1(1), 'LineWidth',p);
set(plot1(2), 'LineWidth',p);
legend( plot1, 'Lab', 'Sim', 'Location', 'NorthEast' );
xlabel({'Degrees'}, 'FontSize',q);
ylabel({'Force (N)'}, 'FontSize',q);
title({'Tangential trial 3'}, 'FontSize',o);
subplot4 = subplot(3,2,4,'Parent',figure19);
ylim(subplot4,[0 500]);
box(subplot4,'on');
set(subplot4,'FontSize',r);
hold(subplot4,'all');
plot1=plot(Degrees,LabTan(:,4),Degrees,SimTan(:,4));
set(plot1(1), 'LineWidth',p);
set(plot1(2), 'LineWidth',p);

```

```

legend( plot1, 'Lab', 'Sim', 'Location', 'NorthEast' );
xlabel({'Degrees'},'FontSize',q);
ylabel({'Force (N)'},'FontSize',q);
title({'Tangential trial 4'},'FontSize',o);
subplot5 = subplot(3,2,5, 'Parent',figure19);
ylim(subplot5,[0 500]);
box(subplot5,'on');
set(subplot5,'FontSize',r);
hold(subplot5,'all');
plot1=plot(Degrees,LabTan(:,5),Degrees,SimTan(:,5));
set(plot1(1),'LineWidth',p);
set(plot1(2),'LineWidth',p);
legend( plot1, 'Lab', 'Sim', 'Location', 'NorthEast' );
xlabel({'Degrees'},'FontSize',q);
ylabel({'Force (N)'},'FontSize',q);
title({'Tangential trial 5'},'FontSize',o);

% Radial
figure20 = figure('Color',[1 1 1]);
subplot1 = subplot(3,2,1, 'Parent',figure20);
ylim(subplot1,[-600 600]);
box(subplot1,'on');
set(subplot1,'FontSize',r);
hold(subplot1,'all');
plot1=plot(Degrees,LabRad(:,1),Degrees,SimRad(:,1));
set(plot1(1),'LineWidth',p);
set(plot1(2),'LineWidth',p);
legend( plot1, 'Lab', 'Sim', 'Location', 'NorthEast' );
xlabel({'Degrees'},'FontSize',q);
ylabel({'Force (N)'},'FontSize',q);
title({'Radial trial 1'},'FontSize',o);
subplot2 = subplot(3,2,2, 'Parent',figure20);
ylim(subplot2,[-600 600]);
box(subplot2,'on');
set(subplot2,'FontSize',r);
hold(subplot2,'all');
plot1=plot(Degrees,LabRad(:,2),Degrees,SimRad(:,2));
set(plot1(1),'LineWidth',p);
set(plot1(2),'LineWidth',p);
legend( plot1, 'Lab', 'Sim', 'Location', 'NorthEast' );
xlabel({'Degrees'},'FontSize',q);
ylabel({'Force (N)'},'FontSize',q);
title({'Radial trial 2'},'FontSize',o);
subplot3 = subplot(3,2,3, 'Parent',figure20);
ylim(subplot3,[-600 600]);
box(subplot3,'on');
set(subplot3,'FontSize',r);
hold(subplot3,'all');
plot1=plot(Degrees,LabRad(:,3),Degrees,SimRad(:,3));
set(plot1(1),'LineWidth',p);
set(plot1(2),'LineWidth',p);
legend( plot1, 'Lab', 'Sim', 'Location', 'NorthEast' );
xlabel({'Degrees'},'FontSize',q);
ylabel({'Force (N)'},'FontSize',q);
title({'Radial trial 3'},'FontSize',o);
subplot4 = subplot(3,2,4, 'Parent',figure20);
ylim(subplot4,[-600 600]);
box(subplot4,'on');
set(subplot4,'FontSize',r);

```

```

hold(subplot4, 'all');
plot1=plot(Degrees, LabRad(:,4), Degrees, SimRad(:,4));
set(plot1(1), 'LineWidth', p);
set(plot1(2), 'LineWidth', p);
legend( plot1, 'Lab', 'Sim', 'Location', 'NorthEast' );
xlabel({'Degrees'}, 'FontSize', q);
ylabel({'Force (N)'}, 'FontSize', q);
title({'Radial trial 4'}, 'FontSize', o);
subplot5 = subplot(3,2,5, 'Parent', figure20);
ylim(subplot5, [-600 600]);
box(subplot5, 'on');
set(subplot5, 'FontSize', r);
hold(subplot5, 'all');
plot1=plot(Degrees, LabRad(:,5), Degrees, SimRad(:,5));
set(plot1(1), 'LineWidth', p);
set(plot1(2), 'LineWidth', p);
legend( plot1, 'Lab', 'Sim', 'Location', 'NorthEast' );
xlabel({'Degrees'}, 'FontSize', q);
ylabel({'Force (N)'}, 'FontSize', q);
title({'Radial trial 5'}, 'FontSize', o);

% Break
Samples3=1:1:6001; % Creating array for subplot
figure21 = figure('Color', [1 1 1]);
subplot1 = subplot(3,2,1, 'Parent', figure21);
box(subplot1, 'on');
set(subplot1, 'FontSize', r);
hold(subplot1, 'all');
plot1=plot(Samples3, LabBreakForce(14000:20000,2), Samples3, SimBreakForce(14000:20000,2));
set(plot1(1), 'LineWidth', p);
set(plot1(2), 'LineWidth', p);
legend( plot1, 'Lab', 'Sim', 'Location', 'NorthEast' );
xlabel({'Degrees'}, 'FontSize', q);
ylabel({'Force (N)'}, 'FontSize', q);
title({'Break trial 1'}, 'FontSize', o);
subplot2 = subplot(3,2,2, 'Parent', figure21);
box(subplot2, 'on');
set(subplot2, 'FontSize', r);
hold(subplot2, 'all');
plot1=plot(Samples3, LabBreakForce(18000:24000,3), Samples3, SimBreakForce(18000:24000,3));
set(plot1(1), 'LineWidth', p);
set(plot1(2), 'LineWidth', p);
legend( plot1, 'Lab', 'Sim', 'Location', 'NorthEast' );
xlabel({'Degrees'}, 'FontSize', q);
ylabel({'Force (N)'}, 'FontSize', q);
title({'Break trial 2'}, 'FontSize', o);
subplot3 = subplot(3,2,3, 'Parent', figure21);
box(subplot3, 'on');
set(subplot3, 'FontSize', r);
hold(subplot3, 'all');
plot1=plot(Samples3, LabBreakForce(18000:24000,4), Samples3, SimBreakForce(18000:24000,4));
set(plot1(1), 'LineWidth', p);
set(plot1(2), 'LineWidth', p);
legend( plot1, 'Lab', 'Sim', 'Location', 'NorthEast' );
xlabel({'Degrees'}, 'FontSize', q);
ylabel({'Force (N)'}, 'FontSize', q);

```

```

title({'Break trial 3'}, 'FontSize', o);
subplot4 = subplot(3,2,4, 'Parent', figure21);
box(subplot4, 'on');
set(subplot4, 'FontSize', r);
hold(subplot4, 'all');
plot1=plot(Samples3, LabBreakForce(14000:20000, 5), Samples3, SimBreakForce(14000:20000, 5));
set(plot1(1), 'LineWidth', p);
set(plot1(2), 'LineWidth', p);
legend( plot1, 'Lab', 'Sim', 'Location', 'NorthEast' );
xlabel({'Degrees'}, 'FontSize', q);
ylabel({'Force (N)'}, 'FontSize', q);
title({'Break trial 4'}, 'FontSize', o);
subplot5 = subplot(3,2,5, 'Parent', figure21);
box(subplot5, 'on');
set(subplot5, 'FontSize', r);
hold(subplot5, 'all');
plot1=plot(Samples3, LabBreakForce(17000:23000, 6), Samples3, SimBreakForce(17000:23000, 6));
set(plot1(1), 'LineWidth', p);
set(plot1(2), 'LineWidth', p);
legend( plot1, 'Lab', 'Sim', 'Location', 'NorthEast' );
xlabel({'Degrees'}, 'FontSize', q);
ylabel({'Force (N)'}, 'FontSize', q);
title({'Break trial 5'}, 'FontSize', o);

% Bump front wheel
Samples4=1:1:2001; % Creating array for subplot
figure22 = figure('Color', [1 1 1]);
subplot1 = subplot(3,2,1, 'Parent', figure22);
box(subplot1, 'on');
set(subplot1, 'FontSize', r);
hold(subplot1, 'all');
plot1=plot(Samples4, LabBumpFForce(11250:13250, 2), Samples4, SimBumpFForce(11250:13250, 2));
set(plot1(1), 'LineWidth', p);
set(plot1(2), 'LineWidth', p);
legend( plot1, 'Lab', 'Sim', 'Location', 'NorthEast' );
xlabel({'Degrees'}, 'FontSize', q);
ylabel({'Force (N)'}, 'FontSize', q);
title({'Front wheel trial 1'}, 'FontSize', o);
subplot2 = subplot(3,2,2, 'Parent', figure22);
box(subplot2, 'on');
set(subplot2, 'FontSize', r);
hold(subplot2, 'all');
plot1=plot(Samples4, LabBumpFForce(12000:14000, 3), Samples4, SimBumpFForce(12000:14000, 3));
set(plot1(1), 'LineWidth', p);
set(plot1(2), 'LineWidth', p);
legend( plot1, 'Lab', 'Sim', 'Location', 'NorthEast' );
xlabel({'Degrees'}, 'FontSize', q);
ylabel({'Force (N)'}, 'FontSize', q);
title({'Front wheel trial 2'}, 'FontSize', o);
subplot3 = subplot(3,2,3, 'Parent', figure22);
box(subplot3, 'on');
set(subplot3, 'FontSize', r);
hold(subplot3, 'all');
plot1=plot(Samples4, LabBumpFForce(12500:14500, 4), Samples4, SimBumpFForce(12500:14500, 4));

```

```

set(plot1(1), 'LineWidth', p);
set(plot1(2), 'LineWidth', p);
legend( plot1, 'Lab', 'Sim', 'Location', 'NorthEast' );
xlabel({'Degrees'}, 'FontSize', q);
ylabel({'Force (N)'}, 'FontSize', q);
title({'Front wheel trial 3'}, 'FontSize', o);
subplot4 = subplot(3,2,4, 'Parent', figure22);
box(subplot4, 'on');
set(subplot4, 'FontSize', r);
hold(subplot4, 'all');
plot1=plot(Samples4, LabBumpFForce(13000:15000, 5), Samples4, SimBumpFForce(13000:15000, 5));
set(plot1(1), 'LineWidth', p);
set(plot1(2), 'LineWidth', p);
legend( plot1, 'Lab', 'Sim', 'Location', 'NorthEast' );
xlabel({'Degrees'}, 'FontSize', q);
ylabel({'Force (N)'}, 'FontSize', q);
title({'Front wheel trial 4'}, 'FontSize', o);
subplot5 = subplot(3,2,5, 'Parent', figure22);
box(subplot5, 'on');
set(subplot5, 'FontSize', r);
hold(subplot5, 'all');
plot1=plot(Samples4, LabBumpFForce(12750:14750, 6), Samples4, SimBumpFForce(12750:14750, 6));
set(plot1(1), 'LineWidth', p);
set(plot1(2), 'LineWidth', p);
legend( plot1, 'Lab', 'Sim', 'Location', 'NorthEast' );
xlabel({'Degrees'}, 'FontSize', q);
ylabel({'Force (N)'}, 'FontSize', q);
title({'Front wheel trial 5'}, 'FontSize', o);

% Bump rear wheel
figure23 = figure('Color', [1 1 1]);
subplot1 = subplot(3,2,1, 'Parent', figure23);
ylim(subplot1, [-30000 30000]);
box(subplot1, 'on');
set(subplot1, 'FontSize', r);
hold(subplot1, 'all');
plot1=plot(Samples4, LabBumpRForce(11250:13250, 2), Samples4, SimBumpRForce(11250:13250, 2));
set(plot1(1), 'LineWidth', p);
set(plot1(2), 'LineWidth', p);
legend( plot1, 'Lab', 'FBD', 'Location', 'NorthEast' );
xlabel({'Degrees'}, 'FontSize', q);
ylabel({'Force (N)'}, 'FontSize', q);
title({'Rear wheel trial 1'}, 'FontSize', o);
subplot2 = subplot(3,2,2, 'Parent', figure23);
ylim(subplot2, [-30000 30000]);
box(subplot2, 'on');
set(subplot2, 'FontSize', r);
hold(subplot2, 'all');
plot1=plot(Samples4, LabBumpRForce(12000:14000, 3), Samples4, SimBumpRForce(12000:14000, 3));
set(plot1(1), 'LineWidth', p);
set(plot1(2), 'LineWidth', p);
legend( plot1, 'Lab', 'FBD', 'Location', 'NorthEast' );
xlabel({'Degrees'}, 'FontSize', q);
ylabel({'Force (N)'}, 'FontSize', q);
title({'Rear wheel trial 2'}, 'FontSize', o);

```

```

subplot3 = subplot(3,2,3,'Parent',figure23);
ylim(subplot3,[-30000 30000]);
box(subplot3,'on');
set(subplot3,'FontSize',r);
hold(subplot3,'all');
plot1=plot(Samples4,LabBumpRForce(12500:14500,4),Samples4,SimBumpRForce(12500:14500,4));
set(plot1(1),'LineWidth',p);
set(plot1(2),'LineWidth',p);
legend( plot1, 'Lab', 'FBD', 'Location', 'NorthEast' );
xlabel({'Degrees'},'FontSize',q);
ylabel({'Force (N)'},'FontSize',q);
title({'Rear wheel trial 3'},'FontSize',o);
subplot4 = subplot(3,2,4,'Parent',figure23);
ylim(subplot4,[-30000 30000]);
box(subplot4,'on');
set(subplot4,'FontSize',r);
hold(subplot4,'all');
plot1=plot(Samples4,LabBumpRForce(13000:15000,5),Samples4,SimBumpRForce(13000:15000,5));
set(plot1(1),'LineWidth',p);
set(plot1(2),'LineWidth',p);
legend( plot1, 'Lab', 'FBD', 'Location', 'NorthEast' );
xlabel({'Degrees'},'FontSize',q);
ylabel({'Force (N)'},'FontSize',q);
title({'Rear wheel trial 4'},'FontSize',o);
subplot5 = subplot(3,2,5,'Parent',figure23);
ylim(subplot5,[-30000 30000]);
box(subplot5,'on');
set(subplot5,'FontSize',r);
hold(subplot5,'all');
plot1=plot(Samples4,LabBumpRForce(12750:14750,6),Samples4,SimBumpRForce(12750:14750,6));
set(plot1(1),'LineWidth',p);
set(plot1(2),'LineWidth',p);
legend( plot1, 'Lab', 'FBD', 'Location', 'NorthEast' );
xlabel({'Degrees'},'FontSize',q);
ylabel({'Force (N)'},'FontSize',q);
title({'Rear wheel trial 5'},'FontSize',o);

```

### 3.6.3 Optimization

```

%% Clears Workspace
clear all

```

```

%% Calculating the energi lost to deforming the structure
F=[0 644.4*2 0]; % Total force applied to the pedal in SW

```

```

% S1 Top 1.25mm, S2 Top 1.5mm, S3 Top 2mm, S4 Front 33.7x4, S5 Rear 33.7x4
D(:,2)=[0.899 0.843 0.751 0.494 0.671]/1000; % Corresponding displacement in SW

```

```

% Calculating the area of the triangle made by the force and displacement
for i=1:5
    E(i,1)=F(:,2)*D(i,2)/2;
end

```

```

% Calculating joule saved per 100 g weight increase
JO=0.579;

```

```

JS=[0.543 0.484 0.318 0.432];
J=JO-JS;
W=[35.8 107.2 51.6 47.9];

for i=1:4
    EW(i)=J(i)/W(i)*1000;
end

%% Plot
% Creating data for subplot
D(:,3)=[0 0 0 0 0]; % Creating a column of zeros
x1=[D(1,1:end-1);D(1,1:end-1);D(1,2:end);D(1,2:end)];
x2=[D(2,1:end-1);D(2,1:end-1);D(2,2:end);D(2,2:end)];
x3=[D(3,1:end-1);D(3,1:end-1);D(3,2:end);D(3,2:end)];
x4=[D(4,1:end-1);D(4,1:end-1);D(4,2:end);D(4,2:end)];
x5=[D(5,1:end-1);D(5,1:end-1);D(5,2:end);D(5,2:end)];
y1=[zeros(1,2);F(1:end-1);F(2:end);zeros(1,2)];

o=40; % Font size for marker and title
p=4; % Font size for linewidth
q=35; % Font size for axes and label
r=20; % Font size for axes on subplots

% Subplot for energyloss due to deformation while accelerating
figure25 = figure('Color',[1 1 1]);
subplot1 = subplot(3,2,1,'Parent',figure25);
xlim(subplot1,[0 0.001]);
box(subplot1,'on');
set(subplot1,'FontSize',r);
hold(subplot1,'all');
plot1=plot(D(1,:),F);
p = patch(x1,y1,'b','LineWidth',1.5);
xlabel({'Displacement (m)'},'FontSize',q);
ylabel({'Force (N)'},'FontSize',q);
title({'Study 1'},'FontSize',o);
subplot2 = subplot(3,2,2,'Parent',figure25);
xlim(subplot2,[0 0.001]);
box(subplot2,'on');
set(subplot2,'FontSize',r);
hold(subplot2,'all');
plot1=plot(D(2,:),F);
p = patch(x2,y1,'b','LineWidth',1.5);
xlabel({'Displacement (m)'},'FontSize',q);
ylabel({'Force (N)'},'FontSize',q);
title({'Study 2'},'FontSize',o);
subplot3 = subplot(3,2,3,'Parent',figure25);
xlim(subplot3,[0 0.001]);
box(subplot3,'on');
set(subplot3,'FontSize',r);
hold(subplot3,'all');
plot1=plot(D(3,:),F);
p = patch(x3,y1,'b','LineWidth',1.5);
xlabel({'Displacement (m)'},'FontSize',q);
ylabel({'Force (N)'},'FontSize',q);
title({'Study 3'},'FontSize',o);
subplot4 = subplot(3,2,4,'Parent',figure25);
xlim(subplot4,[0 0.001]);
box(subplot4,'on');

```

```

set(subplot4,'FontSize',r);
hold(subplot4,'all');
plot1=plot(D(4,:),F);
p = patch(x4,y1,'b','LineWidth',1.5);
xlabel({'Displacement (m)'},'FontSize',q);
ylabel({'Force (N)'},'FontSize',q);
title({'Study 4'},'FontSize',o);
subplot5 = subplot(3,2,5,'Parent',figure25);
xlim(subplot5,[0 0.001]);
box(subplot5,'on');
set(subplot5,'FontSize',r);
hold(subplot5,'all');
plot1=plot(D(5,:),F);
p = patch(x5,y1,'b','LineWidth',1.5);
xlabel({'Displacement (m)'},'FontSize',q);
ylabel({'Force (N)'},'FontSize',q);
title({'Study 5'},'FontSize',o);

```